ХИМИЯ сериясы
№ 4(80)/2015
Серия ХИМИЯ

ҚАРАҒАНДЫ УНИВЕРСИТЕТІНІҢ ХАБАРШЫСЫ

ВЕСТНИК КАРАГАНДИНСКОГО УНИВЕРСИТЕТА

ISSN 0142-0843

ҚАРАҒАНДЫ УНИВЕРСИТЕТІНІҢ
ХАБАРШЫСЫ
ВЕСТНИК
КАРАГАНДИНСКОГО УНИВЕРСИТЕТА

ISSN 0142-0843

ХИМИЯ сериясы
№ 4(80)/2015
Серия ХИМИЯ

Қазан–қараша–желтоқсан
30 желтоқсан 2015 ж.
1996 жылдан бастап шығады
Жылына 4 рет шығады

Октябрь–ноябрь–декабрь
30 декабря 2015 г.
Издается с 1996 года
Выходит 4 раза в год

Собственник РГП **Карагандинский государственный университет**
имени академика Е.А.Букетова

Адрес редакции: 100028, г. Караганда, ул. Университетская, 28
Тел.: (7212) 77-03-69 (внутр. 1026); факс: (7212) 77-03-84.
E-mail: vestnick_kargu@ksu.kz. Сайт: vestnik.ksu.kz

Редактор *Ж.Т.Нурмуханова*
Техн. редактор *В.В.Бутяйкин*

Издательство Карагандинского
государственного университета
им. Е.А.Букетова
100012, г. Караганда,
ул. Гоголя, 38,
тел., факс: (7212) 51-38-20
e-mail: izd_kargu@mail.ru

Басуға 29.12.2015 ж. қол қойылды.
Пішімі 60×84 1/8.
Офсеттік қағазы.
Көлемі 11,62 б.т.
Таралымы 300 дана.
Бағасы келісім бойынша.
Тапсырыс № 306.

Подписано в печать 29.12.2015 г.
Формат 60×84 1/8.
Бумага офсетная.
Объем 11,62 п.л. Тираж 300 экз.
Цена договорная. Заказ № 306.

Отпечатано в типографии
издательства КарГУ
им. Е.А.Букетова

Зарегистрирован Министерством культуры и информации Республики Казахстан.
Регистрационное свидетельство № 13110–Ж от 23.10.2012 г.

МАЗМҰНЫ

ОРГАНИКАЛЫҚ ХИМИЯ

ФИЗИКАЛЫҚ ХИМИЯ

ХИМИЯЛЫҚ ТЕХНОЛОГИЯ ЖӘНЕ МҰНАЙ ХИМИЯСЫ

СОДЕРЖАНИЕ

ОРГАНИЧЕСКАЯ ХИМИЯ

ФИЗИЧЕСКАЯ ХИМИЯ

ХИМИЧЕСКАЯ ТЕХНОЛОГИЯ И НЕФТЕХИМИЯ

UDC 547.891.1

L.K.Salkeyeva[1], Ye.V.Minayeva[1], Ye.K.Taishibekova[1], A.A.Zhortarova[2],
G.T.Khassenova[2], R.M.Zhakupov[1], L.M.Sugralina[1], A.K.Salkeyeva[3]

[1]Ye.A.Buketov Karaganda State University;
[2]Charles University, Prague, Czech Republic;
[3]Karaganda State Technical University
(E-mail: LSalkeeva@mail.ru)

Study of degree of basicity of 2-amino 4-phenylthiazole and 2-amino-4-oxothiazole by mineral acids protonation

There was studied protonation of aminothiazoles of mineral acids of different strength in order to research the basicity of nitrogen atoms of free amino group and nitrogen of thiazole ring. The results obtained showed high ambidentity of 2-amino-4-phenylthiazole and 2-amino-4-oxothiazole associated with a high degree of delocalization of both the lone pair of electrons of the amino group and the thiazole ring nitrogen atom which creates opportunities for chemical modification of the aminoheterocycles with the free amino group and the ring nitrogen atom. Complexing ability of 2-amino-4-oxothiazole with cobalt (II) chloride caused by high degree of basicity of cyclic nitrogen atom was also studied.

Key words: aminoheterocycles, aminothiazoles, mineral acids, protonation, ambidentity, basicity, nucleophilicity, complexones.

It is known that interest to heterocyclic compounds is associated with a wide variety of biologically active properties characteristic for representatives of this class. In particular it does not cease the interest to azaheterocyclic compounds, including derivatives of thiazole, having great importance for the pharmaceutical industry, biochemistry, technology, clinical and experimental medicine. Thiazole derivatives possess antiviral, antiparasitic, antipyretic, antihemolytic, antihypertensive properties and are widely used in medical practice [1]. They are also used in engineering as effective components of the polymeric materials which increase their stability, possess the ability to inhibit the oxidation and corrosion processes, and exhibit complexing properties.

Among practically important thiazole derivatives mercaptothiazoles used as vulcanization accelerators in the rubber industry are well known [2].

Continuing investigations in the field of search and the synthesis of new interesting in practical terms thiazole derivatives, it seems interesting for us to continue researching the structural features of this class of compounds due to the dual reactivity. In this aspect as subjects of research we selected 2-aminothiazole derivatives known to have great importance for the pharmaceutical industry, biochemistry, technology, clinical and experimental medicine. A feature of these compounds is associated with the presence of the free amino group and a nitrogen atom of the heterocycle.

Among the best known amine derivatives of thiazole are 2- and 5-aminothiazoles which can exist in two tautomeric forms but with an evident predominance of the amino form that creates opportunities for their experimental studies aimed at the synthesis of compounds with practically useful properties.

2-Amino-4-phenylthiazole and 2-amino-4-oxothiazole were chosen as subjects of this study. These compounds are characterized by a number of structural features associated with the possibility of high delocalization of the lone pair of electrons (LPE) of the nitrogen atom of free amino group and the nitrogen atom of the heterocycle, and obviously allowance must be made for the presence of the exocyclic carbonyl group in 2-amino-4-oxothiazole which is also capable to participate in the resonance. The presence of the phenyl substituent in the 4 position of the ring undoubtedly contributes to the distribution of the electron density in the molecule. The study of the influence of electronic and structural factors on the chemical behavior of the subjects investigated makes it possible to predict and control the behavior of such structures in the reactions of chemical modification. In this regard we consider that study of the processes of protonation may shed light on the behavior of the reaction centers under different conditions, as the usage of mineral acids of different strength may determine the most important nucleophilic center.

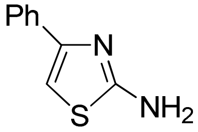
(I)

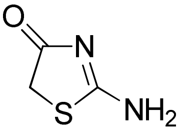
(II)

2-Aminothiazole is known to have sufficiently low basicity ($\mathrm{p}K_a$ 5.39). The chemical structure of 2-amino-4-phenylthiazole suggests the possibility of chemical modification involving the free amino groups and electrophilic substitution reactions in the thiazole ring in the position 5. Some references confirm the ease of electrophilic substitution in position 5 and ease of nucleophilic substitution at the position 2 [3–5]. Nevertheless the presence of LPE at the extracycle nitrogen atom enhances the degree of aromaticity of the thiazole ring due to delocalization. This factor generally reduces the nucleophilic properties of the free amino group, but an increase in the basicity and nucleophilicity of the nitrogen atom of the ring is observed. All these factors taken together cause ambident behavior of 2-amino-4-phenylthiazole in reactions with electrophilic reagents, in particular the possibility of intramolecular proton transfer.

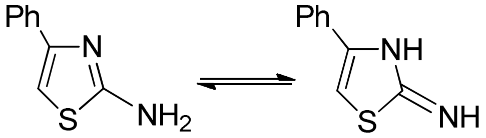

In this regard the study of the intramolecular proton transfer process using mineral acids of different strength will clarify determination of degree of the nucleophilicity of the nitrogen atoms and, consequently, the direction of the reactions with various electrophiles.

There are quite controversial opinions in the literature relative to the basicity of free amino group in the aminothiazole. So it is known that the lone pair of electrons of the nitrogen atom can easily enter into conjugation with thiazole ring which ultimately reduces the basicity of the amino group.

On the one hand the presence of LPE at the nitrogen atom of the thiazole ring can increase its nucleophilicity and hence reactivity in regard to different electrophiles, and on the other hand increases the basicity and nucleophilicity of the free amino group.

All of these factors together create conditions for ambident behavior of molecules of substituted 2-aminothiazoles in reactions with electrophilic reagents.

Thus research of direction of electrophiles attack, in particular the ability to form salts with one equivalent of a mineral acid, is highly informative regarding to basicity of exocyclic nitrogen atom of the amino group and the nitrogen atom of the thiazole ring.

Usage of mineral acids with different degrees of acidity can solve the problem to some extent. For this purpose concentrated hydrochloric acid ($\mathrm{p}K_\alpha$ 7.0), nitric ($\mathrm{p}K_\alpha$ 1.64) and sulfuric acids ($\mathrm{p}K_\alpha$ 3.0) were used.

Study of protonation reactions of aminothiazole derivatives by mineral acids of different strength and structure of salts synthesized determines the strength of basicity and nucleophilicity of the free amino group and the ring nitrogen atom. Obviously during the research at least basicity and nucleophilicity of the free amino groups are changed symbatically.

The reaction of 2-amino-4-phenylthiazole (I) with hydrochloric acid was carried out in ethanol under heating for 2 hours, then upon cooling there was observed precipitating yellow crystals of thiazole hydrochloride (I), which a melting point exceeds significantly the melting point of the starting material and is 220 °C. Control of the reaction was monitored by TLC.

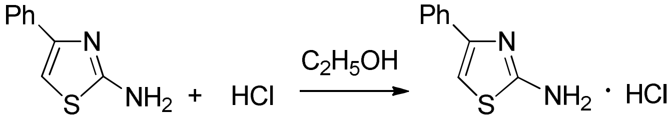

(I a)

Investigation of (Ia) salt structure by IR and NMR spectroscopy indicates the presence of the bound amino group giving the evidence of the significant broadening of absorption bands in the 3300–3400 cm^{-1}.

We used nitric acid as stronger acid, and the reaction is also carried out in ethanol under heating. Nitrate salt of blue color was separated upon reaction (m.p. 168 °C). (Ib) Salt structure was also confirmed by IR and NMR spectroscopy proving protonation at the nitrogen atom of free amino group.

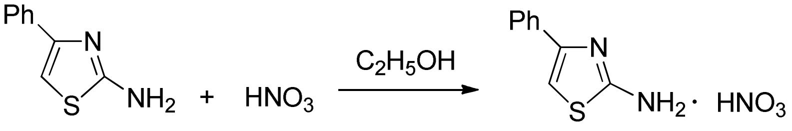

(Ib)

To complete the study of protonating ability of sulfuric acid with respect to 2-amino-4-phenylthiazole was investigated. The reaction was carried out under similar conditions, as a result of which was salt of dark brown color obviously due to strong oxidation and carbonization of substance through the activated aromatic system was obtained. According data of spectral studies salt structure corresponds to the hydrosulfate of the aminothiazole (Ic) according to the following scheme:

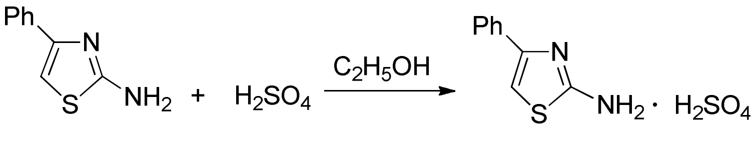

(I c)

The results obtained testify to the high basicity of the free amino group which with forms the corresponding ammonium salts with one equivalent of strong mineral acids. The structure of salts obtained was proved by spectral methods.

As another subject of the study we selected 2-amino-4-oxothiazole which structure is distinguished by the presence of the exocyclic carbonyl group capable of additional polarization and delocalization due to the ring nitrogen atom and amino group. The presence of the C=O group can significantly affect the redistribution of the electronic density of the aminothiazole ring, because the polarization of the delocalized system in the direction of an oxygen atom can significantly decrease the basicity and thus nucleophilicity of the free amino group.

The starting 2-amino-4-oxothiazole was prepared according to a well-known procedure by interacting ethyl ester of monochloroacetic acid with thiourea in 95 % ethanol. After dissolving in 1.2 l hot boiled water crude hydrochloride obtained was treated with an aqueous solution of sodium acetate. Yield of the target product, m.p. 255–258 ºC, was 79–82 %. The structure of compound obtained was confirmed by ^{1}H NMR, ^{13}C NMR spectra.

The reaction proceeds according to the following scheme:

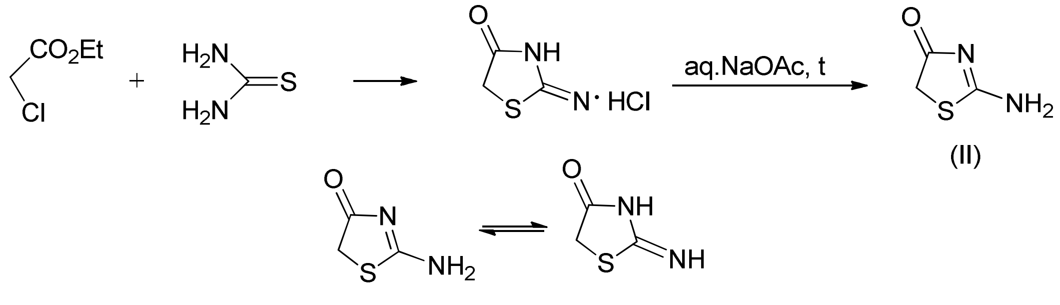

(II)

Protonation of the 2-amino-4-oxothiazole by hydrochloric acid was carried out in acetonitrile while heating for several hours at the reflux temperature, following cooling of reaction mixture leads to precipitation of the desired salt (IIa).

The reaction proceeds according to the following scheme:

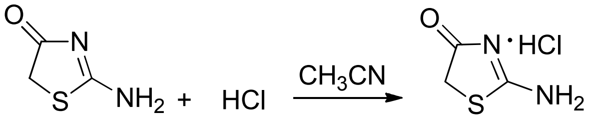

(II a)

The results of spectral studies confirm the occurrence of protonation at the nitrogen atom of the thiazole cycle since IR-spectrum contains two absorption bands of free amino groups in the 3300 cm^{-1}. The resulting salt is a crystalline yellow solid, m.p. 200 °C.

Undoubtedly the basicity of the free amino group is significantly reduced due to a significant resonance with the LPE of cyclic nitrogen atom, which in its turn is delocalized with π — electrons of the C = O bond.

Thus the resonance with the participation of an electron pair of the free amino group has the greatest influence on the distribution of the electron density in the thiazole ring which is obviously due to its enhanced donor capacity.

To confirm these assumptions we used nitric acid as a stronger acid. The reaction was also carried out in acetonitrile under heating. After heating for 2 hours nitrate salt of blue color (IIb) was separated (m.p. 153 ºC).

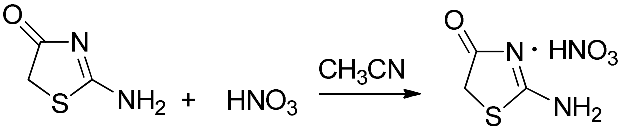

(II b)

To complete the study we investigated the protonating ability of sulfuric acid with respect to 2-amino-4-oxothiazole. The reaction is carried out under the same conditions, thus compound obtained was colored in dark brown. Obviously coloring recess as in the case of aminothiazole (I) is caused by the strong oxidation and degradation due to activation of the thiazole ring as a result of coupling of free amino group with a conjugated system C=N−C=O.

We believe that the structure of the resulting salt (IIc) corresponds to the following scheme:

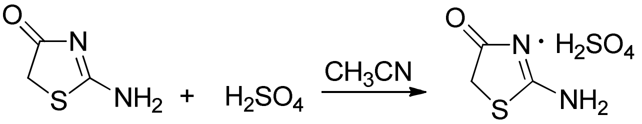

(II c)

The findings of the research carried out show sufficient basicity of the cyclic nitrogen atom of 2-amino-4-hydroxythiazole due to conjugation of electrons of the amino group with a cyclic nitrogen atom, which in its turn is conjugated with the strongly polarized carbonyl group.

The structure of 2-amino-4 oxothiazole synthesized assumes its complexing ability which we showed at investigating its reaction with cobalt chloride with gentle heating for 24 hours in acetonitrile upto reflux.

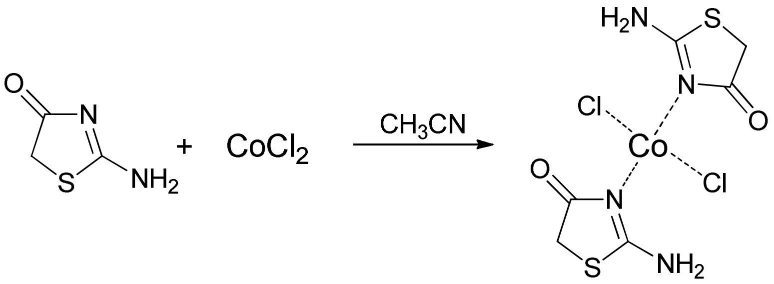

(IV)

The high degree of basicity of the cyclic nitrogen atom is eloquently confirmed by its ability to coordinate with the vacant d-orbitals of cobalt (II) chloride. Thus as a result of studies of complexing ability of 2-amino-4-oxothiazole chloride with cobalt (II), stable complex (IV) of blue colour was obtained, m.p. 260 ºC.

The structure of the complex obtained was confirmed by X-ray diffraction, according to which the complexation of 2-amino-4-oxothiazole with cobalt (II) chloride proceeds on a cyclic nitrogen rather than the free amino group (see Fig.).

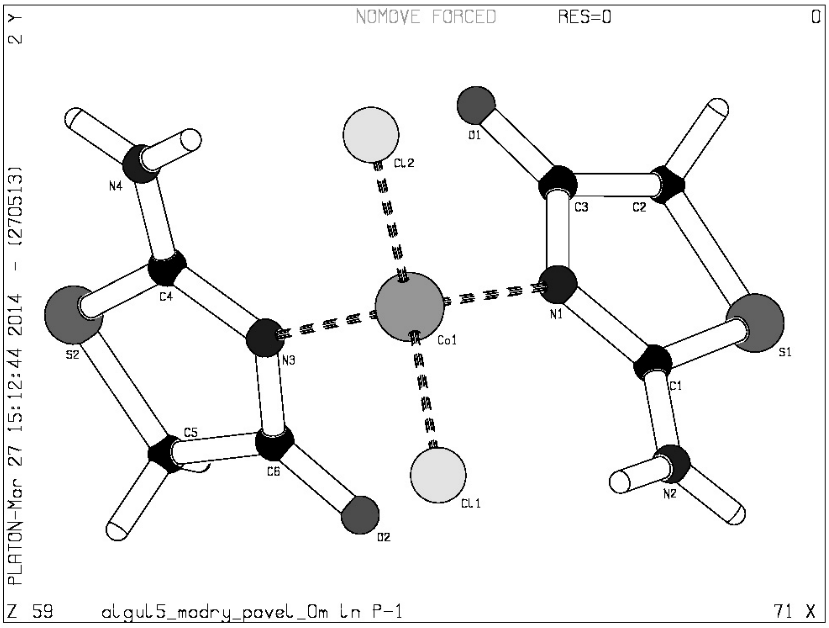

Figure. X-ray analysis of the complex of 2-amino-4-oxothiazole with cobalt (II) chloride

Moreover according to the computer bioprognostication data the complex obtained potentially possesses pharmacological activity such as antiparasitic, antiasthmatic, antiallergic, psychotropic, antiepileptic, and no doubt can be widely used in medical practice.

As a result of the study of protonation reaction of 2-amino-4-oxothiazole by mineral acids of different strength of acidity, it was found that the basicity of the nitrogen atom of the ring is much higher than basicity of the free amino group. X-ray diffraction proved the possibility of chelation of 2-amino-4-oxothiazole with cobalt (II) chloride, and the structure of the complex obtained was established indicating the higher basicity of the cyclic nitrogen atom of 2-amino-4-oxothiazole.

Thus the results obtained show a high ambidentity of 2-amino-4-phenylthiazole and 2-amino-4-oxothiazole caused by the high degree of delocalization of both the lone pair of electrons of the amino group and the one of the ring nitrogen atom which creates great opportunities for chemical modification of such aminoheterocycles with participation of the free amino group and the ring nitrogen atom.

References

1 *Ivanov E.I., Grischuk L.V., Vysotskaya V.V., Stepanov D.E.* Synthesis and antimicrobial activity of derivatives of benzothiazole, thiazolo- and furazanoazepinone // Chem.-Pharm. Journal. — 1993. — No. 7 (27). — P. 37–39.

2 *Georgiev T.R., Davarski K., Shirev F.* About the possibility of the use of 2-aminothiazole as sulfuric vulcanization accelerators // Annual Journal of Chemical Technol. Institute of Burgas. — 1983. — Vol. 18, No. 2. — P. 55–65.

3 *Mishra V.K., Bahel S.C.* The synthesis of thiazole derivatives as potential fungicides // J. Indian Chem. Soc. Pharmacol. — 1984. — Vol. 61, No. 10. — P. 916–918.

4 *Enderfild R.* Heterocyclic Compounds. — Leningrad: Chemistry, 1955. — 539 p.

5 *Gilchrist T.* Chemistry of Heterocyclic Compounds. — Moscow: Mir, 1996. — 464 p.

Л.К.Сәлкеева, Е.В.Минаева, Е.К.Тайшибекова, А.А.Жортарова,
Г.Т.Хасенова, Р.М.Жакупов, Л.М.Сугралина, А.К.Сәлкеева

Минералды қышқылдармен протондау арқылы 2-амино-4-фенилтиазолдың және 2-амино-4-оксотиазолдың негізділік деңгейін зерттеу

Бос амин тобының азот атомы және тиазол сақинасының азот атомының негізділігін зерттеу мақсатымен аминотиазолдардың күші әр түрлі минералды қышқылдармен протондануы зерттелді. Алынған мәліметтер амин тобының бөлініспеген электрон жұбының және тиазол сақинасындағы азот атомының делокализациялану деңгейінің жоғарылығымен байланысқан, 2-амино-4-фенилтиазолдың және 2-амино-4-оксотиазолдың жоғары амбиденттігін көрсетті. Бұл осындай гетероциклдердің бос амин тобының және сақинадағы азот атомының қатысуымен химиялық түрленулерін жүргізуге кең мүмкіндіктер береді. Сонымен қатар циклдегі азот атомының жоғары негізділігімен байланысты 2-амино-4-оксотиазолдың кобальт (II) хлоридімен комплекс түзу қабілеті зерттелді.

Л.К.Салькеева, Е.В.Минаева, Е.К.Тайшибекова, А.А.Жортарова,
Г.Т.Хасенова, Р.М.Жакупов, Л.М.Сугралина, А.К.Салькеева

Исследование степени основности 2-амино 4-фенилтиазола и 2-амино-4-оксотиазола путем протонирования минеральными кислотами

Изучено протонирование аминотиазолов минеральными кислотами различной силы с целью исследования основности атомов азота свободной аминогруппы и азота тиазольного цикла. Полученные результаты показали высокую амбидентность 2-амино-4-фенилтиазола и 2-амино-4-оксотиазола, связанную с высокой степенью делокализации неподеленной пары электронов как аминогруппы, так и атома азота тиазольного кольца, что создает широкие возможности химической модификации подобных аминогетероциклов с участием свободной аминогруппы и атома азота кольца. Также была изучена комплексообразующая способность 2-амино-4-оксотиазола с хлоридом кобальта (II), обусловленная высокой степенью основности циклического атома азота.

UDC 541.64 + 678.744

A.N.Klivenko[1], G.S.Tatykhanova[2, 3], Nurxat Nuraje[4], S.E.Kudaibergenov[2, 3]

[1]*Al-Farabi Kazakh National University, Almaty;*
[2]*K.I.Satpayev Kazakh National Research Technical University, Almaty;*
[3]*Institute of Polymer Materials and Technology, Almaty;*
[4]*Department of Chemical Engineering, Texas Tech University, Lubbok, USA*
(E-mail: skudai@mail.ru)

Hydrogenation of *p*-nitrophenol by gold nanoparticles immobilized within macroporous amphoteric cryogel based on N,N-dimethylaminoethylmethacrylate and methacrylic acid

Macroporous amphoteric cryogel based on N,N-dimethylaminoethylmethacrylate and methacrylic acid (DMAEM-MAA) was used for immobilization of gold nanoparticles (AuNPs). The structure of AuNPs immobilized within macroporous amphoteric cryogel represents the triangular, hexagonal, spherical and rod-like species the sizes of which are varied from 3 to 10 μm. Amphoteric cryogel with immobilized AuNPs was tested as flow-through catalytic reactor in reduction of 4-nitrophenol by $NaBH_4$.

Key words: macroporous amphoteric cryogels, gold nanoparticles, catalytic activity, flow-through reactor.

Introduction

Information on stabilization of AuNPs by amphoteric polyelectrolytes is very limited. A new regular polyampholyte, namely poly-(N,N-diallyl-N,N-dimethylammonium-alt-N-octyl-maleamic carboxylate) is proved to be an efficient reducing and stabilizing agent for the formation of gold colloids [1]. Water-soluble and durable Au nanoclusters, smaller than 4 nm with a narrow size distribution, were supported on a pH- and solvent-responsive water-soluble polyampholyte (SPES) [2]. The phase separation and sensitivity of the SPES-stabilizing Au nanoclusters permitted a facile separation of the clusters from the reaction mixture without any negative aggregation. Diblock polyampholytes poly(methacrylic acid)-block-poly(N,N-dimethylaminoethyl methacrylate), having different molecular weight and block ratio were used for stabilization of AuNPs [3]. Supporting of noble and transition metal ions in bulk of amphoteric nano-, micro-, macrogels followed by reduction to zero-valent state will open new perspectives for development of effective catalytic systems for decomposition, isomerization, hydrogenation, and oxidation of various organic substrates [4–6]. In this context design of monolithic support with microporous structure that can provide both nanoparticle loading and liquid flux is challenging task. A considerable effort of researchers is devoted to construct the catalytic system that is highly active, selective, stable, easy to handle, reusable and simple to separate the product from the reaction medium [7]. Literature survey reveals that the most studied superporous cryogels for immobilization of metal nanoparticles exhibit anionic or cationic character. Superporous cryogels of poly(acrylic acid) [8], poly(4-vinylpyridine) [9] and poly(2-acrylamido-2-methyl-1-propansulfonic acid) [10] and their templated metal nanoparticle composites were used in hydrogen generation from the hydrolysis of $NaBH_4$ and hydrogenation of 4-nitrophenol. The idea of application of amphoteric macroporous cryogels with immobilized nanoparticles of metals as flowing reactors in catalysis was outlined for the first time in our previous publications [4–6] and mentioned only in passing for chitosan-based cryogels [11].

In the present communication we report for the first time the catalytic activity of AuNPs immobilized within cryogel matrix in reduction of 4-nitrophenol.

Experimental section

Materials and Methods. Monomers, catalyst and initiator — methacrylic Acid (MAA, 99 % purity), N,N-dimethylaminoethylmethacrylate (DMAEM, 99 % purity), N,N,N',N'-tetramethylethylenediamine (TMED, 99 % purity), ammonium persulfate (APS, 99 % purity), and crosslinking agent N,N'-methylenbisacrylamide (MBAA, 99 % purity) — were purchased from Sigma-Aldrich Chemical Co., Milwaukee, WI, USA and used without further purification. Standard aqueous solution of tetrachlorauric acid $HAuCl_4$ with concentration 100 mg·L^{-1}, *p*-nitrophenol (*p*-NPh) and sodium boronhydride ($NaBH_4$) were purchased from Sigma-Aldrich. Concentration of gold in supernatant was determined by ion-coupled plasma atomic emission spectroscopy ICP-AES «Optima 5100DV» (Perkin Elmer, USA). Scanning electron microscopy (SEM) images were recorded on a JEOL JSM–6490LA (Japan) and on a high resolution SEM **(**Zeiss Merlin High-resolution SEM).

Synthesis of Amphoteric Cryogels. Mixture of MAA (343 mg or 4 mmol), DMAEM (626 mg or 4 mmol), MBAA (31 mg or 0.2 mmol) corresponding to molar ratio of monomers MAA:DMAEM = = 50:50 mol.%/mol.% was dissolved in 9 mL of deionized water, bubbled by nitrogen during 10 min and degassed under vacuum for about 5 min to eliminate the dissolved oxygen. After addition of 10 μL of TMED the solution was cooled in an ice bath for 5 min. Then 0.1 mL of aqueous solution of APS (10 wt.%) preliminary cooled in an ice bath for 5 min was added and the reaction mixture was stirred for 5 min. The total volume of reaction mixture was divided into 10 parts and each part containing 1 mL of reaction mixture was placed into the 10 glass cylinder with diameter 5 mm with closed outlet at the bottom. The solution in glass cylinder was frozen at minus 12 °C followed by cryopolymerization on cryothermostate Lauda Proline RP 845 (Germany) during 48 h. After completion of the reaction the sample was thawed at room temperature. The prepared cryogel sample was washed out thoroughly by distilled water every 2–3 hours during several days then successively washed out by 25, 50, 75 and 96 % ethanol to dehydrate then dried in air and finally in vacuum oven to constant mass at room temperature. Thus amphoteric cryogel with initial molar ratio of [MAA]:[DMAEM] = 50:50 mol.%/mol.% crosslinked by 5 mol.% of MBAA was synthesized (Fig. 1).

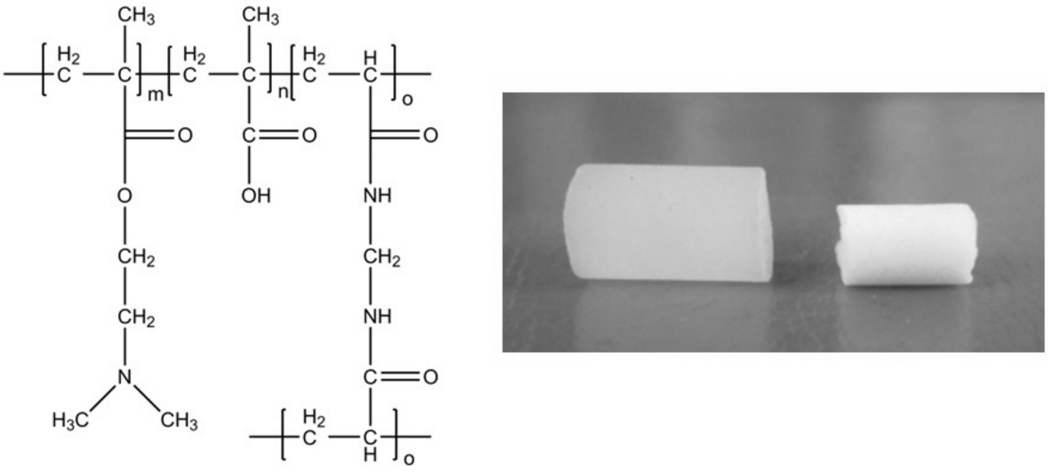

Figure 1. Structural units of amphoteric cryogels derived from MAA and DMAEM (left), dry and swollen in water cryogel samples (right)

Immobilization of AuNPs within the pores of DMAEM-MAA cryogel. 9.5 mL of deionized water was added to 0.5 mL $HAuCl_4$ with concentration 100 mg·L^{-1}. 0.5 g dry gel was immersed to 10 mL of prepared solution and boiled. After 30 min boiling the colorless DMAEM-MAA cryogel turned into raspberry-red color that is specific for AuNPs due to surface plasmon resonance effect. Further the DMAEM-MAA cryogel with immobilized AuNPs is abbreviated as DMAEM-MAA/AuNPs.

Evaluation of the catalytic activity of DMAEM-MAA/AuNPs. 10 mL aqueous solution composed of 0.5 mL $1{\cdot}10^{-3}$ mol·L^{-1} *p*-NPh, 0.5 mL $1{\cdot}10^{-2}$ mol·L^{-1} $NaBH_4$ and 9 mL of deionized water was pumped through the flow-type reactor containing AuNPs with the help of peristaltic pump (the flowing rate is 1.5 mL·min^{-1}). The concentration of *p*-NPh and *p*-APh was determined spectrophotometrically at 400 and 300 nm respectively.

Results and discussion

Morphology of DMAEM-MAA cryogel and AuNPs immobilized macroporous cryogel. According to SEM images the average pore size of DMAEM-MAA sample is varied from 40 to 80 μm (Fig. 2a). The structure of AuNPs immobilized within macroporous amphoteric cryogel represents the myriads of gold nanoparticles distributed in both surface and inner parts of macropores (Fig. 2b). Most of them are triangulars although the hexagonal, spherical and rod-like species are observed (Fig. 2c). The bigger sizes of AuNPs triangles immobilized within DMAEM-MAA cryogels are varied from 3 to 10 μm.

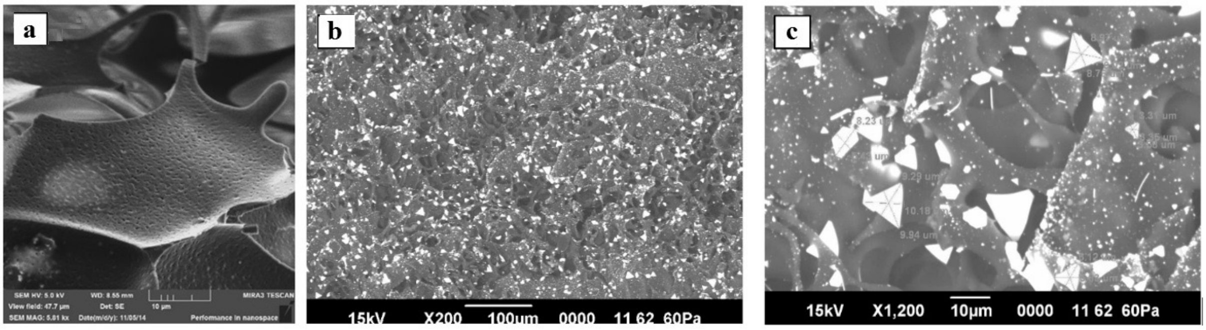

Figure 2. Morphology of pristine (*a*) and AuNPs immobilized macroporous amphoteric cryogel (*b*, *c*)

Catalytic activity of AuNPs immobilized within cryogel pores in hydrogenation of p-NPh. The reduction of *p*-NPh to *p*-APh by $NaBH_4$ (or hydrogen) as model reaction is easily monitored by measurement of the absorption spectra of substrate and reaction product at 400 and 300 nm respectively [12]. In our case the cryogel specimen containing AuNPs served as continuous-flow tank reactor for hydrogenation of *p*-NPh to *p*-APh. The flow-through catalytic reactor represents a glass tube with inner diameter 6–7 mm and height 100 mm which is filled by dry cryogel pieces with diameter 5 mm and height 10 mm. The bottom part of the glass tube is closed by Shott filter ended by valve. At first 10 or 15 mL of deionized water is passed through the cryogel sample. Due to quick swelling of cryogel the tight sealing between the inner wall of the glass tube and swollen sample takes place. Such simple construction allows the mixture of substrate and reducing agent to flow through the cryogel pores and to create enough contacts between the catalyst and reaction mixture. Passing of the mixture of *p*-NPh and $NaBH_4$ through amphoteric cryogel containing AuNPs immediately produces *p*-APh (Fig. 3a, b). The 95 % conversion is reached during 4 min after 5 times repeated passing of 10 mL mixture of *p*-NPh and $NaBH_4$ through the catalytic reactor (Fig. 3a). The same conversion degree is reached during 13 min after the successive fluxing of 50 mL mixture of *p*-NPh and $NaBH_4$ (Fig. 3b). The DMAEM-MAA/AuNPs preserved the high catalytic activity even after passing of 100 mL of *p*-NPh and $NaBH_4$ mixture. In our mind 100 % conversion of *p*-NPh is not reachable due to capturing of some amounts of substrate in deadly volume of cryogel. It should be noted that neither the mixture of *p*-NPh and $NaBH_4$ itself, nor the mixture of *p*-NPh and $NaBH_4$ fluxed through the DMAEM-MAA cryogel does not produce *p*-APh in absence of immobilized AuNPs.

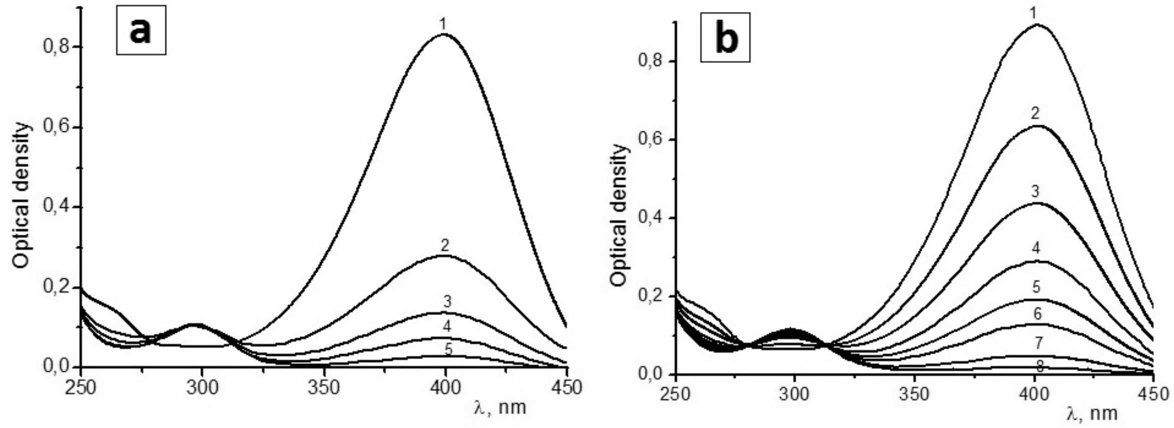

t, min: 0 (curve 1); 1 min (curve 2), 2 (curve 3), 3 (curve 4), 4 (curve 5), 5 (curve 6), 8 (curve 7), 11 (curve 8)

Figure 3. The time dependent absorbance spectra of *p*-NPh and *p*-APh during the 1st (*a*) and 5th (*b*) process cyclicity

The reduction rate constant of *p*-NPh has the pseudo-first-order and depends on the concentartion of nitrophenolate-anion rather than concentration of $NaBH_4$ due to its excess [12]. The kinetics of *p*-NPh reduction is expressed by equation:

$$\ln\left(\frac{C_t}{C_0}\right)=\ln\left(\frac{D_t}{D_0}\right)=-k\times t, \qquad (1)$$

where C_t and C_0 are concentrations of nitrophenolate-anions at definite time t and $t = 0$.

The logarithmic dependence of the equation (1) has linear character and shows that the first cycle is completed during 4 min with 95 % conversion, the second cycle — after 6 min, while the 95 % conversion of *p*-NPh to *p*-APh during 10 cycles requires 11 min (Fig. 4). The apparent rate constants (k_{app}) found from the slopes of kinetic curves of Figure 5 during the 1st, 2nd, 5th, and 10th reduction cycles of *p*-NPh are equal to $13.5{\cdot}10^{-3}$ s^{-1}; $8{\cdot}10^{-3}$ s^{-1}; $6.3{\cdot}10^{-3}$ s^{-1} $4.6{\cdot}10^{-3}$ s^{-1}. Thus, the k_{app} value decreases with increasing of process cyclicity. Cryogel catalyst sustained over 10 cycles without loss of activity.

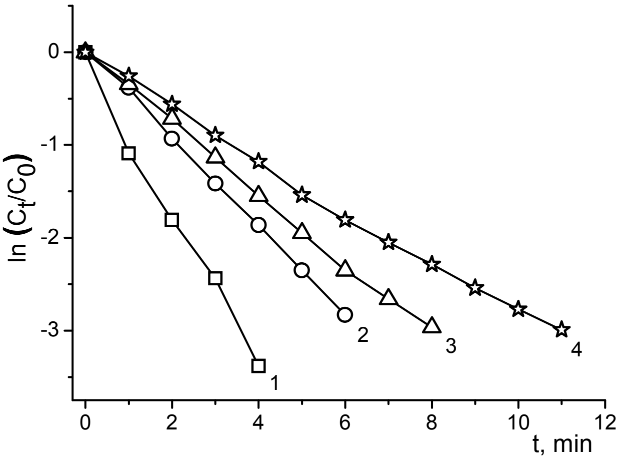

The 1st cycle (1), the 2nd cycle (2), the 5th cycle (3), the 10th cycle (4)

Figure 4. The reaction kinetic curves of ln(C_t/C_0) *versus* time as a function of process cyclicity

The kinetic rate constant of DMAEM-MAA/AuNPs for the reduction of *p*-NPh to *p*-APh was compared with literature data (see Table).

Table

The rate constants of the reduction of *p*-NPh to *p*-APh catalyzed by metal nanoparticles supported on various polymers

Type of catalyst	Rate constant, $\times10^{-2}$ s^{-1}	Ref.
PEI/AuNPs	4.6	[13]
PEI-C_{12}/AuNPs	5.2	[13]
HPEI-IBAM/AuNPs	≈ 2–3	[12]
Chitosan/AuNPs	0.24	[14]
Resin/AuNPs	2.5	[15]
Chitosan/FeNPs	0.24	[16]
PEC/AuNPs	0.5	[17]
PEC/PdNPs	0.394	
PEC/AgNPs	0.142	
PEC/AuNPs$_{50}$/AgNPs$_{50}$	0.678	
PEC/AuNPs$_{50}$/AgNPs$_{25}$/PdNPs$_{25}$	0.983	
PAMAM dendrimers/AuNPs	2.51	[18]
PAMAM dendrimers/AgNPs	0.71	
PAMAM dendrimers/CuNPs	2.43	
PD1–2/AuNPs	≈ 2.8	[19]
DMAEM-MAA/AuNPs	1.35	present work

Comparative analysis shows that DMAEM-MAA/AuNPs catalyst occupies intermediate position among the catalytic systems used for reduction of *p*-NPh to *p*-APh. It is commonly accepted that the reduction process involves chemisorption of 4-nitropenolate anions onto catalytic surface of AuNPs, interfacial electron transfer to reduce the 4-nitropenolate anions and desorption of 4-aminophenol from the surface. In our mind the *p*-NPh molecules are stabilized within the inner surface of DMAEM-MAA/AuNPs via hydrogen bonds between OH groups of substrate and COOH (or —$N(CH_3)_2$) groups of cryogel. The immobilized AuNPs in cryogel pores generates hydrogen atoms from the $NaBH_4$ that in its turn hydrogenate the nitro groups. Detachment of *p*-APh molecules from the surface of DMAEM-MAA/AuNPs takes place due to electrostatic repulsion, e.g. the negatively charged surface of AuNPs repels the same charged 4-nitrophenolate anions from the reaction mixture. The detailed mechanism of the reduction of *p*-NPh on the surface of AuNPs is given by authors. The lifetime of the catalyst is usually expressed through the turnover number (TON) that is the number of moles of substrate that a mole of the catalyst can convert before inactivation [20].

The stability of DMAEM-MAA/AuNPs catalyst, the so-called TON that is defined as

$$\mathrm{TON} = \frac{[p-\mathrm{NPh}]}{[\mathrm{AuNPs}]} \times \mathrm{OCT} \tag{2}$$

(where [*p*-NPh] and [AuNPs] are the molar concentrations of substrate and catalyst, OCT is the overall catalytic time) and the turnover frequency (TOF) calculated (for the first cycle) according to equation

$$\mathrm{TOF} = \frac{[p-NPh]\cdot[conversion]}{[AuNPs]\cdot t} \tag{3}$$

was equal to TON = 38,17 and TOF = 21,56 h^{-1} respectively.

Conclusions

Amphoteric cryogels of DMAEM-MAA were synthesized by cryopolymerization technique. SEM images of cryogels show sponge-like porous structure composed of interconnected channels. The structure AuNPs immobilized within the porous structure of cryogel is represented by triangular, hexagonal, spherical and rod-like species which play the role of catalytic centres in hydrogenation of substrates. The potential application of amphoteric cryogel samples with immobilized AuNPs as effective flow-through units for continuous hydrogenation of *p*-NPh is demonstrated.

Financial support from the Ministry of Education and Science of the Republic of Kazakhstan (1004/GF4 2015–2017) is greatly acknowledged.

References

1 *Note C., Koetz J., Wattebled L., Laschewsky A.* Effect of a new hydrophobically modified polyampholyte on the formation of inverse microemulsions and the preparation of gold nanoparticles // J. Colloid and Interface Sci. — 2007. — Vol. 308. — P. 162–169.

2 *Li S., Wu Y., Wang J., Zhang Q., Kou Y., Zhang S.* Double-responsive polyampholyte as a nanoparticle stabilizer: Application to reversible dispersion of gold nanoparticles // J. Mater. Chem. — 2010. — Vol. 20. — P. 4379–4384.

3 *Mahltig B., Cheval N., Gohy J.F., Fahmi A.* Preparation of gold nanoparticles under presence of the diblock polyampholyte PMAA-b-PDMAEMA // J. Polym. Res. — 2010. — Vol. 17. — P. 579–588.

4 *Kudaibergenov S.E., Nuraje N., Khutoryanskiy V.V.* Amphoteric nano-, micro- and macrogels, membranes, and thin films // Soft Matter. — 2012. — Vol. 8. — P. 9302–9321.

5 *Tatykhanova G., Sadakbayeva Zh., Berillo D., Galaev I., Abdullin Kh., Adilov Zh., Kudaibergenov S.* Metal Complexes of Amphoteric Cryogels based on Allylamine and Methacrylic Acid // Macromolecular Symposia. — 2012. — Vol. 317–318. — P. 7–17.

6 *Kudaibergenov S., Adilov Zh., Berillo D., Tatykhanova G., Sadakbaeva Zh., Abdullin Kh., Galaev I.* Novel Macroporous Amphoteric Gels: Preparation and Characterization // eXPRESS Polymer Letters. — 2012. — Vol. 6, No 5. — P. 346–353.

7 *Koga H., Kitaoka T.* One-step synthesis of gold nanocatalysts on a microstructured paper matrix for the reduction of 4-nitrophenol // Chem. Eng. J. — 2011. — Vol. 68. — P. 420–425.

8 *Sahiner N., Seven F.* The Use Of Superporous P(Aac(Acrylic Acid)) Cryogels As Support For Co and Ni Nanoparticle Preparation And As Reactor In H-2 Production From Sodium Borohydride Hydrolysis // Energy. — 2014. — Vol. 71. — P. 170–179.

9 *Sahiner N., Yildiz S.* Preparation of Superporous Poly(4-Vinyl Pyridine) Cryogel And Their Templated Metal Nanoparticle Composites for H-2 Production Via Hydrolysis Reactions // Fuel Process. Technol. — 2014. — Vol. 126. — P. 324–331.

10 *Sahiner N., Seven F.* Energy And Environmental Usage of Super Porous Poly(2-Acrylamido-2-Methyl-1-Propan Sulfonic Acid) Cryogel Support // RSC Advances. — 2014. — Vol. 4. — P. 23886–23897.

11 *Berillo D., Mattiasson B., Kirsebom H.* Cryogelation of Chitosan Using Noble-Metal Ions: In Situ Formation of Nanoparticles // Biomacromolecules. — 2014. — Vol. 15. — P. 2246–2255.

12 *Liu X.-Y., Cheng F., Liu Y., Liu H.J., Chen Y.* Preparation and characterization of novel ther-moresponsive gold nanoparticles and their responsive catalysis properties // J. Mater. Chem. — 2010. — Vol. 20. — P. 360–368.

13 *Veerakumar P., Velayudham M., Lu K.-L., Rajagopal S.* Polyelectrolyte encapsulated gold nanoparticles as efficient active catalyst for reduction of nitro compounds by kinetic method // Appl. Catal., A. — 2012. — Vol. 439. — P. 197–205.

14 *Seoudi R., Said D.A.* Studies on the Effect of the Capping Materials on the Spherical Gold Nanoparticles Catalytic Activity // World J. Nanoscience Eng. — 2011. — Vol. 1. — P. 51–61.

15 *Shah D., Kaur H.* Resin-Trapped Gold Nanoparticles: An Efficient Catalyst for Reduction of Nitro Compounds and Suzuki-Miyaura Coupling // J. Mol. Catal. A: Chem. — 2014. — Vol. 381. — P. 70–76.

16 *Lu H., Xueliang Q.X., Wang W., Tan F., Xiao Z., Chen J.* Chitosan stabilised nanozero-valent iron for the catalytic reduction of p-nitrophenol // Micro & Nano Letters. — 2014. — Vol. 9, Iss. 7. — P. 446–450.

17 *Islam M.Sh., Choi W.S., Lee H.-J.* Nonstoichiometric polyelectrolyte complexes: Smart nanomaterials for alloy and multimetallic catalyst // International Journal of Materials, Mechanics and Manufacturing. — 2014. — Vol. 2, Iss. 1. — P. 1–4.

18 *Nemanashi M., Meijboom R.* Synthesis and characterization of Cu, Ag and Au dendrimer-encapsulatednanoparticles and their application in the reduction of 4-nitrophenolto 4-aminophenol // J. Colloid Interface Sci. — 2013. — Vol. 389. — P. 260–267.

19 *Liu Y., Fan Y., Yuan Y., Chen Y., Cheng F., Shi-Chun J.* Amphiphilic hyperbranched copolymers bearing a hyperbranched core and a dendritic shell as novel stabilizers rendering gold nanoparticles with an unprecedentedly long lifetime in the catalytic reduction of 4-nitrophenol // J. Mater. Chem. — 2012. — Vol. 22. — P. 21173–21182.

20 *Hagen J.* Industrial Catalysis — A Practical Approach, 2nd ed. — Wiley-VCH: Weinheim, 2006.

А.Н.Кливенко, Г.С.Татыханова, Нұршат Нұраджи, С.Е.Құдайбергенов

Алтынның нанобөлшектері иммобилденген N,N-диметиламиноэтилметакрилат және метакрил қышқылы негізіндегі макроторлы амфотерлі криогель көлемінде *п*-нитрофенолды гидрлеу

N,N-диметиламиноэтилметакрилат және метакрил қышқылы (МАҚ–ДМАЕМ) негізіндегі макроторлы амфотерлі криогель алтынның нанобөлшектерін иммобилизациялауға қолданылды. Макроторлы амфотерлі криогель көлеміндегі алтынның нанобөлшектері үшбұрышты, алтыбұрышты, сфералық және түтікше тәрізді күйде кездеседі және көлемдері 3 пен 10 мкм аралығында. Алтын нанобөлшектері иммобилизацияланған амфотерлі криогель үлгісін ағымды каталитикалық реактор ретінде 4-нитрофенолды $NaBH_4$ гидрлеу реакциясына сыналды.

А.Н.Кливенко, Г.С.Татыханова, Нуршат Нураджи, С.Е.Кудайбергенов

Гидрирование *п*-нитрофенола наночастицами золота, иммобилизованными в макропоры амфотерного криогеля на основе N,N-диметиламиноэтилметакрилата и метакриловой кислоты

Макропористый амфотерный криогель на основе N,N-диметиламиноэтилметакрилата и метакриловой кислоты (МАА–ДМАЕМ) использован для иммобилизации наночастиц золота. Структура иммобилизованных в макропоры амфотерного криогеля наночастиц золота представляет собой треугольные, шестиугольные, сферические и стержнеподобные частицы, размеры которых варьируются от 3 до 10 мкм. Амфотерный криогель с иммобилизованными наночастицами золота тестирован в качестве проточного каталитического реактора в реакции гидрирования 4-нитрофенола $NaBH_4$.

UDC 543:541.1

Sh.K.Amerkhanova[1], Bohari M. Yamin[2], Azwan Mat Lazim[2], A.S.Uali[1], M.Nurgalieva[1]

[1]Ye.A.Buketov Karaganda State University;
[2]University Kebangsaan Malaysia, Kuala Lumpur, Malaysia
(E-mail: amerkhanova_sh@mail.ru)

Complexing ability of 2,8,14,20-tetrabenzol-sulfo-calix[4]resorcenarene in relation to Cs^+, Pd^{2+}, Ce^{3+}, Eu^{3+} ions in aqueous solution

The stability constants of complexes formed in a result of interaction «host-guest» of water-soluble calix[4]resorcinarene with metal ions (Cs^+, Pd^{2+}, Ce^{3+}, Eu^{3+}) in ratio 1:1 and thermodynamic parameters of their formation were calculated. The dependence of the Gibbs energy change of formation of complexes on the atomic number of the element was constructed. It is shown that the value of stability constants depends on the degree of deprotonation of the rim of the calix[4]resorcinarene. It is found that the guest-cations — Ce^{3+} and Eu^{3+} are characterized by high charge density, whereby they form the complexes which are relatively strong, and more hydrated.

Key words: water-soluble calix[4]resorcinarene, complex formation, pH-metric study, stability of complexes, thermodynamics.

In recent years a sharp increase in the number of publications devoted to the design of multifunctional ligands — hetero-ditopic receptors prone to the simultaneous binding of cations and anions [1–4] is observed, this interest is due to the possibility of their usage as sensors for monitoring biological systems and the environment, etc. The ability to bind cations by calixarenes is well known. The anions, anions that act, binding of metal ions, are included in the structure of hetero-ditopic receptors which are based on calixarenes. Despite the fact that the anion play a key role in chemistry and biology, receptors negatively charged particles are poorly studied, and the design of such compounds is a current trend in modern organic chemistry.

Calix[n]resorcinarenes form complexes with organic molecules and metal cations, including 4f- and 5f-elements, and are used in the creation of catalysts for chemical reactions, extractants, chemical sensors, ion-selective electrodes, the active compounds.

In the study of the complexation oxygen containing macrocyclic compounds with metal ions has been found that the formation of stable complexes depends, firstly, on the physical-chemical characteristics of the metal (size and charge of metal ion), and secondly, on the structure and size of the macrocycle (size of cavity of macrocycle, coplanarity of oxygen atoms, their symmetrical arrangement). All the above conditions determine the effectiveness of the interaction between the metal ion and macroheterocycles.

To understand the laws of these processes it is necessary to consider the thermodynamic aspects of the chelation process of «host-guest» in solution.

Calix[n]arenas and Calix[n]resorcinarenes are the most widely used class of artificial receptors, however, the thermodynamics of complexes is not well understood. 2,8,14,20-tetrabenzol-sulfo-calix[4]resorcinarene soluble in water fairly well and dissociates stepwise to forms anion $[H_{4-n}L]^{n-}$ in an aqueous medium. The effectiveness of the host-guest complex formation increases as a result of the ionized groups on the rim of calix[n]resorcinarene [5].

The aim of this study is to evaluate the thermodynamic stability of the complexes formed by the interaction of macrocyclic receptor with cesium (+), palladium (2+), cerium (3+), Eu (3+) ions in an aqueous solution.

Experimental

Tetrabenzol-2,8,14,20-sulfo-calix[4]resorcinarene (hereinafter referred to as L) with gross formula: $C_{52}H_{40}O_{20}S_4$ (structural formula shown in Figure 1) was used as ligand. 2,8,14,20-tetrabenzol-sulfo-calix[4]-resorcinarene was synthesized by research group of Professor Bohari Yamin in the University Kebangsaan in Malaysia.

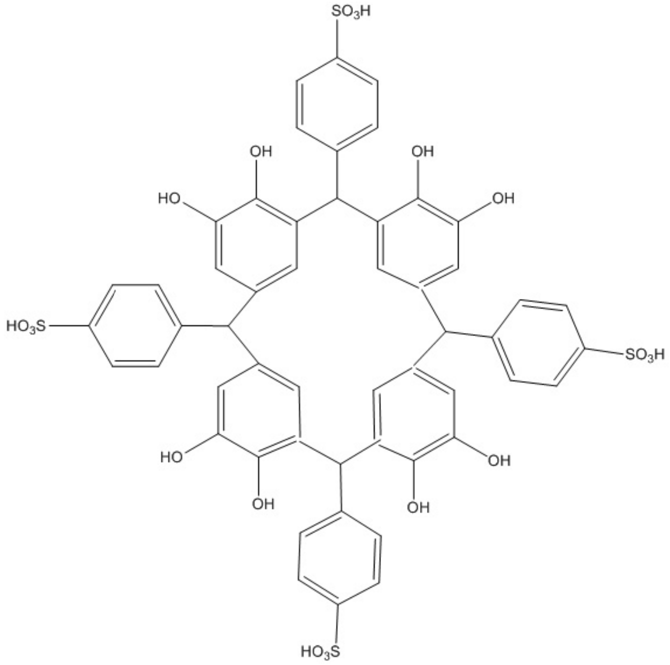

Figure 1. Structure of 2,8,14,20-tetrabenzol-sulfo-calix[4]resorcinarene

Relative molecular mass of this compound is 1109.09 g·mole$^{–1}$, the results of elemental analysis, % are C (56.31), H (3.27), G (28.85), S (11.56).

Solutions containing ions of Cs^+, Pd^{2+}, Ce^{3+}, Eu^{3+} with a concentration of $10^{–4}$ mole·L^{-1} were prepared by dissolving the corresponding salts accurately weighed CsI, $PdCl_2$, $Ce_2(SO_4)_3$, $Eu_2(CO_3)_3$ in distilled water.

The ionic strength was created with the help of sodium nitrite (0; 0.1; 0.25; 0.5; 0.75; 1). Determination of the acidity constant of the ligand was carried out according to standard procedures by conductometric method [6].

pH titration was performed on a pH meter 827 Lab (Metrohm) with the help of 6.0256.600 combined electrode. The temperature was 298, 308, 318 K.The pH titration was carried out by the method of B'errum [7]. The ratio of M:L is 1:1 (on concentration and volume).

Approximation of Ulikh was used to calculate the enthalpy, Gibbs-Helmholtz equation — to calculate the entropy and the Gibbs — Gibbs free energy.

Results and discussion

The constant value of acidity equal to $5.62 \cdot 10^{–7}$ was calculated according to the conductivity depending on the concentration of ligand solutions. According to the classification of Lewis, it can be attributed to the group of bases which form characterized by higher strength complexes.

It is known that the calix[4]resorcinarene are a group of universal macrocyclic compounds capable to form complexes by type guest–host with neutral molecules and ions, and supramolecular aggregates, a specific supramolecular structure having catalytic activity. Chemical modification of these macrocycles yields new complex compounds with Cs^+, Pd^{2+}, Ce^{3+}, Eu^{3+} ions. If we judge on the ability of complexing Cs^+, Pd^{2+}, Ce^{3+}, Eu^{3+} ions, it should be noted that the cesium (1+) and palladium (2+) ions have a low propensity to form complexes. And cerium (3+) and europium (3+) ions belonging to the group of lanthanides react with molecules of the macrocyclic ligands and the bond preferably ionic character.

It is known [3] that the set of complexes between ionized calix[4]resorcinarenes and cations can be divided into two types: cell-like and inclusive, and as a result of polycenter electrostatic interaction between the positively charged cations and negatively charged groups allegedly calix[4]resorcinarene complex formation should occur without any noticeable dive the metal ion into the cavity of calix[4]resorcinarenes.

The ionization calixarene rim occurs as a result of deprotonation of H_4L, leading to an increase of complexing ability with metal ions. Table 1 shows the stability constants of complexes (lg*K*), which are the equilibrium constants between guests-metal ions and anions $[H_{4-n}L]^{n-}$, where *n* = 1–4 in aqueous solution:

$$Cat^{m+}+[H_{4-n}L]^{n-}\leftrightarrow [CatH_{4-n}L]^{n-m} \quad (1)$$

Also Table 1 shows the characteristics of the ions of metal-complexing agents.

Table 1

Characteristics of ions of metal-complexing agents, lg*K* of complexes formed by the interaction with ligand

Complexing ion	Ionic radius (*r*), nm	Ion charge	Electronic configuration of the atom	lgK (298 K, I=0.1)
Cs^+	**0.181 (CN=6)** 0.202 (CN=12)	1	$4s^23d^{10}4p^65s^24d^{10}5p^66s^1$	0.66
Pd^{2+}	0.078 (CN 4) **0.100 (CN 6)**	2	$4s^2p^6d^{10}5s^0$	0.70
Eu^{3+}	**0.109 (CN 6)**	3	$4s^2p^6d^{10}f^75s^2p^66s^2$	0.84
Ce^{3+}	**0.115 (CN 6)** 0.134 (CN 9)	3	$4s^2p^6d^{10}f^15s^2p^6d^16s^2$	1.02

The results in Table 1 show that with the increasing polarizability of complexing ions the strength of formed complexes enhances.

Influence of ionic strength on the stability constants. The following figure 2 shows the stability constants of the complexes formed by the interaction of Cs^+, Pd^{2+}, Ce^{3+}, Eu^{3+} ions with 2,8,14,20-tetrabenzol-sulfo-calix[4]resorcinarene.

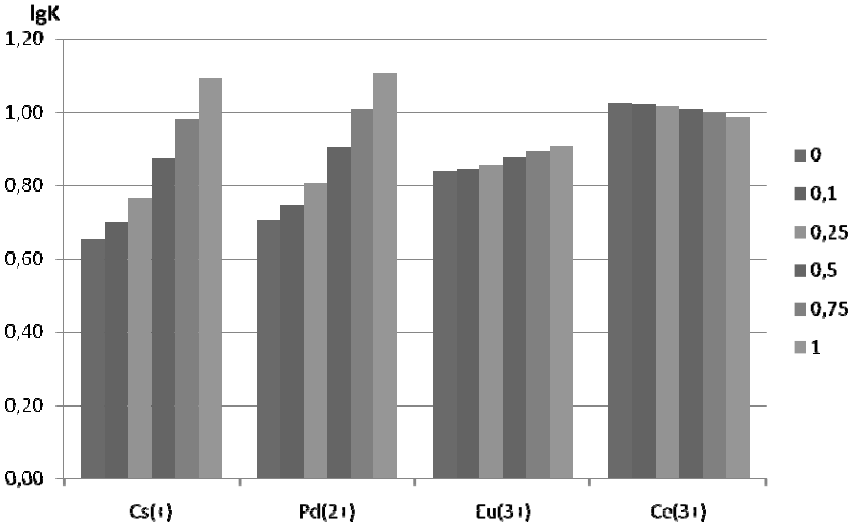

Figure 2. Dependence of the stability constants of complexes 2,8,14,20-tetrabenzol-sulfo-calix[4]resorcinarene with Cs^+, Pd^{2+}, Eu^{3+}, Ce^{3+} ions under the influence of ionic strength

It is known that the effect of forming a bond «metal-ligand» is determined by interaction of metal ions with a solvent and ligand. With increasing charge and decreasing the radius of the ion-metal increases its complexing ability, which can be seen from the data, with the most stable complexes which are formed with ions of cerium (3+) and europium (3+).

The binding energy is determined as well as by the steric and electronic factors. The greater is ligand size, the more probably the occurrence of steric hindrance to the coordination of the ligand, since other ligands presenting in the system (in this case — nitrate ions, water molecules) are also involved in the complex formation. In our case, this pattern is observed for complexes Ce (3+), increasing the concentration of the supporting electrolyte reduces the strength of the formed complexes.

The reverse situation is noted in the case of cesium (+), palladium (2+), europium (3+) ions. This can be attributed to the stabilizing effect of the supporting electrolyte, caused by dehydration of the ligand and metal, as well as the formation of a negatively charged sphere of the outer contour of the complex, separating it from the solvent molecules in the bulk solution.

Moreover, cerium ion is most polarizing from the four-studied ions of metal-complexing agents hence it will be very active to attract ions of the supporting electrolyte compared to the ligand ions and palladium (2+) and cesium (+), Eu (3+) ions are less polarizable, so they increasing number of nitrate ions in the bulk solution will not have such a high impact, wherein for ions of palladium (2+) stability constants are higher at medium ionic strength, and for cesium (+) ions at high ionic strength.

Effect of temperature on the stability constants. Figure 3 shows the constant temperature resistance complexes dependence at constant ionic strength of I = 1.

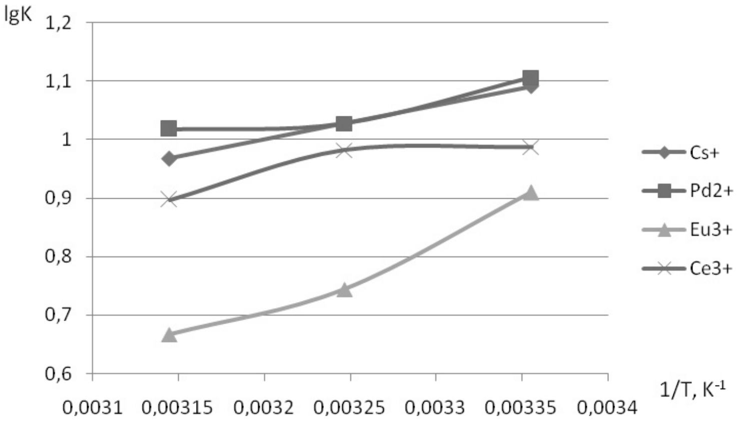

Figure 3. Dependence of the stability constants of complexes 2,8,14,20-tetrabenzol-sulfo-calix[4]resorcinarene with Cs^+, Pd^{2+}, Eu^{3+}, Ce^{3+} ions from temperature

In all cases, the increase in temperature leads to the decrease in the stability of complex compounds. The value of the Gibbs energy of complexation was estimated based on the data on the stability constants. The dependence of the change in Gibbs free energy from the atomic number of element is shown in Figure 4 (T = 298 K, I = 1).

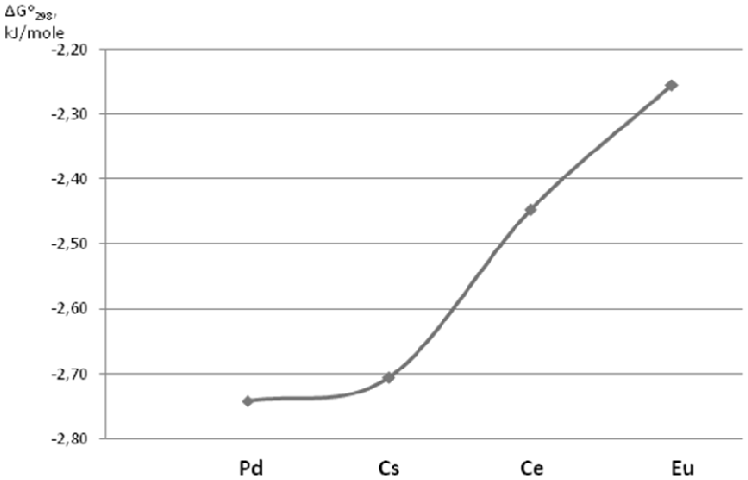

Figure 4. Dependence of Gibbs energy of formation from the atomic number of element

Thermodynamic parameters were calculated on the basis of the temperature dependence of the stability constants (Table 2).

Table 2

Thermodynamic parameters of reactions of Cs^+, Pd^{2+}, Ce^{3+}, Eu^{3+} metal ions complexes formation at 298 K

Thermodynamic parameters	Metal ion	I					
		0	0.1	0.25	0.5	0.75	1
$\Delta_r H_T^o$, kJ·mole^{-1}	Cs^+	10.14	4.16	–4.82	–49.70	–34.74	–19.78
	Pd^{2+}	34.52	27.8	17.73	0.94	–15.84	–32.63
	Ce^{3+}	9.43	9.07	8.54	7.66	6.78	5.90
	Eu^{3+}	–109.36	–120.80	–86.55	–86.44	–93.46	–92.58
$\Delta_r G_T^o$, kJ·mole^{-1}	Cs^+	–1.62	–1.73	–1.89	–2.16	–2.44	–2.71
	Pd^{2+}	–1.74	–1.84	–1.99	–2.24	–2.49	–2.74
	Ce^{3+}	–2.08	–2.10	–2.12	–2.17	–2.21	–2.25
	Eu^{3+}	–2.54	–2.53	–2.51	–2.49	–2.47	–2.45
$\Delta_r S_T^o$, J·mole^{-1}·K^{-1}	Cs^+	146.10	148.30	6.34	7.10	8.06	9.01
	Pd^{2+}	5.97	147.94	6.75	7.53	8.31	9.09
	Ce^{3+}	60.50	148.63	74.03	88.78	103.53	118.28
	Eu^{3+}	8.15	8.08	8.15	8.07	7.97	7.90

Transition from endothermic to exothermic effect with increasing ionic strength indicates metal-ligand bond strength increase; negative values of Gibbs energy change of complex formation also confirm a relatively high resistance to dissociation of the complex in solution. It can be assumed that polycenter electrostatic interactions of cations of cesium and palladium with negatively charged rim require greater desolvation calix[4]resorcenarene (according to equation (1)) than the interaction with cations of cerium and europium.

Conclusion

In general, increasing the concentration of the supporting electrolyte leads to an increase in entropy systems containing ions of Cs^+ and Pd^{2+}, is apparently due to the fact that in these cases the formation of complexes cell-like type since this process is entropically favorable process ($\Delta S>0$). While guests–cations of Ce^{3+} and Eu^{3+} are characterized by high charge density, whereby they form the complexes are relatively strong, and more hydrated.

References

1 *Gutsche C.D.* Calixarene ReVisited / Ed. J.F.Stoddart // Monographs in Supramolecular Chemistry. — Cambridge, U.K.: Royal Society of Chemistry, 1998.

2 *Mandolini L., Ungaro R.* Calixarene in Action. — London: Imperial College Press, 2000.

3 *Lumetta G.J., Rogers R.D., Gopalan A.S.* Calixarenes for Separations. — Washington, DC: American Chemical Society, 2000.

4 *Yu Liu, Dong-Sheng Guo, Heng-Yi Zhang, Yu-Hong Ma, En-Cui Yang.* The Structure and Thermodynamics of Calix[4]arene Complexes with Dipyridines and Phenanthroline in Aqueous Solution Studied by Microcalorimetry and NMR Spectroscopy // J. Phys. Chem. B. — 2006. — Vol. 110. — P. 3428–3434.

5 *Мустафина А.Р., Скрипачева А.Р., Губайдуллин А.Т., Коновалов А.И.* Структурные и термодинамические аспекты комплексообразования каликс[4]резорцинарена с катионами различной структуры в водно-органических растворителях // Журн. структурной химии. — 2005. — Т. 46. — С. 76–83.

6 *Gelb R.I.* Conductometric determination of pKa values. Oxalic and squaric acids // Anal. Chem. — 1971. — No. 43(8). — P. 1110–1113.

7 *Amerkhanova Sh.K., Shlyapov R.M., Uali A.S.* Synthesis and Complex Ability of N-[2-(2-Morpholinoacetyl)hydrazinocarbothioy]benzamide // Russian Journal of General Chemistry. — 2012. — Vol. 82, No. 8. — P. 1815–1818.

Ш.К.Амерханова, Bohari M.Yamin, Azwan Mat Lazim, А.С.Уәли, М.Нұрғалиева

2,8,14,20-Тетрабензол-сульфо-каликс[4]резорцинареннің сулы ерітіндіде Cs^+, Pd^{2+}, Ce^{3+}, Eu^{3+} иондарына қатысты комплекс түзу қабілеті

Суда еритін каликс[4]резорцинареннің металл иондарымен (Cs^+, Pd^{2+}, Ce^{3+}, Eu^{3+}) әрекеттесуі нәтижесінде «ие-қонақ» (1:1 қатынасында) комплекстердің тұрақтылық константалары және түзілу процестерінің термодинамикалық параметрлері есептелді. Комплекстердің түзілуінің Гиббс энергиясы өзгеруінің элементтің реттік нөмірінен тәуелділігі тұрғызылды. Тұрақтылық константасының шамасы каликс[4]резорцинареннің жиегінің депротондану дәрежесіне тәуелді екені көрсетілді. Ce^{3+} и Eu^{3+} қонақ–катиондарының заряд тығыздығы жоғары болғандықтан, олар түзетін комплекстер салыстырмалы тұрақты және гидратталуы жоғарырақ болады.

Ш.К.Амерханова, Bohari M.Yamin, Azwan Mat Lazim, А.С.Уали, М.Нургалиева

Комплексообразующая способность 2,8,14,20-тетрабензол-сульфо-каликс[4]резорцинарена по отношению к ионам Cs^{+}, Pd^{2+}, Ce^{3+}, Eu^{3+} в водном растворе

Были рассчитаны константы устойчивости комплексов и термодинамические параметры процессов комплексообразования «хозяин-гость» (в соотношении 1:1) при взаимодействии водорастворимого каликс[4]резорцинарена с ионами металлов (Cs^{+}, Pd^{2+}, Ce^{3+}, Eu^{3+}). Построена зависимость изменения энергии Гиббса образования комплексов от порядкового номера элемента. Показано, что величина константы устойчивости зависит от степени депротонизации ободка каликс[4]резорцинарена. Установлено, что гости — катионы Ce^{3+} и Eu^{3+} характеризуются высокой плотностью заряда, за счет чего образуемые ими комплексы являются относительно прочными и более гидратированными.

References

1 Gutsche C.D. *Calixarene ReVisited*, Ed. J.F.Stoddart, Monographs in Supramolecular Chemistry, Cambridge, UK: Royal Society of Chemistry, 1998.

2 Mandolini L., Ungaro R. *Calixarene in Action*, London: Imperial College Press, 2000.

3 Lumetta G.J., Rogers R.D., Gopalan A.S. *Calixarenes for Separations*, Washington, DC: American Chemical Society, 2000.

4 Yu Liu, Dong-Sheng Guo, Heng-Yi Zhang, Yu-Hong Ma, En-Cui Yang. *J. Phys. Chem. B.*, 2006, 110, p. 3428–3434.

5 Mustafina A.R., Skripacheva A.R., Gubaydullin A.T., Konovalov A.I. *Journal of Structural Chemistry*, 2005, 46, p. 76–83.

6 Gelb R.I. *Anal. Chem.*, 1971, 43(8), p. 1110–1113.

7 Amerkhanova Sh.K., Shlyapov R.M., Uali A.S. *Russian Journal of General Chemistry*, 2012, 82, 8, p. 1815–1818.

UDC 544.3:544.412.3:549.743.12/13

V.N.Fomin[1, 2], I.E.Rozhkovoy[1, 2], D.B.Gogol[2, 3], D.L.Ponomarev[2]

[1]*Ye.A.Buketov Karaganda State University;*
[2]*Public association «Grazhdane Kazakhstana», Karaganda;*
[3]*Institute of problems of complex development of mineral resources, Karaganda*
(E-mail: vitfomin@mail.ru)

Thermodynamic parameters of reactions of basic copper carbonates formation with participation of organic complexing agents

In the article some of thermodynamic parameters for the processes which are possible in nature during the formation of the malachite and azurite are described. The authors have shown that the formation of basic carbonates from copper sulfide ores is thermodynamically more favorable than that from its oxide minerals. The presence of complexing agents promote the dissolution of oxide forms of copper and involve its ions into secondary mineralogenesis. It is found that the hydroxy acids largely promote the formation of a malachite and azurite than the similar amino acids.

Key words: malachite, azurite, complexing agents, thermodynamic of mineralogenesis.

Natural processes of the minerals formation are characterized by variety and frequently high complexity. In the most general case they can be divided on endogenous and exogenous processes. Among other, process of formation of malachite and azurite from a sulphidic copper ores by oxidation and a carbonatization in the water environment belongs to the exogenous one [1–4]. Natural malachite $Cu_2[CO_3](OH)_2$ is a valuable decorative and ornamental stone, and also important ore of copper, as well as related mineral azurite $Cu_3[CO_3]_2(OH)_2$, especially in a zone of the copper field oxidation. The studying of thermodynamic aspects of the malachite and azurite formation was published in a number of works [5–9] and it is still very interesting in respect to formation from various primary copper minerals.

The various organic complexing agents which contains in soils can participate in the formation processes of basic copper carbonates [10–13]. The occurring in these cases reactions, as a rule, are studied insufficiently from the thermodynamic point of view. A number of different factors influence on these processes; the chemical character of complexing agents and initial carbonates is significant among them. The thermodynamic evaluating the possibility of passing for these reactions give essential contribution in the knowledge of mineral formation processes.

For studying thermodynamics of malachite and azurite formation reactions a number of thermodynamic calculations of changes of enthalpy, entropy and Gibbs energy of reaction at 273–373 K with participation of various initial substances has been carried out. Besides various copper minerals, they included carbonate agents in the form of the carbonate ion, the dissolved and gaseous carbon dioxide; an oxidizer — oxygen in the dissolved and gaseous form; and also water and hydroxide ions. As a source of copper ions the sulphidic and oxidized minerals, such as covellite CuS and tenorite CuO, were investigated.

At the first stage of calculations the model reactions equations have been presented in the ionic form for elimination of influence of the secondary factors connected with antiions. So, for reactions:

$$2Cu^{2+} + CO_2 + 4OH^- = Cu_2[CO_3](OH)_2 + H_2O$$

$$2Cu^{2+} + CO_3^{2-} + 2OH^- = Cu_2[CO_3](OH)_2$$

absolute value of enthalpy change of reaction decreased at transition from a gaseous form of carbon dioxide to dissolved and further to a carbonate ion while value of entropy change increased. Value of change of Gibbs energy for the reaction remained in the range from –250 to –185 kJ/mol (at 298.15 K). When the oxygen in the system is added, there is a further decrease in magnitudes of thermodynamic characteristics: enthalpy change of reaction makes from –505 to –475 kJ/mol, change of Gibbs energy from –395 to –420 kJ/mol. Thus, oxidation allows to increase efficiency of the proceeding reactions. Besides, in the right part of the equations there are free electrons that points to possibility of electrochemical stimulation of the considered processes.

At the second stage, the reactions of formation of malachite and azurite from sulphidic (such as covellite and chalcocite) and the oxidized copper minerals (tenorite, cuprite) were considered:

$$Cu_2S + CaCO_3 + 3H_2O + 2.5O_2 = Cu_2[CO_3](OH)_2 + CaSO_4{\cdot}2H_2O$$

$$3CuS + 3CaCO_3 + H_2O + 6O_2 = Cu_3[CO_3]_2(OH)_2 + 3CaSO_4 + CO_2$$

$$2CuO + CO_2 + H_2O = Cu_2[CO_3](OH)_2$$

$$3CuO + 2CO_2 + H_2O = Cu_3[CO_3]_2(OH)_2$$

Formation of malachite from sulphidic minerals is characterised by very high thermodynamic parameters: enthalpy change from –930 to –1620 kJ/mol, enthropy change from –550 to –730 J/mol·K, and change of Gibbs energy from –770 to –1400 kJ/mol. The formation of azurite from sulphidic minerals at oxidation is also has high thermodynamic parameters (change of Gibbs energy up to –2000 kJ/mol). Formation of copper carbonates from the oxidized minerals has less thermodynamic efficiency due to bigger stability of the oxygen substances; value of Gibbs energy is close to zero and even in certain cases has positive magnitude at higher temperatures. Thus, it is possible to increase efficiency of mineralogenesis by using of coordination substances.

Under natural conditions the most widespread geochemical complexing substances are humic and fulvic acids. At this stage we made thermodynamic estimation of basic copper carbonates formation probability with participation of primary structural fragments of humus acids such as the simplest α-hydroxy and α-amino acids. The following reactions were considered — without complexants:

$$2CuS + 2CaCO_3 + H_2O + 4O_2 = Cu_2[CO_3](OH)_2 + 2CaSO_4 + CO_2 \tag{1}$$

$$2CuO + CaCO_3 + 2H_2O = Cu_2[CO_3](OH)_2 + Ca(OH)_2 \tag{2}$$

$$3CuS + 3CaCO_3 + H_2O + 6O_2 = Cu_3[CO_3]_2(OH)_2 + 3CaSO_4 + CO_2 \tag{3}$$

$$3CuO + 2CaCO_3 + 3H_2O = Cu_3[CO_3]_2(OH)_2 + 2Ca(OH)_2 \tag{4}$$

with complexant Na-glycolate (in salt forms to neutralize formed acid in reactions with sulfide minerals):

$$CuS + 2CH_2(OH)COONa + 2O_2 = Cu(CH_2(OH)COO)_2 + Na_2SO_4 \tag{5}$$

$$CuO + 2CH_2(OH)COOH = Cu(CH_2(OH)COO)_2 + H_2O \tag{6}$$

and analogical reactions with participation of Na-lactate (7, 8), K-glycinate (9, 10) and Ca-alanate (11, 12):

$$CuS + 2CH_3CH_2(OH)COONa + 2O_2 = Cu(CH_3CH_2(OH)COO)_2 + Na_2SO_4 \tag{7}$$

$$CuO + 2CH_3CH_2(OH)COOH = Cu(CH_3CH_2(OH)COO)_2 + H_2O \tag{8}$$

$$CuS + 2CH_2NH_2COOK + 2O_2 = Cu(CH_2NH_2COO)_2 + K_2SO_4 \tag{9}$$

$$CuO + 2CH_2NH_2COOH = Cu(CH_2NH_2COO)_2 + H_2O \tag{10}$$

$$CuS + Ca(CH_3CH_2NH_2COO)_2 + 2O_2 = Cu(CH_3CH_2NH_2COO)_2 + CaSO_4 \tag{11}$$

$$CuO + 2CH_3CH_2NH_2COOH = Cu(CH_3CH_2NH_2COO)_2 + H_2O \tag{12}$$

and final reactions of malachite (13–16) and azurite (17–20) formation from copper complexes with participation of glycolates (13, 17), lactates (14, 18), glycinates (15, 19) and alanates (16, 20):

$$2Cu(CH_2(OH)COO)_2 + 2CaCO_3 + H_2O = Cu_2[CO_3](OH)_2 + 2Ca(CH_2(OH)COO)_2 + CO_2 \tag{13}$$

$$2Cu(C_2H_5(OH)COO)_2 + 2CaCO_3 + H_2O = Cu_2[CO_3](OH)_2 + 2Ca(C_2H_5(OH)COO)_2 + CO_2 \tag{14}$$

$$2Cu(CH_2NH_2COO)_2 + 2CaCO_3 + H_2O = Cu_2[CO_3](OH)_2 + 2Ca(CH_2NH_2COO)_2 + CO_2 \tag{15}$$

$$2Cu(C_2H_5NH_2COO)_2 + 2CaCO_3 + H_2O = Cu_2[CO_3](OH)_2 + 2CaC_2H_5NH_2COO)_2 + CO_2 \tag{16}$$

$$3Cu(CH_2(OH)COO)_2 + 3CaCO_3 + H_2O = Cu_3[CO_3]_2(OH)_2 + 3Ca(CH_2(OH)COO)_2 + CO_2 \tag{17}$$

$$3Cu(C_2H_5(OH)COO)_2 + 3CaCO_3 + H_2O = Cu_3[CO_3]_2(OH)_2 + 3Ca(C_2H_5(OH)COO)_2 + CO_2 \tag{18}$$

$$3Cu(CH_2NH_2COO)_2 + 3CaCO_3 + H_2O = Cu_3[CO_3]_2(OH)_2 + 3Ca(CH_2NH_2COO)_2) + CO_2 \tag{19}$$

$$3Cu(C_2H_5NH_2COO)_2 + 3CaCO_3 + H_2O = Cu_3[CO_3]_2(OH)_2 + 3Ca(C_2H_5NH_2COO)_2 + CO_2 \tag{20}$$

The results of the calculations at standard temperature are shown in Table 1.

Table 1

Thermodynamic functions of the reactions (1–20) at 298.15 K

Reaction	$\Delta_rH^o(298)$, kJ/mol	$\Delta_rS^o(298)$, J/(mol·K)	$\Delta_rG^o(298)$, kJ/mol
1	2	3	4
1	–1475.85	–700.378	–1267.031
2	50.010	–47.502	64.173
3	–2264.92	–963.737	–1977.583
4	134.111	–74.488	156.32
5	–815.109	–558.696	–648.534
6	–91.872	–219.646	–26.384
7	–810.004	–551.583	–645.550
8	–88.943	–220.901	–23.081

1	2	3	4
9	–841.594	–432.506	–712.642
10	–29.940	–37.998	–18.611
11	–858.41	–493.467	–711.286
12	–17.480	–14.630	–13.118
13	73.193	291.353	–13.674
14	71.352	289.680	–15.016
15	195.785	245.329	122.640
16	185.910	220.225	120.250
17	112.373	366.041	3.238
18	109.612	363.531	1.225
19	296.26	297.005	207.708
20	281.449	259.349	204.124

The reactions with participation of copper sulphide are characterized with high values of parameters at direct mineral formation and reactions with intermediate formation of copper complexes. It is seen that complexants promote the transition of oxidized copper into solution (Fig. 1). The malachite and azurite precipitation from copper complexes with hydroxy acids is thermodynamically probable, especially at case of lactates. The reactions with participation of amino acids have positive magnitudes of Gibbs energy change; nevertheless, it can be marked some tendency to decrease the value at increasing of carbon chain.

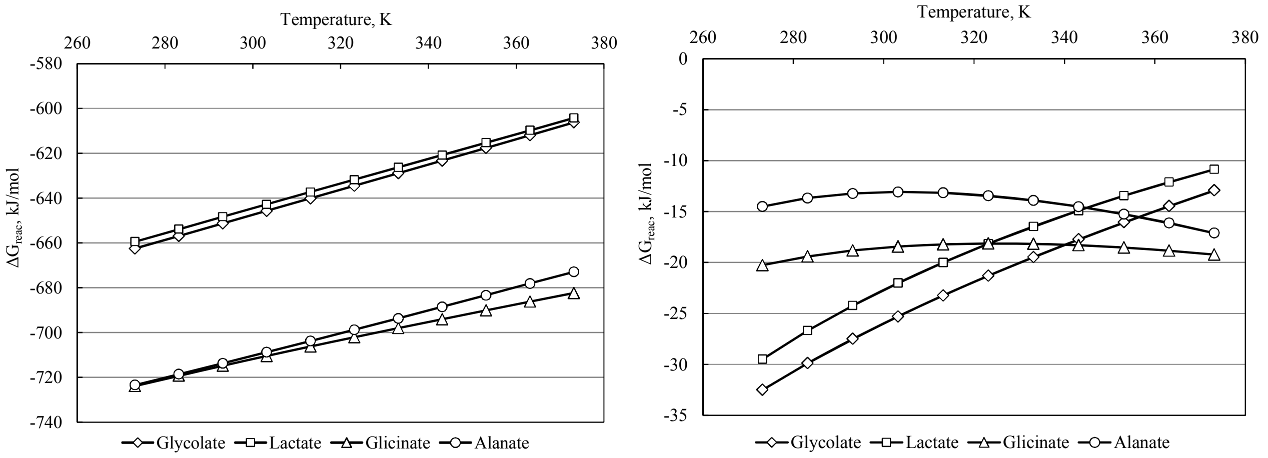

Figure 1. Temperature dependence of Gibbs energy change in reactions of dissolution of sulphide (left) and oxide (right) copper minerals with participation of complexing agents

Lactic (L-2-hydroxypropanoic) acid is one from complexing agents occurring in the nature. Lactic acid is available in industrial quantities and can be viewed as potential reagent for intensification of the mineralogenesis processes. In this case the important advantage is its ecological safety. The formation of copper complexes with lactate-ions prevent its fast precipitation in poorly soluble compounds; this fact enlarge a migration route of copper ions in environment.

The main sources of carbonate-ions at natural conditions are carbonates of calcium and magnesium. Thus, the thermodynamical parameters for reactions of copper (II) lactate with mostly widespread in the nature calcium and magnesium carbonates — calcite, magnesite and dolomite — were considered:

$$2Cu(C_3H_5O_3)_2 + 2CaCO_3 + H_2O = Cu_2[CO_3](OH)_2 + 2Ca(C_3H_5O_3)_2 + CO_2$$

$$2Cu(C_3H_5O_3)_2 + 2MgCO_3 + H_2O = Cu_2[CO_3](OH)_2 + 2Mg(C_3H_5O_3)_2 + CO_2$$

$$2Cu(C_3H_5O_3)_2 + CaCO_3{\cdot}MgCO_3 + H_2O = Cu_2[CO_3](OH)_2 + Ca(C_3H_5O_3)_2 + Mg(C_3H_5O_3)_2 + CO_2$$

The thermodynamic calculations in temperature range 273–373 K show that the malachite formation is possible in the reactions with participation all of considered carbonate rocks (Table 2). The upper negative value of Gibbs energy change is observed for reaction with calcium carbonate; the reaction with participation of magnesium carbonate is considerably more profitable in energy aspect. It is may to expect some mean values for the reaction with participation of dolomite, but its thermodynamic parameters are closer to the reaction with participation of calcite.

Table 2

Thermodynamic functions of malachite formation reactions at 298.15 K

Mineral	$\Delta_r H^o(298)$, kJ/mol	$\Delta_r S^o(298)$, J/(mol·K)	$\Delta_r G^o(298)$, kJ/mol	log K_{eq}
Calcite	71.35	289.7	–15.02	2.631
Magnesite	5.128	178.1	–47.96	8.404
Dolomite	61.94	272.7	–19.36	3.392

The reactions of azurite formation at these circumstances are characterized by higher values of enthalpy change and entropy change, as well as positive value of Gibbs energy change at environmental temperatures (Fig. 2). Thus, the reactions of azurite formation with participation of complexing agents are less probable thermodynamically than the reactions of malachite formation.

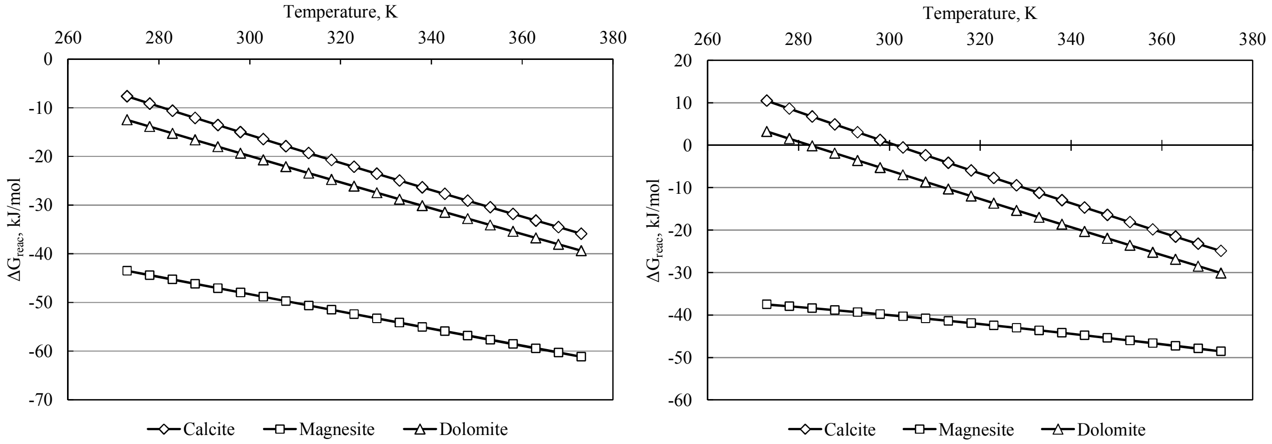

Figure 2. Temperature dependence of Gibbs energy change in reactions of precipitation of malachite (left) and azurite (right) from copper complexes with lactate-ions on various carbonate collectors

It should be noted that the using in the calculations thermodynamic data for hydrated forms of initial and final substances has an effect on thermodynamics of the processes. At the same time, in most causes, the value of Gibbs energy change stay negative.

Small values of Gibbs energy change and equilibrium constant snow that the reaction with participation of lactates are carried out closely to equilibrium conditions. This fact indicate at possibility of formation of well-shaped malachite aggregates.

The research is supported by the Science Committee of the Ministry of Education and Science, the Republic of Kazakhstan, under the Scientific grant No. 0214/GF4 «Developing methods aimed to stimulate the secondary mineral formation of malachite in copper deposits and waste dumps».

References

1 *Woods T.L., Garrels R.M.* Use of oxidized copper minerals as environmental indicators // Applied Geochemistry. — 1986. — Vol. 1. — P. 181–187.

2 *Yang F., Mao J., Pirajno F., Yan Sh., Liu G., Zhou G., Zhang Zh., Liu F., Geng X., Guo Ch.* A review of the geological characteristics and geodynamic setting of Late Paleozoic porphyry copper deposits in the Junggar region, Xinjiang Uygur Autonomous Region, Northwest China // Journal of Asian Earth Sciences. — 2012. — Vol. 49. — P. 80–98.

3 *Hazen R.M., Downs R.T., Kah L., Sverjensky D.* Carbon mineral evolution // Reviews in Mineralogy & Geochemistry. — 2013. — Vol. 75. — P. 79–107.

4 *Seltmann R., Porter T.M., Pirajno F.* Geodynamics and metallogeny of the central Eurasian porphyry and related epithermal mineral systems: A review // Journal of Asian Earth Sciences. — 2014. — Vol. 79. — P. 810–841.

5 *Stiff M.J.* Copper/bicarbonate equilibria in solutions of bicarbonate ion at concentrations similar to those found in natural water // Water Research. — 1971. — Vol. 5. — P. 171–176.

6 *Symes J.L., Kester D.R.* Thermodynamic stability studies of the basic copper carbonate mineral, malachite // Geochimica et Cosmochimica Acta. — 1984. — Vol. 48. — P. 2219–2229.

7 *Balitsky V.S., Bublikova T.M.* Physico-chemical foundations of malachite synthesis and structural-morphological peculiarities and properties of its man-made jewelry quality varieties // Progress in Crystal Growth and Characterization. — 1990. — Vol. 21. — P. 139–161.

8 *Kiseleva I.A., Ogorodova L.P., Melchakova L.V., Bisengalieva M.R., Becturganov N.S.* Thermodynamic properties of copper carbonates malachite $Cu_2(OH)_2CO_3$ and azurite $Cu_3(OH)_2(CO_3)_2$ // Physics and Chemistry of Minerals. — 1992. — Vol. 19. — P. 322–333.

9 *Preis W., Gamsjäger H.* Solid–solute phase equilibria in aqueous solution. XVI. Thermodynamic properties of malachite and azurite — predominance diagrams for the system Cu^{2+}–H_2O–CO_2 // Journal of Chemical Thermodynamics. — 2002. — Vol. 34. — P. 631–650.

10 *Wagemann R., Barica J.* Speciation and rate of loss of copper from lakewater with implications to toxicity // Water Research. — 1971. — Vol. 13. — P. 515–523.

11 *Stevenson F.J., Krastanov S.A., Ardakani M.S.* Formation constants of Cu^{2+} complexes with humic and fulvic acids // Geoderma. — 1973. — Vol. 9. — P. 129–141.

12 *Ernst R., Allen H.E., Mancy K.H.* Characterization of trace metal species and measurement of trace metal stability constants by electrochemical techniques // Water Research. — 1975. — Vol. 9. — P. 969–979.

13 *Mantoura R.F.C., Dickson A., Riley J.P.* The complexation of metals with humic materials in natural waters // Estuarine and Coastal Marine Science. — 1978. — Vol. 6. — P. 387–408.

В.Н.Фомин, И.Е.Рожковой, Д.Б.Гоголь, Д.Л.Пономарев

Органикалық комплекстүзушілердің қатысуымен жүретін негізгі мыс карбонаттарының түзілу реакцияларының термодинамикалық өлшемдері

Мақалада табиғатта пайда болатын малахит мен азуриттың кейбір термодинамикалық процестері сипатталған. Авторлардың зерттеуі бойынша, оксидті минералдарға қарағанда сульфидті кендерден алынатын негізгі карбонаттар термодинамикалық жағынан тиімдірек. Комплекс түзушілердің жүйеде болуы мыстың оксидті формаларын ерітуге әсер етеді және мыс иондарының екіншілік минерал түзуіне мәжбүр етеді. Аналогты аминқышқылдармен салыстырғанда гидроксиқышқылдар малахит пен азуриттың пайда болуына көбірек мүмкіндік туғызады.

В.Н.Фомин, И.Е.Рожковой, Д.Б.Гоголь, Д.Л.Пономарев

Термодинамические параметры реакций образования основных карбонатов меди в присутствии органических комплексообразователей

В статье описаны некоторые термодинамические процессы, которые могут протекать при образовании малахита и азурита в природе. Авторами показано, что образование основных карбонатов из сульфидных руд меди термодинамически более выгодно, чем из ее оксидных минералов. Присутствие комплексообразователей способствует растворению оксидных форм меди и вовлечению ее ионов во вторичное минералообразование. Установлено, что гидроксикислоты в большей степени способствуют образованию малахита и азурита, чем аналогичные аминокислоты.

UDC 697.32

Sh.K.Amerkhanova, R.M.Shlyapov, A.S.Uali

Ye.A.Buketov Karaganda State University
(E-mail: amerkhanova_sh@mail.ru)

Evaluation of interrelation of electrochemical properties and thermal storage capacity of the melt of crystal hydrates of inorganic substances on the basis of $Na_2S_2O_3{\cdot}5H_2O$

Research of conductivity of concentrated salt solutions are of great interest in connection with the structural changes in electrolytes. The heat storage properties of the mixture of sodium thiosulfate pentahydrate and sodium tellurate dihydrate were calculated. Firstly the coefficients of temperature dependence of heat capacity of sodium tellurate were calculated. Melting temperature of mixtures at ratios (50:1, 25:1, 10:1), which are equal to 349 K, 307 K, 326 K, were determined. The specific melting heat of mixtures was calculated. It was shown, that heat of fusion of mixture $Na_2S_2O_3{\cdot}5H_2O$ — $Na_2TeO_4{\cdot}2H_2O$ (10:1) is maximal and equals to 238.5 $kJ{\cdot}kg^{-1}$. An analysis of the temperature dependence of the electrical conductivity was carried out. It showed the presence of high activity and mobility of tellurate-ions. It was shown that crystallization process is changed from quasi-equilibrium to the «explosive» at low temperatures ranging from T=318 K.

Key words: heat storage properties, sodium thiosulfate pentahydrate, electrical conductivity, specific melting heat, kinetic characteristics, sodium tellurate.

Researches on the conductivity of concentrated salt solutions became the subject of great interest in connection with the structural changes in electrolytes. It is known that concentrated and saturated solutions of electrolytes refer to the third type of liquids organization with the lack of water structure according to the classification formed by the results of measurement of the dielectric permittivity [1].

At the same time a number of theories were suggested for the mechanism of electrical conductivity: hydrodynamic, where ions are presented in the form of balls moving in a viscous medium [2], theory of Debye-Hückel-Onsager in which the movement of ions is caused by electrostatic forces under the influence of an electric field, and braking is caused due to the formation and disappearance of the ion atmosphere [3], in Eyring's theory ion is hopping from one equilibrium position to another [4], Ivashkevich theory, where the electrical conductivity is determined by the equation of communication between the concentration of ions and the medium viscosity. On the other hand, inorganic compounds containing some crystallized water show the ability to store heat, as a result of *solid – liquid* phase transition, which is then released into the environment during crystallization. In most cases the heat storage based on phase transition is understood as the accumulation of fusion heat.

The heat content (internal energy) of a liquid or solid phase is often used as an addition to the heat of the phase transition. It increases the capacity of the battery, but makes it impossible to take advantage of heating at constant temperature [5].

It is known from the literature sources that the enthalpy of melting of sodium thiosulfate crystalline is higher than the one of anhydrous salt, i.e. in the reverse process of crystallization into the environment more heat will be generated, therefore the substance may have been selected as a material having some heat storage properties, and on the basis of their costs, the storage capacity and reliability of heat during repeated thermal cycling [6]. Furthermore, the effect of adding the sodium sulfate decahydrate on the process of crystallization of sodium thiosulfate pentahydrate is also marked [7].

In connection with this the evaluation of the electrochemical properties of heat storage materials based on mixtures of crystal hydrates $Na_2S_2O_3{\cdot}5H_2O$ — $Na_2TeO_4{\cdot}2H_2O$ is the task of the theoretical and practical plan which gives the opportunity to perform the modification of the base crystal hydrates. The aim is to determine the heat storage capacity and electrochemical properties of mixtures of crystal hydrates $Na_2S_2O_3{\cdot}5H_2O$ — $Na_2TeO_4{\cdot}2H_2O$.

Sodium thiosulfate pentahydrate ($Na_2S_2O_3{\cdot}5H_2O$) chemically pure, telluric acidic sodium dihydrate ($Na_2TeO_4{\cdot}2H_2O$) analytical grade have been used as the starting materials for heat storage materials.

Inorganic mixtures are obtained by mixing sodium thiosulfate pentahydrate and sodium tellurate dihydrate in various proportions by weight of (50:1, 25:1, 10:1), weight 5 g sodium thiosulfate, from which the weight of sodium tellurate dihydrate additives is calculated.

After mixing, the mixtures were heated up to a temperature at which solids are dissolved in the crystallized water. Method for determining the specific heat of fusion [8]. The samples were heated by convection. Temperature control was performed by a thermometer, which was immersed in the sample at a visual and thermal analysis and thermocouple (chromel-alumel (298–1073 K)) during measuring thermal emf. The thermo-emf. was recorded using a voltmeter brand EV2265–1 with divisions of 0.1 mV (Fig. 1).

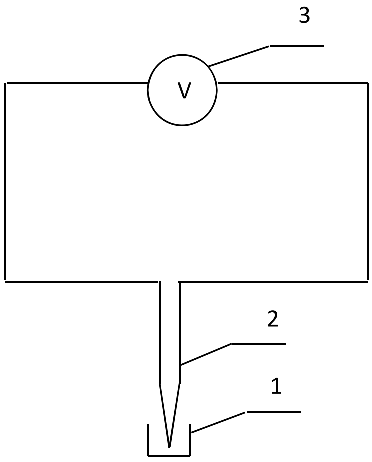

1 — Sample; 2 — Thermocouple chromel-alumel; 3 — Voltmeter

Figure 1. Apparatus for measuring thermal emf.

A method for determining the heat release rate is as follows. After the material in the crucible has melted and reached the temperature higher than the melting temperature, the furnace is turned off, and at regular intervals millivoltmeter readings are fixed.

Conductivity studies were carried out in a thermostated vessel with the capacity of 50 ml. The electrical conductivity was measured in mark OK-102 conductivity meter. The working electrode was made of a pair of platinum plates of 1 cm^2. To recalculate the values of specific conductivity from $Sim{\cdot}cm^{-1}$ to $Ohm{\cdot}cm^{-1}$ the instrument constant has been determined by measuring the χ 0.001 M KCl at standard temperature [9].

According to the graph of the thermocouple (chromel-alumel) capacity dependence on the temperature the graph of temperature dependence on time is made, an exemplary form of which is shown in Figure 2.

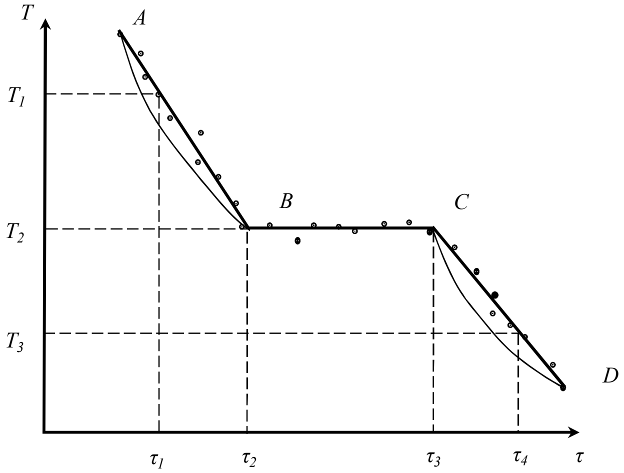

Figure 2. Thermocouple temperature dependence on time

On the graph AB area corresponds to a cooling of the molten metal before the start of crystallization, BC area — to metal crystallization, and CD area — to solid metal cooling (T_2 is the melting point). Replace the resulting graph with the idealized one by connecting points A and B, C and D with straight lines. The amount of heat delivered per time unit by average liquid metal with the crucible during cooling:

$$\frac{Q_1}{\tau}=\frac{(MC_1+mC_2)\cdot(T_1-T_2)}{\tau_2-\tau_1}, \tag{1}$$

where M — melting pot; m — mass of metal; C_1 — specific heat capacity of the melting pot (C_1 =1090 J× ×kg^{-1}·K^{-1}); C_2 — the specific heat of the test liquid metal (for tin — C_2 = 266 J·kg^{-1}·K^{-1}).

When cooling solid metal per unit of time the amount of heat is given:

$$\frac{Q_2}{\tau}=\frac{(MC_1+mC_2^{'})\cdot(T_2-T_3)}{\tau_4-\tau_3}, \tag{2}$$

where $C_2^{'}$ — the specific heat capacity of the investigated solid metal ($C_2^{'}$ = 230 J·kg^{-1}·K^{-1}).

Since during crystallization temperature of the metal does not change, the rate of heat transfer during this period can not be measured directly. The rate of heat transfer, all other things being equal, depends on the temperature difference between the heated body and the environment, so the average speed of cooling before and after crystallization process will be approximately equal to the rate of heat transfer during solidification.

Using this, you can write:

$$\frac{Q_0}{\Delta\tau}=\frac{1}{2}\left(\frac{Q_1}{\Delta\tau}+\frac{Q_2}{\Delta\tau}\right). \tag{3}$$

Using the equations (1), (2) and (3), we have found:

$$\frac{Q_0}{\Delta\tau}=\frac{1}{2}\left((MC_1+mC_2)\frac{T_1-T_2}{\tau_2-\tau_1}+(MC_1+mC_2^{'})\frac{T_2-T_3}{\tau_4-\tau_3}\right). \tag{4}$$

In the graph the times τ_1 and τ_2 are chosen so that:

$$\tau_2-\tau_1=\tau_3-\tau_2;$$

$$\tau_4-\tau_3=\tau_3-\tau_2. \tag{5}$$

We have placed the equation (4) in the expression (2). Taking into account (5), we have obtained:

$$\lambda=\frac{1}{2m}\Big((MC_1+mC_2)(T_1-T_2)+(MC_1+mC_2^{'})(T_2-T_3)\Big). \tag{6}$$

To calculate the kinetic parameters the Arrhenius equation has been used, in which the rate constant was replaced with the specific conductivity. Activation energy of the electrical conductivity has been calculated graphically according to the equation:

$$\lg\chi=\lg A_0-E_a/2.303RT. \tag{7}$$

Calculation of kinetic parameters was performed according to the formulas [4]

$$\Delta H^{\#}=E_a-2RT. \tag{8}$$

Then we have found the value of $\Delta S^{\#}$ according to the equation:

$$\Delta S^{\#}=R\,[2{,}303\lg A_0-2{,}303\lg(\frac{kT}{h})-1]; \tag{9}$$

$$\Delta G^{\#}=\Delta H^{\#}-T\Delta S^{\#}. \tag{10}$$

In this scientific work heat-storage properties have been calculated for example, inorganic salts, sodium thiosulfate and modified salts of elements of (VI) group. It has been shown that sodium thiosulfate is a solvent with respect to the additive, since the melting point of the second component is significantly higher. In this regard, the melt mixture is a solution, the heat capacity of which is different from the heat capacity of the solvent (basic salt). Also for the first time coefficients of the temperature dependence of heat capacity for sodium tellurate were determined by Landia's method [10] in the range 298 K – T_m (Table 1).

Table 1

The coefficients of the temperature dependence of sodium tellurate heat capacity

Compound	C_p, cal·mol^{-1}·K^{-1}			298 – T_m
	a	b·10^3	c·10^5	
Na_2TeO_4	36.04	4.84	0.37	298–1009 K

The indicated coefficients of temperature dependence of sodium tellurate heat capacity (Table 1) can be used for the calculation of heat capacity of the mixture of sodium thiosulfate pentahydrate — sodium tellurate dihydrate. Next, on the base of the kinetic curves of cooling, the melting temperature of mixture, and the fusion heat of the mixtures of sodium thiosulfate pentahydrate with sodium tellurate have been calculated (Table 2).

Table 2

The thermodynamic characteristics of melting mixtures of sodium thiosulfate pentahydrate with sodium tellurate dihydrate

Mixture	T_m, K	C_p(solid), $J \cdot kg^{-1} \cdot K^{-1}$	C_p(melt), $J \cdot kg^{-1} \cdot K^{-1}$	λ, kJ·kg
$Na_2S_2O_3 \cdot 5H_2O$-$Na_2TeO_4 \cdot 2H_2O$ (10:1)	326	885.3	92.25	269.3
$Na_2S_2O_3 \cdot 5H_2O$-$Na_2TeO_4 \cdot 2H_2O$ (25:1)	307	883.2	46.4	60.3
$Na_2S_2O_3 \cdot 5H_2O$-$Na_2TeO_4 \cdot 2H_2O$ (50:1)	349	885.1	30.0	32.9
$Na_2S_2O_3 \cdot 5H_2O$	321	1451.6	12.9	94

Effect of temperature on the conductivity of mixtures of sodium thiosulfate pentahydrate — sodium tellurate dihydrate in a weight ratio (25:1; 50:1) has been investigated. However, high consumption of sodium tellurate dihydrate restricts the use of the mixture as a heat storage material, so it is necessary to evaluate the electrochemical properties providing maximum heat output. The results determining the electrical conductivity for mixtures of sodium thiosulfate pentahydrate – sodium tellurate dihydrate are shown in Figure 3.

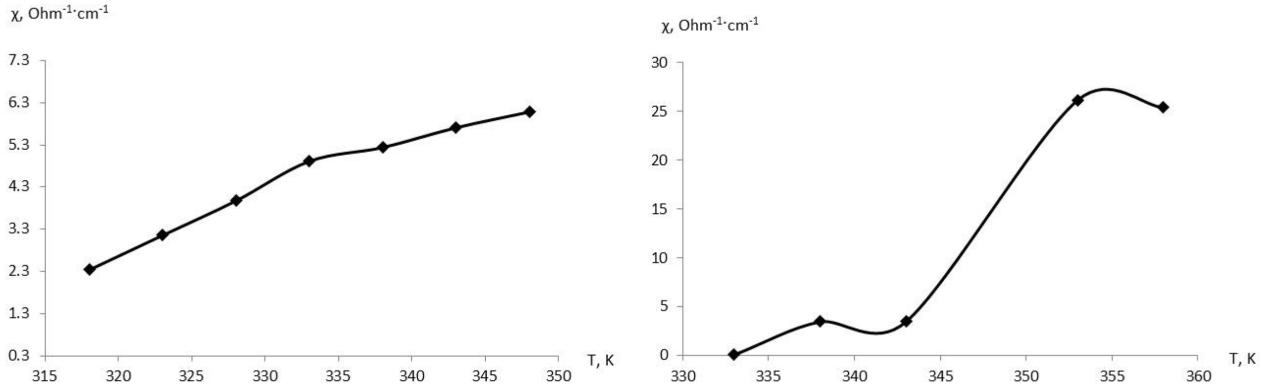

$Na_2S_2O_3 \cdot 5H_2O – Na_2TeO_4 \cdot 2H_2O$ (25:1)

$Na_2S_2O_3 \cdot 5H_2O – Na_2TeO_4 \cdot 2H_2O$ (50:1)

Figure 3. The temperature dependence of the electrical conductivity for the mixture $Na_2S_2O_3 \cdot 5H_2O – Na_2TeO_4 \cdot 2H_2O$

The data in the table show that adding sodium tellurate dihydrate leads to lower specific heat of fusion. The lower mixture melting point compared to a basic salt of sodium thiosulfate pentahydrate is associated with the coordination of tellurate — ions with water molecules.

On the other hand the addition of sodium tellurate dihydrate increases not only the melting point but also the specific heat of melting, due to the formation of the eutectic mixture while removing water. The melting point and fusion heat of these mixtures have been identified, it is shown that the addition of sodium tellurate dihydrate in 10: 1 ratio increases the specific heat of melting to 238.7 $kJ \cdot kg^{-1}$. Thus the mixture of the composition of 90.9 % of sodium thiosulfate, 9.1 % sodium tellurate dihydrate can be used as heat-storage material.

Data given in Figure 3 make it possible to judge about the presence of high activity and mobility of ions due to the absence or reduction of solvents. These conductivity data are in accord with those for the pure molten nitrate salts, alkali metal chlorides, but they are characterized by high melting points.

Figure 4 shows that the change in conductivity and temperature is exponential, which is due to an increase in the ionic contribution to the overall conductivity of the melt. Furthermore, energy characteristics of the melt mixture conduction have been defined, since the fundamental period contributing to the process of heat transfer is cooling (Table 3).

Table 3

Changes in the kinetic characteristics of the electrical conductivity of melts $Na_2S_2O_3·5H_2O$ – $Na_2TeO_4·2H_2O$ (C_1:C_2)

C_1:C_2	T_1–T_2 (heating), K	E_a, kJ·mol^{-1}	lg$A$	T_2–T_1 (cooling), K	E_a, kJ·mol^{-1}	lg$A$	Δ$S^{\#}$, J·mol^{-1} K^{-1}	Δ$H^{\#}$, kJ·mol^{-1}	Δ$G^{\#}$, kJ·mol^{-1}
25:1	318–333	43.30	7.49	343–323	27.11	4.83	60.99	21.41	0.48
							61.01	21.49	0.86
							61.02	21.57	1.25
							61.04	21.65	1.63
							61.05	21.74	2.02
	333–348	14.00	2.97	323–303	48.93	6.64	95.75	43.64	13.19
							95.76	43.72	13.74
							95.78	43.81	14.30
							95.79	43.89	14.86
50:1	323–343	403.49	62.25	353–323	16.06	3.94	43.96	10.19	–5.33
							43.97	10.27	–5.03
							43.99	10.35	–4.73
							44.01	10.44	–4.43
							44.02	10.52	–4.14
	343–348	457.10	70.14				44.04	10.60	–3.84
							44.05	10.69	–3.54
	348–358	–31.50	–3.21	318– 298	40.84	7.85	118.96	35.56	–2.27
							118.97	35.64	–1.60
							118.99	35.72	–0.93
							119.00	35.81	–0.25
							119.02	35.89	0.42

In this case, the activation energy is the minimum kinetic energy required so that an ion could perform a translational motion and for the appearance of electric current. Therefore, heating up to 333 K allows to decrease the activation energy as the melts almost do not contain any crystallized impurities and the process of transferring the atomic charge is flowing in the diffusion mode. On the other hand the activation energy is the sum of the true activation energy, which active ions have and the excess energy needed to perform a jump from one quasi-equilibrium position with the oscillation frequency of the ion ν_1 to the state with the oscillation frequency ν_2 during τ [11].

Since this mixture consists of sodium salts, the common ion is sodium ion, and the center of the quasi-equilibrium state are anions (thiosulfate ion and tellurate ion). Low enough positive pre-exponential factor suggests low values of the relaxation times of ions with respect to the equilibrium position, which are increased when heated and are reduced upon cooling. I.e. in the cooling process there is the destruction of crystal lattice by ions having a high kinetic energy, which they transmit in a collision with the formed lattice sites. Hence the collision of an ion with a lattice site can be viewed as a reaction between a mobile cation and static anion the product of which is the activated complex, i.e., this bimolecular reaction [12]. Therefore, all the kinetic parameters can be applied to the cooling process which relate to bimolecular reactions in condensed matter, namely the activation enthalpy and entropy of activation. The data on the Gibbs energy of activation show that at low temperatures ranging from T = 318 K, the crystallization process proceeds from a quasi-equilibrium and «explosive,» which promotes rearrangement of the crystal lattice, the release of excessive kinetic and potential energy into the environment.

Similar calculations were made for 1:50 ratio, it is shown that the heating process takes place in the diffusion mode, and high values of pre-exponential factor enable us to judge about fairly high mobility of ions. At the same time cooling is accompanied by a decrease in the activation energy and pre-exponential factor, and the crystal lattice is stabilized. This fact is confirmed by the values of Gibbs energy of activation. From the temperature of 318 K cooling is followed by a slight increase in the activation entropy, change of the structure, but it does not lead to a significant change in the amount of heat released into the environment. Therefore, one of the main criteria for the selection of heat-retaining materials is the increment of the Gibbs energy of activation when the temperature changes from T to T_0.

Thus, the value of the electrical conductivity of molten mixture of sodium thiosulfate crystalline — sodium tellurate dihydrate of different composition have been determined. Coefficients of the temperature dependence of the heat capacity of sodium tellurate dihydrate have been calculated. It is shown that the addition of sodium tellurate dihydrate in an amount of 2 % by the weight of sodium thiosulfate pentahydrate increases the heat output. The values of activation entropy, the Gibbs energy of activation, which indicate the electrochemical nature of the transition from a quasi-equilibrium to «explosive» which facilitates the rearrangement of the crystal lattice, the release of excessive kinetic and potential energy into the environment.

The work was financed by the scientific and technical program «International scientific and technical programs and projects for 2013–2015» (№ state registration 0113PK00961).

References

1 *Monica D.M., Petrella G., Sacco A., Bufo S.* Transference numbers in concentrated sodium chloride solutions // Electrochimica Acta. — 1979. — Vol. 24. — P. 1013–1017.

2 *de Diego A., Usobiaga A., Fernaèndez L. A., Madariaga J.M.* Application of the electrical conductivity of concentrated electrolyte solutions to industrial process control and design: from experimental measurement towards prediction through modelling // Trends in analyt. chem. — 2001. — Vol. 20. — P. 65–78.

3 *Fuoss R.M.* Conductimetric determination of thermodynamic pairing constants for symmetrical electrolytes // Proc. Natl. Acad. Sci. USA. — 1980. — Vol. 77. — P. 34–38.

4 *Rubinstein I., Bixon M., Gileadi E.* Confirmation of the Hopping Mechanism of the Conductivity of Bromide Ions in Solutions Containing Bromine// J. Phys. Chem. — 1980. — Vol. 84. — P. 715–721.

5 *Socaciu L.G.* Thermal Energy Storage with Phase Change Material // Leonardo Electronic Journal of Practices and Technologies. — 2012. — Vol. 20. — P. 75–98.

6 *Bhatt V.D., Gohil K., Mishra A.* Thermal Energy Storage Capacity of some Phase changing Materials and Ionic Liquids // International Journal of Chem. Tech. Research. — 2010. — Vol. 2. — P. 1771–1779.

7 *Heine D., Abhat A.* Investigation of Physical and Chemical Properties of Phase Change Materials for Space Heating, Cooling Applications // Proceedings of international Solar Energy Society Congress. — New Delhi, India, Jan., 1978. — Vol. 1. — P. 500–505.

8 *Sklyarchuk V., Plevachuk Yu., Gerbeth G., Eckert S.* Melting-solidification process in Pb-Bi melts // Journal of Physics: Conference Series. — 2007. — Vol. 79. — P. 12–19.

9 *Holmquist D.D., Randall J., Volz D.L.* Chemistry with Vernier. — Vernier Software and Technology, Beaverton, OR, 2004.

10 *Huy H., Stavros A.A.* Mathematical modelling of solidification and melting: a review Modelling Simul. // Mater. Sci. Eng. — 1996. — Vol. 4. — P. 371–396.

11 *Laidler' K.J., Klng M.C.* The Development of Transition-State Theory // J. Phys. Chem. — 1983. — Vol. 87. — P. 2657–2664.

12 *Ferna´ndez-Ramos A., Miller J.A., Klippenstein S.J., Truhlar D.G.* Modeling the Kinetics of Bimolecular Reactions // Chem. Rev. — 2006. — Vol. 106. — P. 4518–4584.

Ш.К.Амерханова, Р.М.Шляпов, А.С.Уәли

$Na_2S_2O_3 \cdot 5H_2O$ негізінде бейорганикалық заттар кристаллогидраттары қоспаларының электрохимиялық қасиеттері және жылужинағыш қабілеттілігі арасындағы өзара байланысты бағалау

Концентрацияланған тұз ерітінділерін зерттеу өткізгіштік электролиттерде құрылымдық өзгерістерге байланысты үлкен қызығушылық тудыруда. Мұнда натрий тиосульфатының пентагидраты және натрий теллуратының дигидрат қоспасының жылу сақтау қасиеттері есептелген. Алғаш рет Ландийдың әдісі мен натрий теллуратының жылу жинағыш қасиетіне температуралық тәуелділік коэффициенттері анықталды. (50:1, 25:1, 10:1) қатынастағы 349 K, 307 K, 326 K тең болатын қоспалардың балқу температуралары есептелді. Қоспалардың ерекше жылулық балқу температуралары белгіленді. Қоспалардың $Na_2S_2O_3 \cdot 5H_2O$ – $Na_2TeO_4 \cdot 2H_2O$ жасырын жылулық балқуы (10:1) максималды және 238,5 кДж/кг тең екені көрсетілді. Электр өткізгіштігінің температура тәуелділігіне талдау жүргізілді. Ол жоғары белсенділігі мен теллурат-ионының қозғалғыштығына негізделген. Кристалдану процесі T = 318 K төмен температурада квазитепе-теңдіктен жарылғышқа дейін өзгереді деп көрсетілген.

Ш.К.Амерханова, Р.М.Шляпов, А.С.Уали

Оценка взаимосвязи электрохимических свойств и теплоаккумулирующей способности расплавов кристаллогидратов неорганических веществ на основе $Na_2S_2O_3 \cdot 5H_2O$

Исследования электропроводности концентрированных растворов солей представляют большой интерес в связи со структурными изменениями в электролитах. Были рассчитаны теплоаккумулирующие свойства смеси пентагидрата тиосульфата натрия и дигидрата теллурата натрия. Впервые методом Ландия были найдены коэффициенты температурной зависимости теплоемкости для теллурата натрия. Определены температуры плавления смесей при соотношениях (50:1, 25:1, 10:1), которые равны 349 K, 307 K, 326 K. Была рассчитана удельная теплота плавления смесей. Показано, что скрытая теплота плавления смеси $Na_2S_2O_3 \cdot 5H_2O$ – $Na_2TeO_4 \cdot 2H_2O$ (10:1) максимальна и равна 238,5 кДж/кг. Проведен анализ температурной зависимости электропроводности. Это обусловлено высокой активностью и подвижностью теллурат-ионов. Показано, что процесс кристаллизации изменяется от квазиравновесного к взрывному при низких температурах от T = 318 K.

UDC 546.02. 544.3

O.A.Golovanova[1], M.V.Kuimova[2]

[1]F.M.Dostoevsky Omsk State University;
[2]National Research Tomsk Polytechnic University, Russia
(E-mail: golovanoa2000@mail.ru)

Study of the influence of inorganic and organic additives on the possibility and regularity of the precipitation process of brushite from aqueous solutions

The article presents a range of issues related to the peculiarities of brushite crystallization in the presence of additives based on thermodynamic calculations and experimental data. The authors studied the regularities of phase formation in the system of $Ca^{2+} – HPO_4^{2-} – H_2O$, an additive in a broad range of variation of concentrations of components and pH. The effect of silicate-, fluoride-, chloride- and hydrocarbonate-ions on the precipitation and the composition of the crystallizing phase was investigated. It was found that brushite and other calcium phosphates co-precipitate from the original system. Studying the influence of organic additives, it has been established that their presence leads to the precipitation of brushite admixed with apatite phase.

Key words: Brushite, thermodynamic calculations, experimental data, silicate-, fluoride-, chloride- hydrocarbonate-ions, crystallizing phase, calcium phosphates, organic additives, apatite phase.

Introduction

In recent years, considerable attention has been paid to the creation of ceramic materials for medical purposes used in reconstruction of bone tissue defects caused by pathological changes in the body, major surgical interferences or trauma. The use of the materials on the basis of calcium phosphates provides unique opportunities, since this group of compounds is characterized by biological compatibility with body tissues, active combination with bone tissue and the formation of new bone tissue. These properties are widely used for the production of artificial bone grafts, which are either entirely made or only surface-coated with biocompatible calcium phosphates. For example, self-hardening cements of calcium orthophosphates are used in bone regeneration, while titanium prostheses coated with a surface layer of calcium orthophosphate are used for endoprosthesis replacement of hip joints and teeth. Porous support structures made of calcium orthophosphates are promising tools in tissue engineering [1–5].

Another reason giving rise to a great deal of interest in studies of these minerals is the fact that apatite is the main part of the inorganic physiogenic (bones, teeth) and pathological (i.e., those appearing due to various diseases) hard tissues. For example, dental caries and osteoporosis occur due to the partial removal of calciferous matter (decalcification) of teeth and bones respectively. This is a consequence of substitution of less soluble and more solid biological apatite with more soluble and soft dicalcium phosphate. Therefore, the processes of both physiogenic and pathological crystallization in vivo are crystallization of calcium phosphate.

This paper deals with brushite — dihydrate dicalcium phosphate $CaHPO_4 \cdot 2H_2O$ (dicalcium phosphate dihydrate — DCPD) which is a quite common but as yet poorly studied biologically important mineral.

DCPD is of frequent occurrence in the composition of pathogenic mineral formations such as dental stones, kidney stones [6–10]. In medicine it is used in cement compositions based on calcium phosphate. DCPD is included in cavity protection toothpastes (in this case it is present together with the fluorine-containing compounds) and is a mild polishing agent [2, 5, 11].

Analysis of the literature [1, 5, 12] shows that the crystallization process of brushite in a greater degree depends on the parameters of the solution (such as initial concentration of the components, the pH of the medium) and the reaction conditions (temperature, time of solid phase crystallization, the rate of solution pouring, the mixing procedure). Since the conditions under which brushite is formed are very diverse, the selection and specification of synthesis parameters of this phase from aqueous solutions are urgent and complex problems of modern science. In addition, the research aimed at studying the nature of the influence of inorganic and organic additives (components of biological fluids of the human body) on the properties of the synthetic solid phase is very important.

The aim of this work is to study the effect of organic and inorganic additives on the opportunity and the regularities of the precipitation process of brushite from aqueous solutions.

Materials and methods

Thermodynamic calculation. At the initial stage of the study, thermodynamic calculation was conducted to determine the feasibility and conditions of precipitation of slightly soluble calcium compounds. Aqueous solutions containing ions of calcium, phosphate, nitrate ions and ammonium were chosen as the systems to study the regularities of crystallization. The concentration of calcium and phosphate ions was varied between 10 and 200 mmol/L, the content of counter-ions in the system corresponded to the equilibrium stoichiometric concentration after dissociating of calcium nitrate and ammonium hydrophosphate in aqueous medium. The consideration of these ions was reduced to the description of their impact on the non-ideality of the solution due to the electrostatic interactions of ions constituents related to the ionic strength of the solution. The calculation of activity ratio of ions was carried out according to the equation of the second approximation of the Debye-Huckel theory [13].

During calculations, the value of acidity ranged from 0 to 14, with a step increment of 0.1. Stepped hydrolysis of phosphate ions in the solution was considered by the introduction of the value of mole fractions of those anion forms that are a part of a slightly soluble composition, in the equation for relative solubility products. According to the existing data [3–5, 11, 12], in aqueous solutions containing calcium ions and phosphate ions, the following slightly soluble compounds are formed: $Ca(H_2PO_4)_2 \cdot H_2O$ (monocalcium phosphate monohydrate), $Ca(H_2PO_4)_2$ (monocalcium phosphate), $CaHPO_4 \cdot 2H_2O$ (brushite), $Ca_8H_2(PO_4)_6 \cdot 5H_2O$ (octacalcium phosphate, OCP), $Ca_{10}(PO_4)_6(OH)_2$ (hydroxyapatite, HA), $\beta\text{-}Ca_3(PO_4)_2$ (tricalcium phosphate, TCP), $Ca(OH)_2$. To determine the feasibility and the conditions of the precipitation of the listed substances, we used the values of thermodynamic solubility products (pK^o_s) corresponding to the instability constants data base of complexes SC-database [SCQUERY Version 1.37 (1993)]. Theoretical determination of feasibility and conditions of precipitation of these slightly soluble calcium compounds in aqueous media was carried out based on calculations of thermodynamic parameters characterizing the degree of the system deviation from equilibrium. The value of supersaturation index (SI) of the system for each of the compounds was calculated according to [14]. The driving force of the crystallization process was characterized by the change in Gibbs' free energy (ΔG) when the system transfers from a supersaturated state to equilibrium [14].

If $SI > 0$, $\Delta G < 0$ and precipitation of the solid phase from the solution is thermodynamically probable.

Experimental modeling. Brushite crystals were obtained by mixing the dilute solutions of calcium nitrate and ammonium hydrogen phosphate as a result of the precipitation reaction:

$$Ca(NO_3)_2 + (NH_4)_2HPO_4 + 2H_2O \rightarrow CaHPO_4 \cdot 2H_2O\downarrow + 2NH_4NO_3$$

The study of the system was carried out at the equimolar concentrations of the solution of $Ca(NO_3)_2$ and $(NH_4)_2HPO_4$ at room temperature (22–25 ºC). During the experiment, the concentration of additives was varied.

The solution was filtered under vacuum after sedimentation of the heterogeneous system during the chosen period of time. The precipitate was dried at a temperature of ~80 ºC to the constant weight for complete removal of the chemically not-bound water. The obtained solid phase was weighed and studied by the methods of X-ray diffraction analysis (XRD) (DRON-3M), by Fourier-transform infrared spectroscopy (FTIR spectrometer FT-801, tablets with KBr) and optical microscopy.

The analysis of variance was performed on the laser diffraction particle size analyzer ShimadzuSALD-2101 (Laser Diffraction Particle Size Analyzer). According to the results of analysis, we obtained a curve of particle size distribution and average particle size in microns using special software (WING-2; WING-3). For more reliable results, the analysis of the samples was carried out in 4–5-fold repetition, and the relative standard deviation for these measurements was Sr = 0.02–0.04.

The statistical data processing was carried out using software StatSoft Statistica 6.0.

Results and their discussion

Thermodynamic modeling. The comparison of the values of solubility products $K_s^{/}$ of studied slightly soluble compounds, calculated taking into account the ionic strength and hydrolysis processes, with values of thermodynamic constants $K_s°$ showed that in all systems in which $C_{Ca(NO_3)_2} / C_{(NH_4)_2HPO_4} = 1.33\text{–}2.00$, crystallization is thermodynamically possible $CaHPO_4 \cdot 2H_2O$; $Ca_{10}(PO_4)_6(OH)_2$; $Ca_8H_2(PO_4)_6 \cdot 5H_2O$, $\beta\text{-}Ca_3(PO_4)_2$ and $Ca(OH)_2$ (for them $K_s^{/} > K_s°$). By increasing the ratio of concentrations of calcium and phosphate ions in the solution, the change of composition and the number of phases (with respect to which the medium is in a supersaturated state) is not observed. The conditions, under which the deposition of a particular solid phase is possible, are virtually unchanged at varying initial concentrations of the ions forming the precipitation. So the diagrams of crystallization of all of the slightly soluble calcium orthophosphates, for which precipitation is possible in the studied systems, are almost invariant with the changes of the parameter Ca/P in the solution (Fig. 1). Consequently, the magnitude $C_{\mathrm{Ca(NO_3)_2}} / C_{\mathrm{(NH_4)_2HPO_4}}$ (when changing from 1.33 to 2.00) does not have a significant influence on the conditions and sequence of crystallization of slightly soluble compounds of calcium.

Acidity of the medium has the greatest influence on the process and depth of the reaction behavior of precipitation. The stability region of $Ca_{10}(PO_4)_6(OH)_2$ ($SI > 0$) is significantly expanded by increasing the pH value, reaching a maximum at pH = 12 (Fig. 1), whereupon the supersaturation is virtually unchanged and remains constant (SI = 3.70). A similar trend is observed for β-$Ca_3(PO_4)_2$ (Fig. 1).

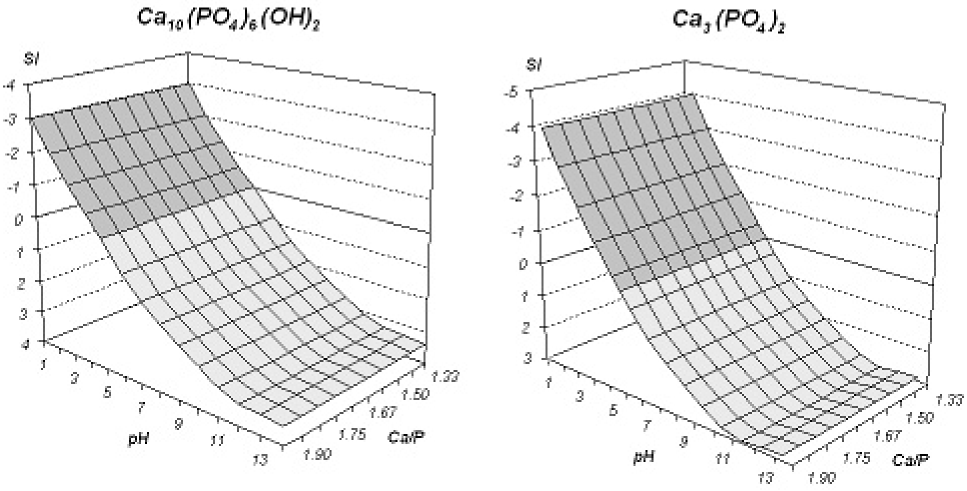

Figure 1. Diagrams of crystallization of calcium orthophosphates ($Ca(NO_3)_2$ / $(NH_4)_2HPO_4$ = 1.67)

The established regularity is due to the fact that with increasing pH value, the mole fraction of orthophosphate ions in the system increases, and at pH>12, the form PO_4^{3-} predominates in the solution, as the phosphorus in the form of trisodium orthophosphate ion is included in the composition of $Ca_{10}(PO_4)_6(OH)_2$ and β-$Ca_3(PO_4)_2$. The supersaturation of the solution concerning the calcium orthophosphates increases, as the pH increases with that the field of their existence expands, the rate and depth of deposition of the reaction increase [14].

It is known that $CaHPO_4 \cdot 2H_2O$ and $Ca_8H_2(PO_4)_6 \cdot 5H_2O$ phases that crystallize in slightly acidic and close to neutral solutions. The areas obtained in the calculations of the possible deposition of the mentioned salts have the boundaries of 5.0–13.7 and 5.7–14, respectively for $CaHPO_4 \cdot 2H_2O$ and $Ca_8H_2(PO_4)_6 \cdot 5H_2O$ (Fig. 1). In practice, in aqueous solutions at pH close to 7, the processes of hydrolysis of the considered calcium orthophosphates with the formation of thermodynamically more stable $Ca_{10}(PO_4)_6(OH)_2$ start. Probably, this is due to the lack of experimental data regarding the availability of $CaHPO_4 \cdot 2H_2O$ and $Ca_8H_2(PO_4)_6 \cdot 5H_2O$ in aqueous alkaline solutions and their stable existence in time. However, according to [12], the range of pH medium of crystallization at the nonequilibrium growth of brushite (in gel media) is significantly wider than the well-known thermodynamic equilibrium range 4<pH<6 and includes all experimentally studied pH range from 3 to 8 [12].

In the transition from dilute solutions to the systems with a higher concentration, a significant decrease in the Gibbs energy of the crystallization process of $Ca_{10}(PO_4)_6(OH)_2$, $Ca_8H_2(PO_4)_6 \cdot 5H_2O$ and β-$Ca_3(PO_4)_2$ is observed [14]. This change reaches 4–6.5 kJ/mol when the concentration of calcium ions and phosphate ions increases in the system by 20 times. The driving force of the deposition process of brushite varies slightly depending on the concentration of precipitation forming ions in the medium and reaches its maximum value (–6.78 kJ/mol) at concentrations = 50–75 mmol/l.

According to the thermodynamic calculations, it is established that in the systems with the concentrations of phosphate ions and calcium ions of 10 to 200 mmol/l and pH from 0 to 14, the deposition of two of calcium phosphates is most likely: at pH ~ 4.7–6.0 and $C \geq 50$ mmol/l — brushite, at pH>6.0 and $C < 50$ mmol/l — apatite, $Ca_8H_2(PO_4)_6 \cdot 5H_2O$ and β-$Ca_3(PO_4)_2$ metastable phases in the studied conditions.

The theoretical results are confirmed during the experimental study of the system of $Ca(NO_3)_2$–$(NH_4)_2HPO_4$–H_2O, containing equivalent amounts of ions of Ca^{2+} and HPO_4^{2-}: at low concentrations (10–50 mmol/l) at the time of pouring of solution the brushite crystallizes, which as it matures in the system, transformes into hydroxyapatite; at higher contents of ions of Ca^{2+} and HPO_4^{2-} in the systems (≥50 mmol/l) brushite deposits, the size of the crystals of brushite increases during ripening in the solution. The crystallization of brushite takes place in the pH range = 5.00–6.00 at adding a solution of $Ca(NO_3)_2$ to the solution of $(NH_4)_2HPO_4$. The particle size decreases with the decrease of the rate of pouring of the reactants.

It should be noted that the constructed thermodynamic model reflects the possibility of the formation of phases only on the basis of the data about their thermodynamic stability in the standard state. It does not take into account kinetic factors influencing the formation process of the solid phase in the actual conditions.

The concentration of precipitation-forming ions is one of the most important parameters influencing the crystallization process, its direction, velocity, nature and properties of the developing slightly soluble compound. At initially low concentrations of Ca^{2+} and HPO_4^{2-} in the calcium phosphate system, according to the data obtained in the thermodynamic calculations, apatite deposition is possible, whereas, with the increase of the initial concentrations of precipitation-forming ions the supersaturation system increases relative to $CaHPO_4{\cdot}2H_2O$, β-$Ca_3(PO_4)_2$ and $Ca_8H_2(PO_4)_6{\cdot}5H_2O$ and the formation of a mixture of phosphates is thermodynamically probable. Theoretically established regularities were tested in the experiment.

With the methods of XRD, IR-spectroscopy and optical microscopy, it was determined that at the initial time (when pouring reagents) from the solutions with the concentrations of 10 and 25 mmol/l, brushite crystallizes. When the precipitation matures in the mother liquor, small rhombic crystals of brushite mostly transform into apatite; this indicates greater stability of the precipitation in the studied conditions and agrees with the data of thermodynamic calculation. The powders obtained after separation from the aqueous phase and drying are biphasic and consist of brushite and HA (Fig. 2, 3).

In the system where the original concentrations of precipitation-forming ions is 50 mmol/l, brushite crystallizes with impurity of apatite according to IR-spectroscopy and optical microscopy (Fig. 2, 3). However, on the diffractograms of the solid phase obtained under these conditions, only reflexes $CaHPO_4{\cdot}2H_2O$ appear and peaks $Ca_{10}(PO_4)_6(OH)_2$ are absent. This is probably due to the low content of basic calcium phosphate in the composition of the precipitate (less than 5 % from the weight of the total solid phase).

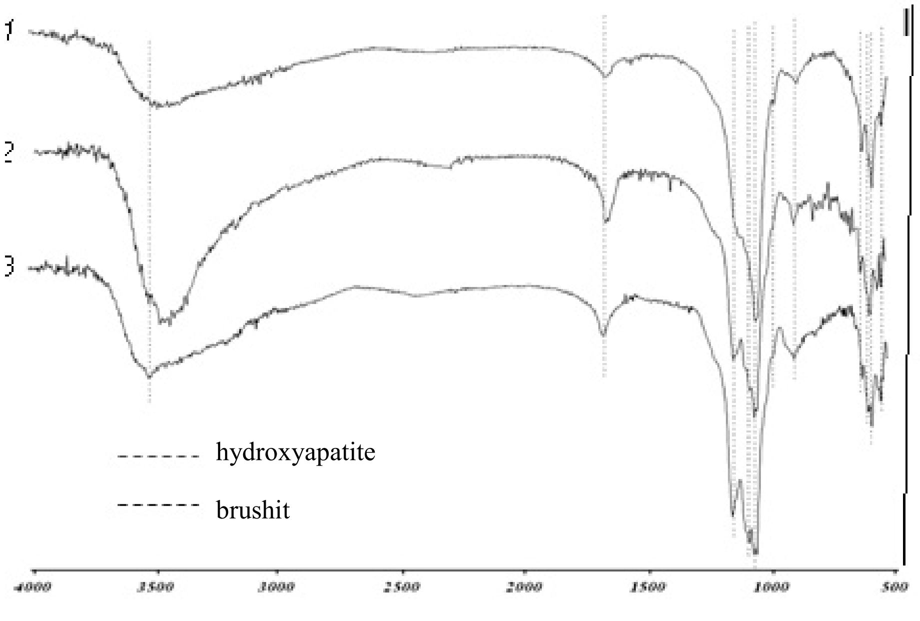

C(Ca^{2+}, HPO_4^{2-})$_{initial}$: *1* — 10 мМ; *2* — 25 мМ; *3* — 50 мМ

Figure 2. IR Spectra of the samples from the systems

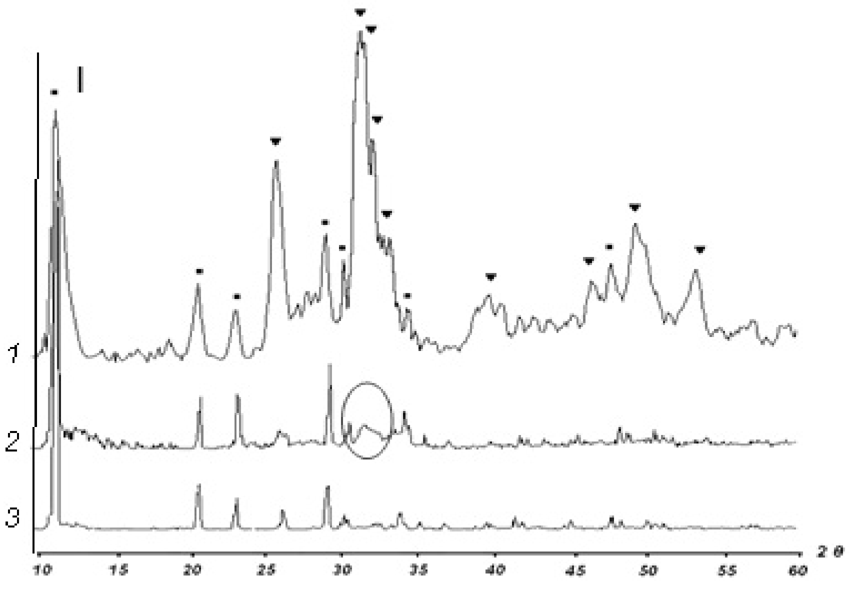

▼ hydroxyapatite ■ brushit

$C(Ca^{2+}, HPO_4^{2-})_{initial}$: *1* — 10 мМ; *2* — 25 мМ; *3* — 50 мМ

Figure 3. Diffractogram of the precipitations from the systems

In the studied systems, crystallization of only brushite phase occurs at higher initial concentrations of calcium ions and phosphate ions ($C \geq 75$ mmol/l). At the initial stage of their formation, the particles have the form of thin prolate plates, diverging rays from the center (Fig. 4*a*). Maturing of the sedimentary substance in the mother liquor leads to the separation of crystals and their enlargement. The greatest growth occurs in the direction of one of the axes, so the ratio of the crystal length to the width is approximately 10:1 (characteristic feature of brushite crystals [12]). The average particle size of the brushite obtained by precipitation in the systems with concentration ≥75 mmol/l is 17.5–22.5 μm.


a *b* *c*

a — at the moment of pouring together; *b*, *c* — 2 days after maturation

Figure 4. Image of brushite particles obtained from the solution with $C_{initial} = 75$ mmol/l

Overall, the results of theoretical and experimental study of the phase formation processes in the system $Ca(NO_3)_2 - (NH_4)_2HPO_4 - H_2O$ agree well with and complement each other. The driving force of the deposition process of brushite was evaluated and the influence of several factors on the regularities of phase formation in the system $Ca(NO_3)_2 - (NH_4)_2HPO_4 - H_2O$ was established. The features of brushite were revealed in the course of comprehensive multicenter study of the spontaneous crystallization of slightly soluble calcium phosphates (controlled by both thermodynamic and kinetic factors). Based on the obtained results it can be stated that further investigation of crystallization of calcium hydrogen phosphate dihydrate in the presence of organic and inorganic substances of biological origin is necessary to clarify the mechanisms of their influence on the processes of mineralization *in vivo.*

Research of the influence of the inorganic anions on the properties of synthetic solid-phase and characteristics of the deposition process

The influence of fluoride ions on the crystallization in the system $Ca(NO_3)_2 – (NH_4)_2HPO_4 – NaF – H_2O$. Theoretically, in the given ionic composition (Ca^{2+}, Na^+, NH_4^+, NO_3^-, $H_2PO_4^-/HPO_4^{2-}/PO_4^{3}$, F^-, H^+, OH^-) the deposition of the following slightly soluble calcium compounds is possible $Ca(OH)_2$, $CaHPO_4{\cdot}2H_2O$, $Ca_8H_2(PO_4)_6{\cdot}5H_2O$, $Ca_xH_y(PO_4)_z{\cdot}nH_2O$, $Ca_{10-x}(HPO_4)_x(PO_4)_{6-x}(OH)_{2-x}$, $Ca_{10}(PO_4)_6(OH)_2$, $Ca_{10}(PO_4)_6F_2$. In the experimental study it was found that in a similar system without the addition of fluoride ions ($pH = 5.50 \pm 0.05$, $t = 22–25$ ºC, $\tau = 48$ h.) the crystallization of only phase brushite occurs — $CaHPO_4{\cdot}2H_2O$. In the presence of anions F^- in the medium of crystallization, the formation of least soluble phase of all currently known calcium phosphates — fluorapatite is probable. Therefore, the experiment on the crystallization of the solid phase in the presence of fluoride ions, whose content in the system ranged from $1.06{\cdot}10^{-5}$ to $1.06{\cdot}10^{-2}$ mol/l (the minimum concentration corresponds to the content of F^- in human stomatic fluid), was conducted to study the influence of fluoride ions on the process of phase formation in the studied conditions.

The study of the obtained solid phases by IR-spectroscopy showed that the value of the initial concentration of fluoride ions has a significant impact on the nature of the crystallizing substance. With the increase of C_{F^-} in the system, there is a change of the type of crystallization process: brushite → mixture of brushite and hydroxyl/fluoro-apatite → fluorapatite.

The analysis of IR spectra of samples synthesized at higher concentrations of fluoride ions (0.53–1.06 mmol/l) showed that in these conditions the formation of additional crystal phase occurs, probably of fluoro-substituted non-stoichiometric hydroxyapatite $Ca_{10-x}(HPO_4)_x(PO_4)_{6-x}(OH)_{2-2x}F_x$. In this case, the samples are biphasic. The complex structure of the spectrum in the near infrared region (ranges 500–650, 1000–1200 cm^{-1}) proves it. Absorption bands of brushite and apatite are jointly present in this region. With further increase of the initial content of F^- in the system (≥5.30 mmol/l), fluorapatite ($Ca_{10}(PO_4)_6F_2$) is presumably the prevaling component of the obtained precipitate. This is evidenced by the presence of intense peaks at 1040 and 1090 cm^{-1} triply degenerate mode of antisymmetric valence vibration of P–O (ν_3) in the composition of apatite and a broad flat absorption band in the range 3300–3500 cm^{-1} (Fig. 5).

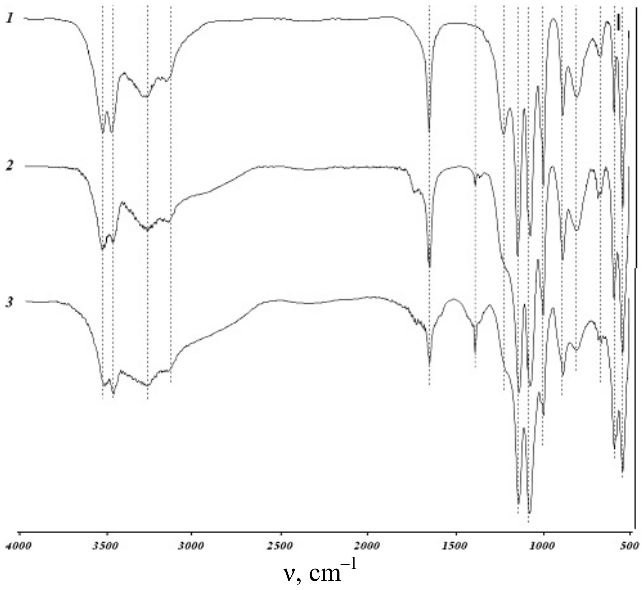

1 — brushite (50mM); *2* — C(F⁻) = 53 mM; *3* — C(F⁻) = 106 mM

Figure 5. IR spectra of solid phases from the solutions without additives and with the impurity of fluoride ions

The conducted analysis of variance of all obtained solid phases showed that the particle size increases with the increase of initial concentration of the additive of fluoride ions in the initial crystallization medium (Fig. 6). Thus, the precipitations obtained from the solutions with $C_{F^-} \leq 106$ μm have large size

(D_{modal} ~ 50–100 micron) compared to brushite, which precipitation occurred in the medium without additives. The increase of fluorine content in the initial solution leads to a further increase in the particle size of the precipitation. Thus, at C_{F^-} = 1.06 mm, the diameter of particles is about 170 µm.

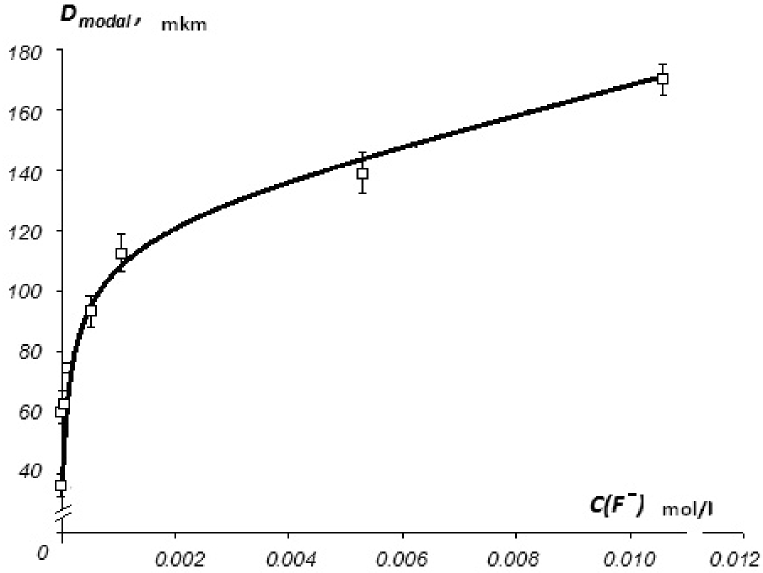

Figure 6. Dependence of the diameter of the particles on the concentration of the fluoride ions in the system

The presence of one peak on the differential curves of the particle size distribution (Fig. 7, 8) indicates a predominance of particles of certain diameter in the composition of the samples extracted from the solutions with C_{F^-} = 0–1.06 µm. For the samples of fluorapatite obtained at 5.30 µm ≤ C_{F^-} ≤ 10.6 µm, the differential curves have two maxima (Fig. 8); therefore, the solid phase is primarily composed of particles of two fractions, for which $D_{modal(1)}$ = 100–200 µm and $D_{modal(2)}$ = 400–500 µm.

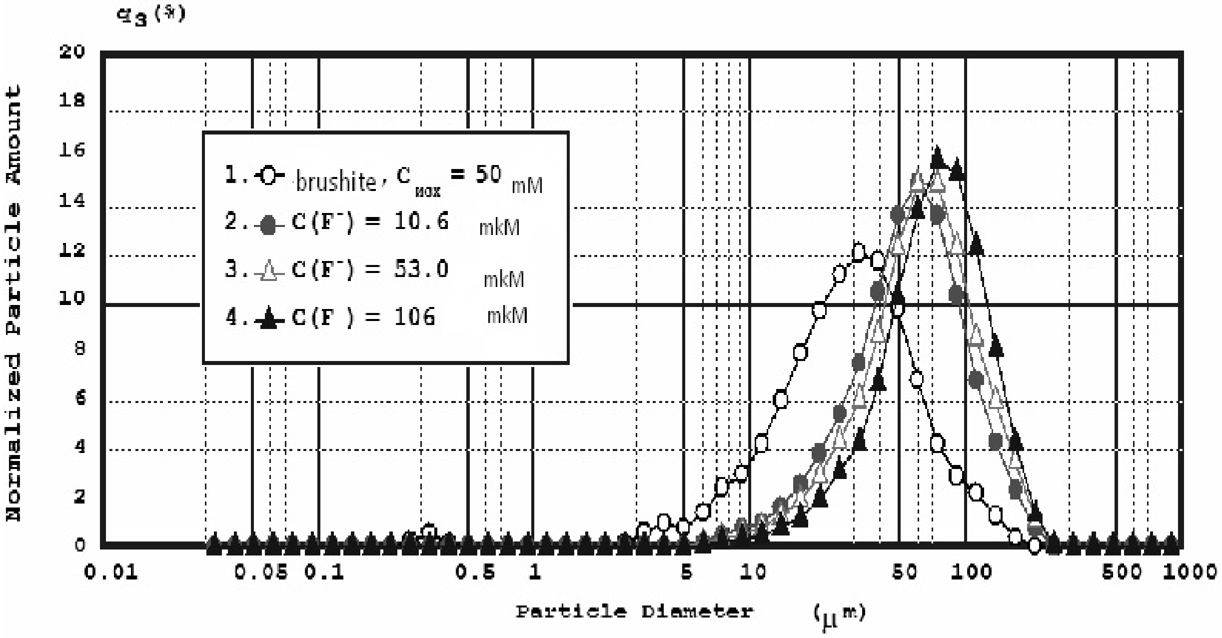

Figure 7. The differential curves of particles size distribution of the solid phases obtained at C_{F^-} = 10.6–106 mkmol/l, µm

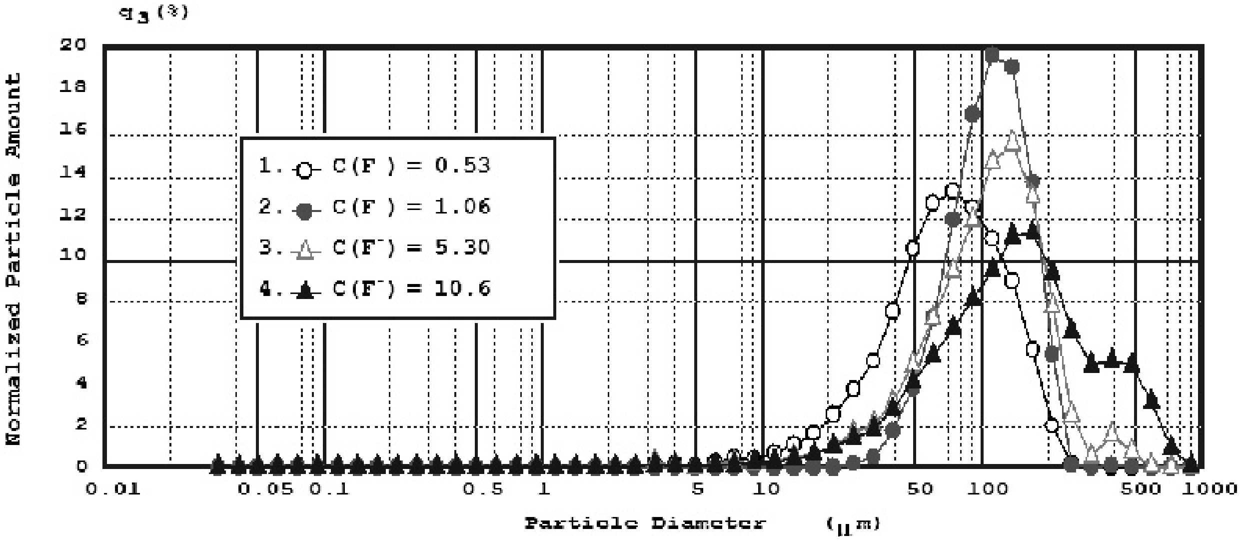

Figure 8. The differential curves of particles size distribution
of the solid phases obtained at C_{F^-} = 0.53–6.10 mkmol/l, µm

The influence of chloride ions on the crystallization in the system $Ca(NO_3)_2 – (NH_4)_2HPO_4 – NaCl – H_2O$. The synthesis of brushite conducted in the presence of chloride ions, whose content in the system was varied in the concentration range 0.010–0.100 mol/l (the content of Cl^- in human stomatic fluid — 0.015 mol/L) to study the influence of additives on the process of phase formation under these conditions.

The study of the obtained phases by the method of IR-Fourier spectroscopy enabled to state that Cl^- ions added to the solution even in a small amount of ($C(Cl) \geq 0.010$ mol/l) cause joint crystallization of brushite and hydroxyapatite. Thus, on the infra-red spectrum of sample absorption there are peaks at 653, 578 cm^{-1} and also 1135 and 1060 cm^{-1}, which are characteristic for HPO_4^{2-} — groups in brushite, and bands due to variations of water: at 1646 cm^{-1} and a broad band in the region 3500–3000 cm^{-1} with a minimum of 3420 cm^{-1} (Fig. 9).

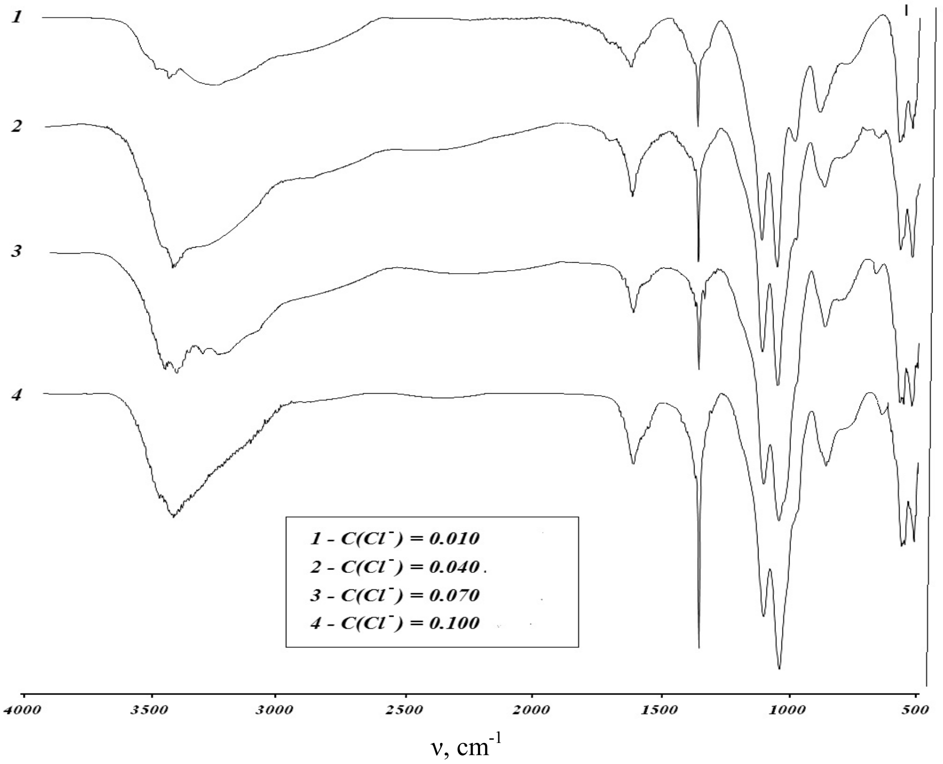

Figure 9. The IR spectra of the synthetic phases in the presence of chloride ions (mol/l)

According to the analysis of variance dispersing composition of synthetic powders the size of the particles of the obtained combinations increases with the concentration of additives in the initial system (see Table). Moreover, for the samples obtained by precipitation from the system with the initial concentration of chloride ions 0.040 and 0.010 mol/l the distribution curves of particle size are bimodal. It indicates the formation of crystals of two fractions (r_{max1} = 30 µm, r_{max1} = 150 µm) (Fig. 10) in the test conditions and shows the presence of two phases in the composition of the precipitation. The dependence with monomodal particle size distribution is characteristic for other synthetic samples, the value of the average diameter of particles ranges from 30 to 70 µm.

Table

Specifications of synthetic solid phases

The concentration of chloride ions in mol/l		Ca/P the precipitate	D, мкм
in the initial solution	solid phase		
0.010	0.002±0.000	1.47±0.04	25.1
0.040	0.002±0.000	1.47±0.04	39.6
0.070	0.005±0.000	1.23±0.13	57.8
0.100	0.008±0.000	1.16±0.04	60.1

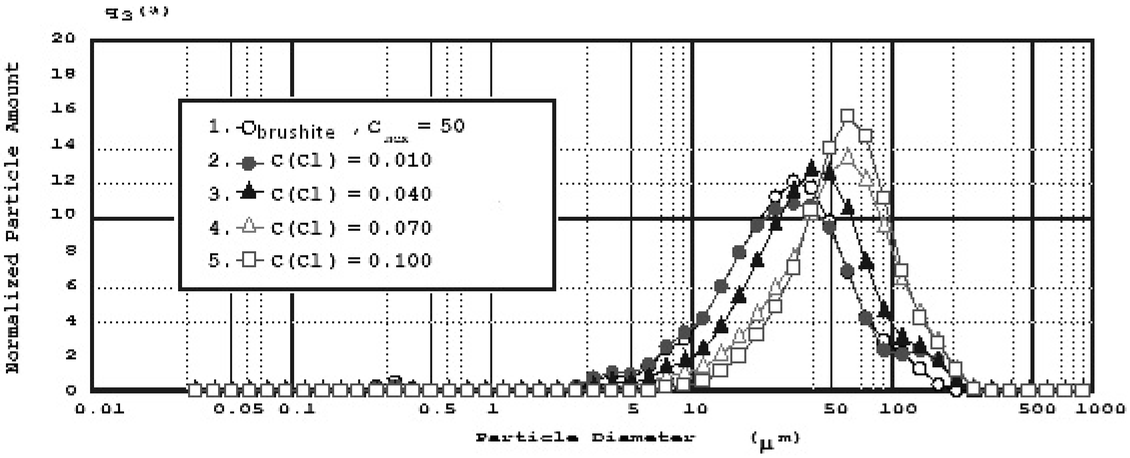

Figure 10. The distribution curve of the particles obtained in the presence of chloride ions (mol/l) in size, µm

The influence of hydrogen carbonate ions on the crystallization ion in the system $Ca(NO_3)_2 - (NH_4)_2HPO_4 - NaHCO_3 - H_2O$. It is known that carbonate ions are a part of the human biological fluid and sometimes may exceed the content of phosphate ions. Therefore, in the following step the influence of hydrocarbonate ions on nature, composition and properties of the precipitated solid phase was studied. The additive concentration ranged from 0.010 to 0.100 mol/l. The investigation by the method of IR-Fourier spectroscopy of the phase composition of the samples obtained from the systems with additives HCO_3^- showed that obtained precipitations are formed with brushite with the admixture of a minor amount of hydroxyapatite, the spectrum is similar (Fig. 9). At this stage of the experimental study it was found that added to the crystallization medium hydrocarbonate ions lead to the precipitation of brushite with the impurity of hydroxyapatite. The increase in the content of the ions of additives in the precipitation is caused by their adsorption on the surface of the solid phase.

The influence of silicate-ions on the crystallization in the system $Ca(NO_3)_2 - (NH_4)_2HPO_4 - Na_2SiO_3 - H_2O$. It is assumed that the bioactivity of the materials is defined by their chemical composition, crystal morphology and properties of surface materials. Therefore, the primary method of managing this property is the chemical modification of calcium orthophosphates. By the example of glass-ceramics produced in the system $CaO–Na_2O–SiO_2–P_2O_5$, it is known that the presence of silicon in the material and at its surface accelerates the union of the implant with the bone. Thus, the use of these materials in medical applications is very promising.

The analysis of the IR-Fourier spectroscopy of the samples with the addition of silicate-ions showed that all precipitations are monophasic and formed by brushite (Fig. 11). There are groups of absorption bands that are characteristic for brushite on the spectra of the obtained samples.

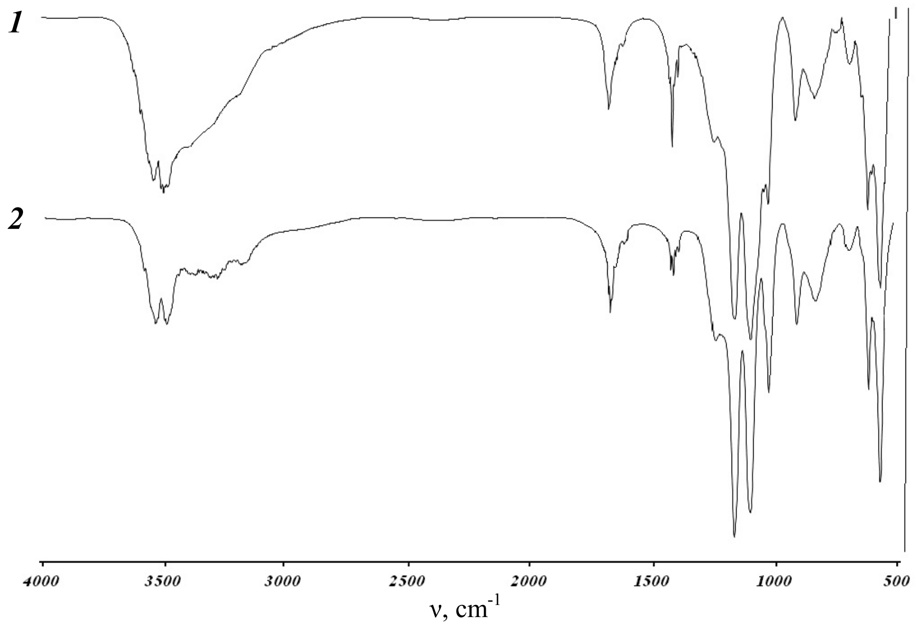

1 — $C(SiO_3^{2-})_{initial}$ = 0.001 M; *2* — $C(SiO_3^{2-})_{initial}$= 0.015 M

Figure 11. IR-spectrum of synthesized phase in the presence of silicate-ions

The study of the influence of organic anions on the properties of synthetic solid phase and characteristics of precipitation process

There are numerous organic components of human biological fluid. It contains simple (albumins, globulins), compound (glycoproteins) proteins, proteins and non-protein nitrogen-containing components — amino acids, urea, et al., as well as carbohydrates and the products of their transformation (pyruvic, citric and acetic acids), vitamins, hormones, lipids, ferment (glycoproteins, mucin, immunoglobulin A, phosphatases, lysozyme, hyaluronidase, ribonuclease and others) [7]. Protein acid-base buffer system plays a role of neutralization, combining the protons of acids with negatively charged groups of aspartate and glutamate: $COO^- + H^+ \leftrightarrow COOH$; the bases are neutralized by a protonated group of radicals of lysine and arginine with the formation of a free amino group and a water molecule: $RN^+H + OH^- \leftrightarrow RNH_2 + H_2O$. The proteins fulfill important functions related to the protection, mineralization processes and participation in digestion. The content of proteins varies within 0.95 — 6.30 g/l according to different authors [6, 7].

The influence of acetate-, citrate- and pyruvate-ions on the crystallization of the solid phase. Three series of syntheses were conducted to study the influence of acetate-, citrate- and pyruvate-ions on the crystallization process of brushite. Organic additives were added into the investigated system $Ca(NO_3)_2 - (NH_4)_2HPO_4 - H_2O$ in the form of sodium salts of the acids, wherein the additive concentration was varied in the range of 10 to 200 mmol/l.

According to IR-Fourier spectroscopy it was revealed that the precipitation of the basic calcium phosphate — hydroxyapatite occurs in the presence, in the medium of crystallization, of additives along with brushite. The increase in the content of impurity ions does not affect the phase composition of the samples. Thus, when the concentration of the additive changes in the range from 10 to 200 mmol/l, after 2 days of maturation, the solid phase is a mixture of brushite and hydroxyapatite (Fig. 12). It is indicated by the joint presence of the absorption bands that are characteristic for these calcium phosphates on the spectra of the samples.

With IR-Fourier spectroscopy it was revealed that under chosen conditions of the synthesis, the impurity ions introduced in the system cause joint crystallization of two calcium phosphates of different stoichiometry. Adsorptive interaction of the ionized form of the additive with the charged regions of the surface of the solid phase leads to the blocking of the active centers of the growth of brushite crystals and the inability of their advancement, i.e. the change of the composition and a more streamlined structure, resulting in the precipitation of an additional phase of apatite.

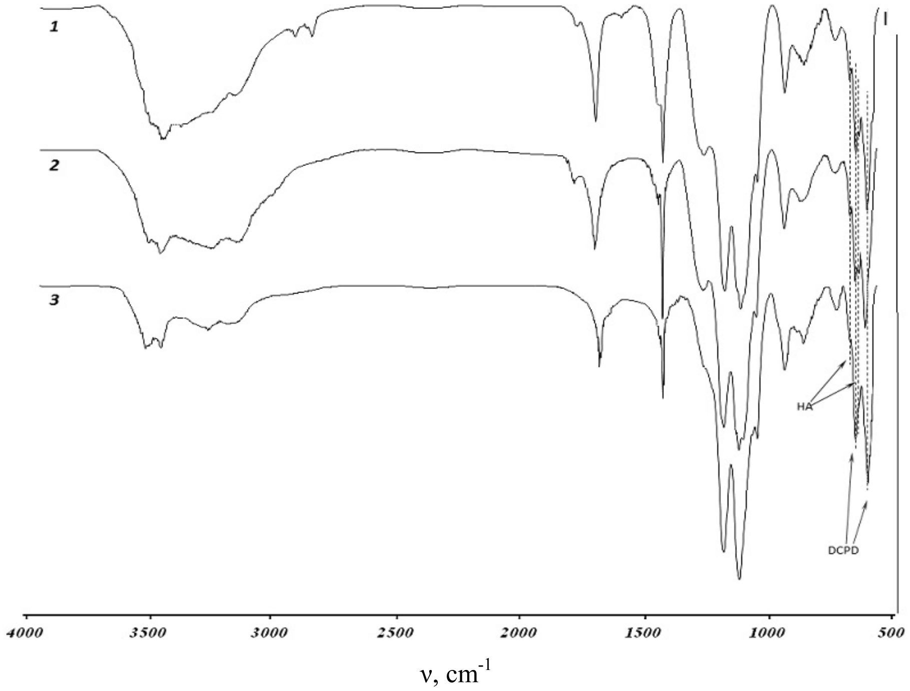

Figure 12. IR-spectra of the synthetic phases obtained in the presence of acetate (1), citrate (2) and pyruvat-ions (3), 200 mkM

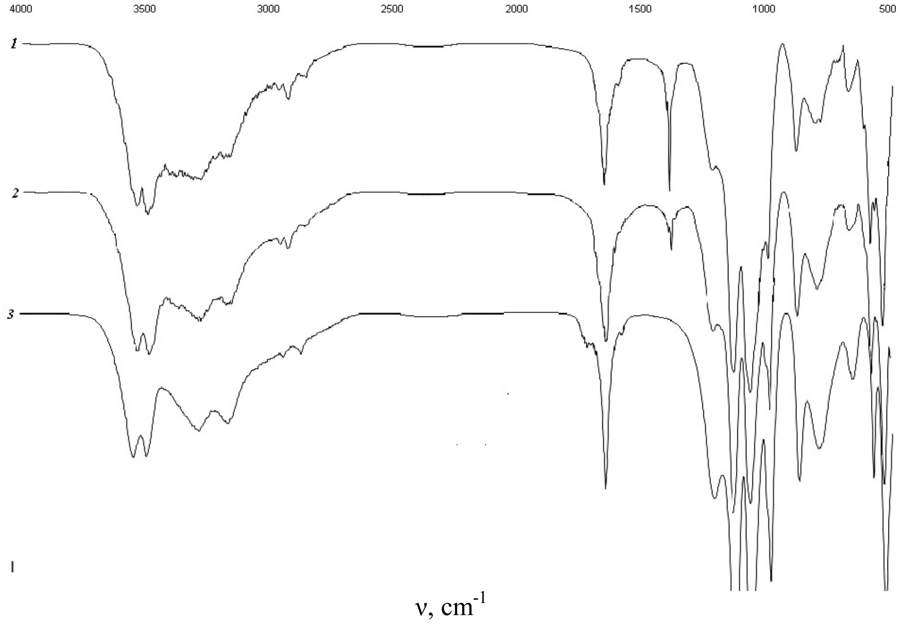

Figure 13. IR-spectra of the synthetic phase obtained in the presence of glucose (1), C_{initial} = 90 mg/l; casein (2), C_{initial} = 1 g/l; gelatin (3), C_{initial} = 2 g/l

The influence of glucose, casein and gelatin on the crystallization of the solid phase. Further we explored the mechanism of the influence of gelatin additives (C_{initial} = 0.5–2.0 g/l), glucose (C_{initial} = 1.8–90 mg/l) and casein (C_{initial} = 0.10–1.00 g/l), the concentration of the latter was chosen based on the data in the composition of human stomatic fluid on the processes of crystallization of the solid phase.

According to the data of IR-spectroscopy, it was established that brushite is present in the composition of precipitations (Fig. 13). Organic component is found in all samples along with the mineral component. On the IR spectra of the samples, the absorption bands of vibrations of bonds of inorganic and organic groups are found: 1010–1050, 600, 570, 480 cm^{-1} — stretching vibrations and deformation vibrations of the bond O–P–O– PO$_4^{3-}$ions; 1420–1460 cm^{-1} — CO$_3^{2-}$ and NO$_3^{-}$ ions; doublet, characteristic for vibrations of the CH bond — in 2980, 2940 cm^{-1}; the absorbance at 640 cm^{-1} — OH. In the near-spectrum region, the intensity is 1650 cm^{-1}, while in the farther there is a broad band of 3150–3400 cm^{-1} corresponding to the vibrations of molecular water.

The conducted studies enabled establishing that the nature of the influence of the organic additives is similar. Organic molecules introduced into the crystallization medium, cause the precipitation of dicalcium phosphate dihydrate with the impurity of apatite phase. Adsorbed on the surface of the solid phase, they inhibit the centers of growth of the germinal crystals of brushite. In addition, there is a possibility for the formation of hydroxyapatite due to the fact that this phase is little resistant under the experimental conditions. As a result, the residual supersaturation of the system is removed by the formation of apatite phase.

Thus, the influence of components of human biological fluids on the possibility and the regularities of the process of precipitation of brushite has been researched. It has been established that the nature of influence of inorganic anions (fluorides, chlorides, hydrocarbonates, silicates) is associated with the change of the phase composition of the crystallizing substance. The influence of organic matter on the process of crystallization is realized by the adsorption mechanism.

This work was partially supported by the Russian Foundation for Basic Research (Grant № 15–29–04839 ofi_m).

References

1 *Abraham J., Grenon M., Sanchez H.J., Perez C., Barrea R.* A case stady of elemental and structural composition of dental calculus during several stages of maturation using SRXRF // Journal Of Biomedical Materials Research. — 2005. — Vol. 75, No 3. — P. 623–628.

2 *Баринов С.М.* Керамические и композиционные материалы на основе фосфатов кальция для медицины // Успехи химии. — 2010. — Т. 79, № 1. — С. 15–32.

3 *Вересов А.Г., Путляев В.И., Третьяков Ю.Д.* Химия неорганических биоматериалов на основе фосфата кальция // Рос. хим. журн. — 2004. — Т. 48, № 4. — С. 52–64.

4 *Dorozhkin S.V.* Calcium orthophosphate cements and concretes // Materials. — 2009. — № 2. — P. 221–291.

5 *Данильченко С.Н.* Структура и свойства апатитов кальция с точки зрения биоминералогии и биоматериаловедения (обзор) // Вестн. СумДУ. Сер. Физика, математика, механика. — 2007. — № 2. — С. 33–59.

6 *Пальчик Т.А., Мороз Т.Н., Леонова И.В., Мирошниченко Л.В.* Минералообразование в организме человека // Биокостные взаимодействия: жизнь и камень: Материалы II Междунар. симпоз. — СПб.: МО РАН, 2004. — С. 186–189.

7 *Голованова О.А.* Патогенные минералы в организме человека. — Омск, 2007. — 395 с.

8 *Пальчик Н.А., Столповская В.Н., Леонова И.В. и др.* Особенности минерального состава и структуры мочевых камней и их распространенность у пациентов из разных районов Новосибирской области // Минералогия техногенеза – 2001. — Миасс: ИМин УрО РАН, 2001. — С. 99–108.

9 *Потапов С.С., Паршина Н.В., Чиглинцев А.Ю. и др.* Статистическое исследование уролитов и уролитиаза жителей Челябинской области // Минералогия техногенеза – 2002. — Миасс: Научмиасс, 2002. — С. 109–123.

10 *Голованова О.А.* Комплексное изучение почечных камней (обзор) // Изв. вузов. Сер. Химия и химическая технология. — 2004. — Т. 47, Вып. 1. — С. 3–12.

11 *Баринов С.М., Комлев В.С.* Биокерамика на основе фосфатов кальция. — М.: Наука, 2005. — 204 с.

12 *Ракин В.И., Каткова В.И.* Неравновесный синтез оксалатов и фосфатов кальция. Образование и трансформация кристаллических фаз. — Сыктывкар: Геопринт, 2005. — С. 16–30.

13 *Васильев В.П.* Аналитическая химия. Кн. 1. Титриметрические и гравиметрические методы анализа. — М.: Дрофа, 2003. — 368 с.

14 *Солоненко А.П., Голованова О.А., Ишутина В.С.* Определение возможности и условий осаждения брушита из водных растворов при варьировании параметров кристаллизационной среды // Бутлеровские сообщения. — 2010. — Т. 21, № 8. — С. 17–27.

О.А.Голованова, М.В.Куимова

Брушиттің сулы ерітінділерден тұнбаға түсу процесінің мүмкіндігі мен заңдылықтарына бейорганикалық және органикалық қоспалардың әсерін зерттеу

Мақалада термодинамикалық есептеулер және тәжірибелік материал негізінде брушиттің қоспалар қатысында кристалдану ерекшеліктерімен байланысты мәселелер комплексі қарастырылды. Ca^{2+} – HPO$_4^{2-}$ – H$_2$O – қоспалар жүйесіндегі фазатүзілу заңдылықтары компоненттердің концентрациялары және pH-тың әр түрлі мәндерінде зерттелді. Кристалданатын фазаның құрамына және тұнбаға түсуіне силикат-, фторид-, хлорид- және гидрокарбонат-иондарының әсері зерттелді. Бастапқы жүйеден брушит және кальцийдің басқа фосфаттарының бірігіп тұнбаға түсетіні көрсетілді. Органикалық қоспалардың әсерін зерттеген кезде олардың брушиттің апатитті фаза қоспаларымен бірге тұнбаға түсетіні анықталды.

О.А.Голованова, М.В.Куимова

Изучение влияния неорганических и органических добавок на возможность и закономерности процесса осаждения брушита из водных растворов

В статье на основе термодинамического расчета и экспериментального материала рассмотрен комплекс проблем, связанных с особенностями кристаллизации брушита в присутствии добавок. Исследованы закономерности фазообразования в системе $Ca^{2+} – HPO_4^{2-} – H_2O$ – добавки в широком интервале варьирования концентраций компонентов и pH. Изучено влияние силикат-, фторид-, хлорид- и гидрокарбонат-ионов на осаждение и состав кристаллизующейся фазы. Получено, что из исходной системы совместно осаждаются брушит и другие фосфаты кальция. При изучении влияния органических добавок установлено, что их присутствие приводит к осаждению брушита с примесью апатитовой фазы.

References

1 Abraham J., Grenon M., Sanchez H.J., Perez C., Barrea R.A. *Journal of Biomedical Materials Research*, 2005, 75, 3, p. 623–628.

2 Barinov S.M. *Russian Chemical Reviews*, 2010, 79, 1, p. 15–32.

3 Veresov A.G., Putlyaev V.I., Tretyakov Yu.D. *Russian Chemical Journal*, 2004, 48, 4, p. 52–64.

4 Dorozhkin S.V. *Materials*, 2009, 2, p. 221–291.

5 Danilchenko S.N. *Bull. of the Sumy State University. Series physics, mathematics, mechanics*, 2007, 2, p. 33–59.

6 Palchik T.A., Moroz T.N., Leonova I.V., Miroshnichenko L.V. *BioBone interaction: life and stone*: Proceedings of the II International Symposium, Saint Petersburg: RAS, 2004, p. 186–189.

7 Golovanova O.A. *Pathogenic minerals in human body*, Omsk, 2007, 395 p.

8 Palchik N.A., Stolpovskaya V.N., Leonova I.V. et al. *Mineralogy of technogenesis – 2001*, Miass: RAS, 2001, p. 99–108.

9 Potapov S.S., Parshina N.V., Chiglintsev A.Yu. et al. *Mineralogy of technogenesis – 2002*, Miass: Nauchmiass, 2002, p. 109–123.

10 Golovanova O.A. *Proceedings of the universities. Ser. Chemistry and chemical technology*, 2004, 47, 1, p. 3–12.

11 Barinov S.M., Komlev V.S. *Bioceramics based on calcium phosphates*, Moscow: Nauka, 2005, 204 p.

12 Rakin V.I., Katkova V.I. *Non-equilibrium synthesis of calcium oxalate and calcium phosphate. Formation and transformation of the crystalline phases*, Syktyvkar: Geoprint, 2005, p. 16–30.

13 Vasiliev V.P. *Analytical chemistry. Book 1. Titrimetric and gravimetric methods of the analysis*, Moscow: Drofa, 2003, 368 p.

14 Solonenko A.P., Golovanova O.A., Ishutina V.S. *Butlerov reports,* 2010, 21, 8, p. 17–27.

UDC 536.7

Kh.B.Omarov, Z.B.Absat, S.K.Aldabergenova, N.J.Rakhimzhanova, A.B.Siyazova

Ye.A.Buketov Karaganda State University
(E-mail: aseka5577@mail.ru)

Comparative analysis of arsenates, antimonates and calcium bismuthates based on *E*–pH diagrams

The article presents the potential-pH diagram systems Ca–As–H_2O, Ca–Sb–H_2O, Ca–Bi–H_2O and the analysis of these systems. The stability region is shown for the followings: $Ca_3(AsO_4)_2$, $Ca_3(AsO_4)_2{\cdot}4H_2O$, $Ca(AsO_2)_2$, $Ca(SbO_3)_2$, $Ca_2Sb_2O_7$, $Ca_3(SbO_4)_2$, $Ca_5Bi_{14}O_{26}$, $Ca_2Bi_2O_5$, $CaBi_2O_4$ in oxidizing, recovering and aquatic environments. The data obtained can be used in predicting the occurrence of hydrometallurgical processes, due to the fact that the E–pH diagram characterizes the behavior of ions in solutions of the compounds.

Key words: diagram of the potential–pH, calcium arsenate, calcium antimonate, calcium bismuthate, thermodynamic analysis.

During the production of non-ferrous metals, arsenic, antimony and bismuth are considered as bad contaminants. During copper electrolysis their transition from anode copper in solution happens as a result contamination of the electrolyte occurs. The accumulation of significant amounts of harmful impurities in the electrolyte can lead to increased resistance, viscosity of the solution, as well as the overuse of electricity, and therefore, there is a problem of cleaning electrolyte copper production. The world practice for these purposes uses different methods, whereas the analysis shows that there is still a question of purifying electrolyte, as applied methods do not allow to reach deep purity solutions.

The aim of this study is a comparative analysis of arsenates, antimonates and calcium bismuthates in order to predict the behavior of arsenic, antimony and bismuth in the process of hydrolytic precipitation of calcium compounds.

In metallurgy, the main characteristics of hydro and pyrometallurgical processes are thermodynamic quantities of reaction components that enable to predict the direction of the process, the probability of the meeting, under certain conditions, the value of the thermal effect.

Characteristic physicochemical properties of aqueous solutions, which define the process of dissolution and precipitation of various compounds are pH and electrochemical or redox potential (*E*).

Thermodynamic analysis, based on the construction of diagrams of *E*–pH is a chemical and thermodynamic basis for addressing assessment of the stability limits of the compounds involved in hydrometallurgical processes to flow any reaction and directed synthesis that allows you to monitor the progress of the processes and effectively carry out these processes in industrial environments [1, 2].

Arsenic-, antimony- and bismuth containing systems are insufficiently studied, despite the fact that the elements are circulating in many non-ferrous metallurgical processes, complicating the process flow, thereby reducing their cost-effectiveness. In this regard, based on charting *E*–pH systems of Ca–As–H_2O, Ca–Sb–H_2O, Ca–Bi–H_2O, we graphically show the stability boundaries and formation of calcium arsenates composition of $Ca_3(AsO_4)_2$, $Ca_3(AsO_4)_2{\cdot}4H_2O$, $Ca(AsO_2)_2$–H_2O, calcium antimonates — $Ca(SbO_3)_2$, $Ca_2Sb_2O_7$, $Ca_3(SbO_4)_2$ and calcium bismuthates — $Ca_5Bi_{14}O_{26}$, $Ca_2Bi_2O_5$, $CaBi_2O_4$.

Calculated (Table 1) and constructed (Fig. 1) diagram *E*–pH of the system Ca–As–H_2O at standard conditions (25 ºC and 1 atm. Total pressure) by combining the private system diagram As–H_2O with private diagram of Ca–H_2O is shown.

According to the *E*–pH diagram of the Ca–As–H_2O system forming calcium arsenates in strongly acidic solutions is preferably than arsenite formation of calcium because for deposition of arsenic as calcium arsenite composition $Ca(AsO_2)_2$ solution pH should not be lower than 4.26.

Calculated (Table 2) and constructed (Fig. 2) diagram *E*–pH of the Ca–Sb–H_2O at standard conditions (25 °C and 1 atm. Total pressure) by combining the private system diagram of Sb–H_2O with private diagram of Ca–H_2O is shown.

Table 1

Calculation equations of interacting systems $Ca(AsO_2)_2$ – $Ca_3(AsO_4)_2$ – H_2O at 25 °C

№	Chemical reaction	Electrode reaction
1	$H_2O_{(L)}=O_{2(g)}+4H^+_{(L)}+4\bar{e}$	$E = 1{,}23–0{,}059pH$
2	$H_{2(g)}=2H^+_{(L)}+2\bar{e}$	$E = –0{,}059pH$
3	$H_3AsO_{3(L)}+H_2O_{(L)}=H_3AsO_{4(L)}+2H^+_{(L)}+2\bar{e}$	$E = 0{,}586+0{,}029\ lg[H_3AsO_4]–0{,}029\ lg[H_3AsO_3]–0{,}059pH$
4	$H_3AsO_{4(L)}=H_2AsO_4^-{}_{(L)}+H^+_{(L)}$	$lgK_p = lg[H_2AsO_4^-]–lg[H_3AsO_4]–pH$; pH=2,19
5	$H_2AsO_3^-{}_{(L)}=HAsO_3^{2-}{}_{(L)}+H^+_{(L)}$	$lgK_p = lg[HAsO_3^{2-}]–lg[H_2AsO_3]–pH$; pH=12,10
6	$HAsO_3^{2-}{}_{(L)}=H^+_{(L)}+AsO_3^{3-}{}_{(L)}$	$lgK_p = lg[AsO_3^{3-}]–lg[HAsO_3^{2-}]–pH$; pH=13,41
7	$H_2AsO_{3(L)}^-+H_2O_{(L)}=AsO_4^{3-}{}_{(L)}+4H^+_{(L)}+2\bar{e}$	$E = 0{,}925–0{,}029\ lg[H_2AsO_3^-]+0{,}029\ lg[AsO_4^{3-}]–0{,}118pH$
8	$HAsO_3^{2-}{}_{(L)}+H_2O_{(L)}=AsO_4^{3-}{}_{(L)}+3H^+_{(L)}+2\bar{e}$	$E = 0{,}567–0{,}029\ lg[HAsO_3^{2-}]+0{,}029\ lg[AsO_4^{3-}]–0{,}088pH$
9	$As_{(т)}+3H_2O_{(L)}=HAsO_3^{2-}{}_{(L)}+5H^+_{(L)}+3\bar{e}$	$E = 0{,}647+0{,}019\ lg[HAsO_3^{2-}]–0{,}098pH$
10	$AsO_3^{3-}{}_{(L)}+H_2O_{(L)}=AsO_4^{3-}{}_{(L)}+2H^+_{(L)}+2\bar{e}$	$E = 0{,}170+0{,}029\ lg[AsO_4^{3-}]–0{,}029\ lg[AsO_3^{3-}]–0{,}059pH$
11	$As_{(т)}+3H_2O_{(L)}=AsO_3^{3-}{}_{(L)}+6H^+_{(L)}+3\bar{e}$	$E = 0{,}912+0{,}0196\ lg[AsO_3^{3-}]–0{,}118pH$
12	$HAsO_4^{2-}{}_{(L)}=H^+_{(L)}+AsO_4^{3-}{}_{(L)}$	$lgK_p = lg[AsO_4^{3-}]–lg[HAsO_4^{2-}]–pH$; pH=11,51
13	$H_2AsO_4^-{}_{(L)}=HAsO_4^{2-}{}_{(L)}+H^+_{(L)}$	$lgK_p = lg[HAsO_4^{2-}]–lg[H_2AsO_4^-]–pH$; pH=6,79
14	$H_2AsO_3^-{}_{(L)}+H_2O_{(L)}=HAsO_4^{2-}{}_{(L)}+3H^+_{(L)}+2\bar{e}$	$E = 0{,}585+0{,}029\ lg[HAsO_4^{2-}]–0{,}029\ lg[H_2AsO_3^-]–0{,}088pH$
15	$As_{(т)}+3H_2O_{(L)}=H_2AsO_3^-{}_{(L)}+4H^+_{(L)}+3\bar{e}$	$E = 0{,}4085+0{,}0196\ lg[H_2AsO_3^-]–0{,}078pH$
16	$As_{(т)}+3H_2O_{(L)}=H_3AsO_{3(L)}+3H^+_{(L)}+3\bar{e}$	$E = 0{,}226+0{,}0196\ lg[H_3AsO_3]–0{,}059pH$
17	$AsH_{3(g)}=As_{(т)}+3H^++3\bar{e}$	$E = –0{,}6268–0{,}059pH$
18	$H_3AsO_{3(L)}+H_2O_{(L)}=HAsO_4^{2-}{}_{(L)}+4H^+_{(L)}+2\bar{e}$	$E = 0{,}858+0{,}029\ lg[HAsO_4^{2-}]–0{,}029\ lg[H_3AsO_3]–0{,}118pH$
19	$H_3AsO_{3(L)}=H_2AsO_3^-{}_{(L)}+H^+_{(L)}$	$lgK_p = lg[H_2AsO_3^-]–lg[H_3AsO_3]–pH$; pH=9,24
20	$H_3AsO_{4(L)}=H_2AsO_4^-{}_{(L)}+H^+_{(L)}$	$lgK_p = lg[H_2AsO_4^-]–lg[H_3AsO_4]–pH$; pH=2,19
21	$3Ca^{2+}+2H_3AsO_4=Ca_3(AsO_4)_2+6H^+$	$lgK_p = –3lg[Ca^{2+}]–2\ lg[H_3AsO_4]–6pH$, pH=2,37
22	$3Ca(AsO_2)_2+8H_2O=Ca_3(AsO_4)_2+4H_3AsO_3+4H^++4\bar{e}$	$E = 0.3354–0.059pH$
23	$Ca^{2+}+2H_3AsO_3=Ca(AsO_2)_2+2H_2O+2H^+$	$lgK_p = –lg[Ca^{2+}]–2\ lg[H_3AsO_3]–2pH$ pH=4,26
24	$3Ca^{2+}+2H_3AsO_3+2H_2O=Ca_3(AsO_4)_2+10H^++4\bar{e}$	$E = 0.97975–0.1475pH$
25	$Ca^{2+}+2As+4H_2O =Ca(AsO_2)_2+8H^++6\ \bar{e}$	$E = 0{,}34983–0.07867pH$
26	$Ca_3(AsO_4)_2+Ca^{2+}+6H_2O =$ $= Ca_3(AsO_4)_2\cdot 4\ H_2O + +Ca(OH)_2 +2H^+$	$lgK_p = –lg[Ca^{2+}]–2pH$; pH=11,20
27	$Ca_3(AsO_4)_2\cdot 4H_2O+2\ H_2O=3Ca(OH)_2+2AsO_4^{3-}+6H^+$	$lgK_p = 2\ lg[AsO_4^{3-}]–6pH$; pH=14,20

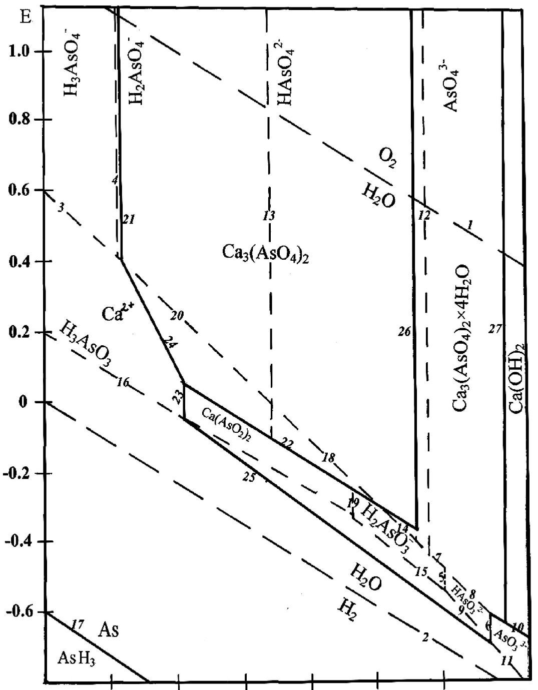

Figure 1. Diagram of E-pH system $Ca(AsO_2)_2$ — $Ca_3(AsO_4)_2$ — H_2O

Table 2

Calculation equations of interacting systems Ca–Sb–H_2O at 25 ºC

№	Reaction equation	Electrode reaction
1	$H_2O_{(L)}=O_{2(g)}+4H^+_{(L)}+4\bar{e}$	$E = 1,23–0,059pH$
2	$H_{2(g)}=2H^+_{(L)}+2\bar{e}$	$E = –0,059pH$
3	$Sb(OH)_2^+ + H_2O= Sb(OH)_3+H^+$	pH=2,17
4	$Sb + 2H_2O= Sb(OH)_2^+ +2H^+ +3\bar{e}$	$E = 0,199 + 0,0197 lg[Sb(OH)_2^+]–0,039pH$
5	$Sb(OH)_3+ 3H_2O= Sb(OH)_6^{-} +3H^+ +2\bar{e}$	$E = 0,729 + 0,118 lg[Sb(OH)_6^-]–0,089pH$
6	$Sb + 3H_2O= Sb(OH)_3+3H^+ +3\bar{e}$	$E = 0,222–0,059pH$
7	$Sb(OH)_2^+ +4 H_2O= Sb(OH)_6^{-} +4H^+ +2\bar{e}$	$E = 0,729 +0,0295 lg[Sb(OH)_6^-]–0,0295 lg[Sb(OH)_2^+]–$ $–0,118pH$
8	$SbH_3= Sb+3H^+ +3\bar{e}$	$E = –0,51–0,0198 lgPSb_3–0,059 pH$
9	$3Ca^{2+}+2Sb(OH)_2^+ +4H_2O=Ca_3(SbO_4)_2+12H^+ +4\bar{e}$	$E = 0,42–0,0443 lg[Ca^{2+}]–0,0295 lg[Sb(OH)_2^+]–0,177pH$
10	$3Ca^{2+}+2Sb(OH)_3+2H_2O=Ca_3(SbO_4)_2+10H^+ +4\bar{e}$	$E = 0,386–0,0443 lg[Ca^{2+}]–0,148pH$
11	$3Ca^{2+}+2Sb+8H_2O=Ca_3(SbO_4)_2+16H^+ +10\bar{e}$	$E = 0,386–0,018 lg[Ca^{2+}]–0,094pH$
12	$2Ca^{2+}+2Sb(OH)_2^+ +4H_2O=Ca_3(SbO_4)_2+12H^+ +4\bar{e}$	$E = 0,42–0,0443 lg[Ca^{2+}]–0,0295 lg[Sb(OH)_2^+]–0,177pH$
13	$2Ca^{2+}+2Sb(OH)_3+H_2O= Ca_2Sb_2O_7+8H^+ +4\bar{e}$	$E = 0,316–0,0295 lg[Ca^{2+}]–0,118pH$
14	$2Ca^{2+}+2Sb+7H_2O= Ca_2Sb_2O_7+14H^+ +10\bar{e}$	$E = 0,386–0,018 lg[Ca^{2+}]–0,094pH$
15	$Ca^{2+}+2Sb(OH)_3=Ca(SbO_3)_2+6H^+ +4\bar{e}$	$E = –0,95–0,0148 lg[Ca^{2+}]–0,089pH$
16	$Ca^{2+}+2Sb+6H_2O= Ca(SbO_3)_2+12H^+ +10\bar{e}$	$E = 0,23–0,006 lg[Ca^{2+}]–0,071pH$
17	$2Sb+ 3Ca(OH)_2+2H_2O=Ca_3(SbO_4)_2+10H^+ +10\bar{e}$	$E = –0,120–0,059pH$
18	$2Sb+ 2Ca(OH)_2+3H_2O=Ca_2Sb_2O_7+10H^+ +10\bar{e}$	$E = –0,012–0,059pH$
19	$2Sb+Ca(OH)_2+4H_2O=Ca(SbO_3)_2+10H^+ +10\bar{e}$	$E = –0,0944–0,059pH$

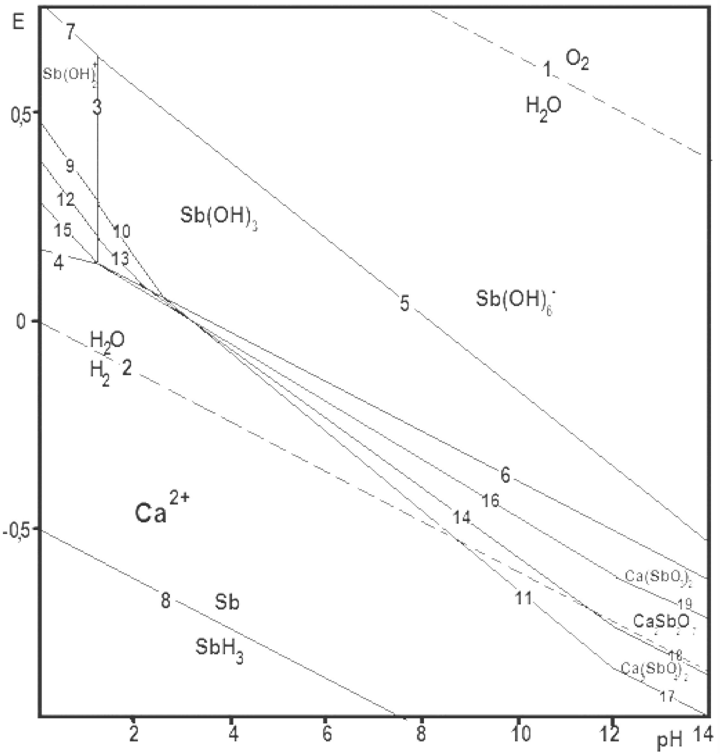

Figure 2. Diagram of *E*–pH system Ca–Sb–H_2O

The first two equations are the equations of the reaction the upper and lower boundaries of the sustainability of water (reaction equations 1, 2). The following reactions at number 3 to 8 meet all the possible interactions of Sb–H_2O, which shows the interaction and existence of dissolved Antimony: $Sb(OH)_2^+$, $Sb(OH)_3$, $Sb(OH)_6^-$, SbH_3 and Sb^0.

Equations numbered from 9 to 19 correspond to the reactions of formation of various calcium antimonates (built based on Sb–H_2O and Ca–H_2O systems). In particular the equations 9, 10, 11, 17 — the boundaries of sustainability of calcium antimonate structure $Ca_3(SbO_4)_2$; Equation 12, 13, 14, 18 — the stability boundary structure of calcium antimonate$Ca_2Sb_2O_7$; Equation 15, 16, 19 — the stability boundary structure of calcium antimonate $Ca(SbO_3)_2$.

Calculated (Table 3) and built (Fig. 3) Diagram *E*–pH of the system Ca–Bi–H_2O at standard conditions (25 °C and 1 atm. Total pressure) by combining the private system diagram of Bi-H_2O with private diagram of Ca–H_2O is shown [3, 4].

Table 3

Calculation equations of interacting systems Ca–Bi–H_2O at 25 °C

№	Reaction equation	Electrode reaction
1	$H_2O_{(L)}=O_{2(g)}+4H^+_{(L)}+4\bar{e}$	$E = 1,23–0,059pH$
2	$H_{2(g)}=2H^+_{(L)}+2\bar{e}$	$E = –0,059pH$
3	$BiH_3 =Bi+3H^++3\bar{e}$	$E = 0,8–0,0591pH–0,0197lgP_{BiH3}$
4	$Bi=Bi^{3+}+3\bar{e}$	$E = 0,215+0,0197lg[Bi^{3+}]$
5	$Bi^{3+}+H_2O=BiOH^{2+}+H^+$	$lg[BiOH^{2+}]/ lg[Bi^{3+}] = –2,0+pH$
6	$2BiOH^{2+}+H_2O=Bi_2O_3+4H^+$	$lg[BiOH^{2+}] = 5,96–2pH$
7	$2Bi+3H_2O= Bi_2O_3+6H^+ +6\bar{e}$	$E = 0,371–0,0591pH$
8	$Bi+H_2O= BiOH^{2+}+H^++3\bar{e}$	$E = 0,254–0,0197pH+0,0197lg[BiOH^{2+}]$
9	$2Bi^{3+}+5H_2O=Bi_2O_5+10H^++4\bar{e}$	$E = 1,759–0,1477pH–0,0295lg[Bi^{3+}]$
10	$2BiOH^{2+}+2H_2O=Bi_2O_4+6H^++2\bar{e}$	$E = 1,792–0,1773pH–0,0591lg[BiOH^{2+}]$
11	$4BiOH^{2+}+3H_2O=Bi_4O_7+10H^++2\bar{e}$	$E = 2,042–0,2295pH–0,1182lg[BiOH^{2+}]$
12	$2Bi_2O_3+H_2O=Bi_4O_7+2H^++2\bar{e}$	$E = 1,338–0,0591pH$
13	$2Bi_4O_7+H_2O=2Bi_2O_4+2H^++2\bar{e}$	$E = 1,541–0,0591pH$
14	$Bi_2O_4+H_2O=Bi_2O_5+2H^++2\bar{e}$	$E = 1,607–0,0591pH$
15	$2Ca^{2+} +6Bi^{3+}+11H_2O=Ca_2Bi_6O_{11}+22H^+$	$pH = 0,42$
16	$2Ca^{2+} +6Bi^0+11H_2O=Ca_2Bi_6O_{11}+22H^++18\bar{e}$	$E = 0,225–00,072pH$
17	$CaBi_2O_4+Ca^{2+}+4Bi^{3+}+7H_2O=Ca_2Bi_6O_{11}+14H^+$	$pH = 1,0$
18	$Ca_2Bi_2O_5 +4Bi^{3+}+6H_2O=Ca_2Bi_6O_{11}+12H^+$	$pH = 1,5$
19	$Ca_5Bi_{14}O_{26} +2BiOH^{2+}+H_2O=5Ca_2Bi_6O_{11}+4H^+$	$pH = 3,73$

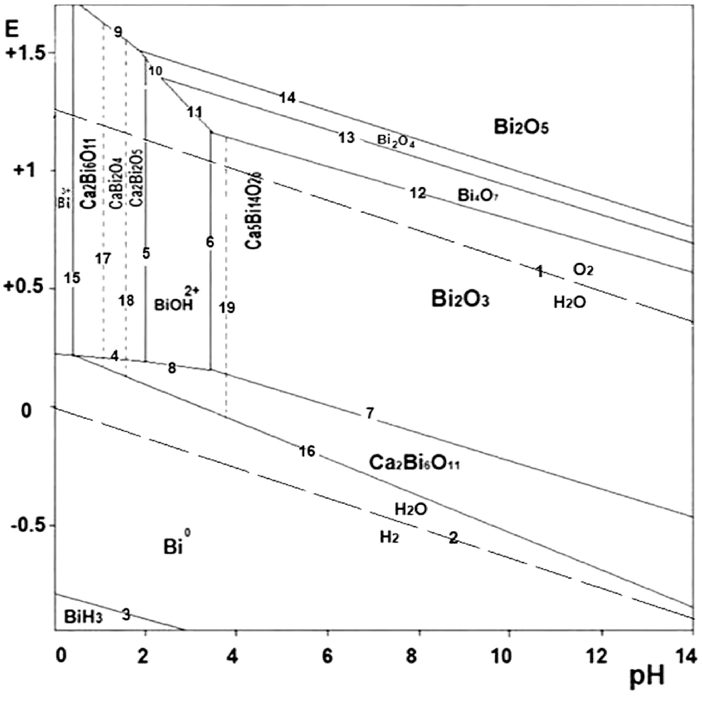

Figure 3. Diagram of *E*–pH systems Ca–Bi–H_2O

The first two equations are the equations of the reaction the upper and lower boundaries of the sustainability of water (reaction equations 1, 2). The following reactions at number from 3 to 14 meet all the possible interactions of the system Bi–H_2O, which shows the interactions and existence of bismuth ions: Bi^0, Bi^{3+}, $BiOH^{2+}$, BiH_3 and bismuth oxide Bi_2O_3, Bi_4O_7, Bi_2O_4, Bi_2O_5.

Equations under the number of 15 to 19 corresponds to the region of existence of calcium bismuthates (systems are built based on Bi–H_2O and Ca–H_2O), in particular, the equations 15 and 16 — the existence of the border calcium bismuthate composition $Ca_2Bi_6O_{11}$. Dash-dotted lines correspond to the boundaries of possible transition bismuthate calcium $Ca_2Bi_6O_{11}$ the next bismuthates: $CaBi_2O_4$ (reaction equation 17), $Ca_2Bi_2O_5$ (reaction equation 18), $Ca_5Bi_{14}O_{26}$ (reaction equation 19).

Such bismuthates as $Ca_3Bi_4O_9$, Ca_7Bi_6O16, $Sa_7Bi_{10}O_{22}$, which subject to limiting interactions of Bi–H_2O system and Ca–H_2O, on this chart are not reflected.

Based on the analysis of the set of diagrams results show that arsenates, antimonates and calcium bismuthates are stable compounds in oxidized, recovered and aqueous media. Calcium arsenate are stable in an oxidizing environment at $E > 0{,}4$ V and the pH range of 2–14; calcium antimonates and calcium bismuthates — throughout the whole pH range. Increase in the number of metal properties in As–Sb–Bi leads to increase of the stability region in the row arsenate – antimonate – calcium bismuthate in acid areas.

References

1 Справочник химика / Под ред. Б.П.Никольского. — Т. 3. — Л.: Наука, 1951. — 1150 с.

2 *Касенов Б.К., Алдабергенов М.К., Пашинкин А.С.* Термодинамические методы в химии и металлургии. — Алматы: Рауан, 1994. — 126 с.

3 *Гаррелс Р.И., Крайст И.А.* Растворы, минералы, равновесия. — М.: Мир, 1968. — 386 с.

4 *Матаев М.М., Алдабергенов М.Қ., Абдраимова М.Р., Досжанова Н.А.* CaO–Fe_2O_3–Bi_2O_3 — жүйесінің триангуляциясы // Теоретическая и экспериментальная химия: Материалы IV Междунар. науч.-практ. конф., посвящ. 80-летию проф. М.И.Бакеева. — Караганда, 2010. — С. 223–227.

Х.Б.Омаров, З.Б.Абсат, С.К.Алдабергенова, Н.Ж.Рахимжанова, А.Б.Сиязова

Кальцийдің арсенаттарын, антимонаттарын және висмутаттарын *E*–pH диаграммасы негізінде салыстыра отырып талдау

Мақалада Ca–As–H_2O, Ca–Sb–H_2O, Ca–Bi–H_2O жүйелерінің *E*–pH диаграммасы көрсетілген және оған талдау жүргізілген. $Ca_3(AsO_4)_2$, $Ca_3(AsO_4)_2{\cdot}4H_2O$, $Ca(AsO_2)_2$, $Ca(SbO_3)_2$, $Ca_2Sb_2O_7$, $Ca_3(SbO_4)_2$, $Ca_5Bi_{14}O_{26}$, $Ca_2Bi_2O_5$, $CaBi_2O_4$ сияқты тұрақты қосылыстардың тұрақтылық аймағы белгіленген. Мақаладағы мәліметтер гидрометаллургия саласында өте қызықты болып табылады, себебі *E*–pH диаграммасы иондар мен қосылыстардың ерітіндідегі қасиетін сипаттайды.

Х.Б.Омаров, З.Б.Абсат, С.К.Алдабергенова, Н.Ж.Рахимжанова, А.Б.Сиязова

Сравнительный анализ арсенатов, антимонатов и висмутатов кальция на основе диаграммы *E*–pH

В статье представлены диаграммы потенциал–pH систем Ca–As–H_2O, Ca–Sb–H_2O, Ca–Bi–H_2O и проведен анализ данных систем. Показаны области устойчивости $Ca_3(AsO_4)_2$, $Ca_3(AsO_4)_2{\cdot}4H_2O$, $Ca(AsO_2)_2$, $Ca(SbO_3)_2$, $Ca_2Sb_2O_7$, $Ca_3(SbO_4)_2$, $Ca_5Bi_{14}O_{26}$, $Ca_2Bi_2O_5$, $CaBi_2O_4$, которые являются устойчивыми соединениями. Данные статьи представляют интерес в гидрометаллургических процессах, в связи с тем, что диаграмма E-pH характеризует поведение ионов, соединений в растворах.

References

1 *Chemist reference book*, Ed. B.P.Nikolsky, Leningrad: Nauka, 1951, 1150 p.

2 Kasenov B.K., Aldabergenov M.K., Pashinkin A.S. *Thermodynamic methods in chemistry and metallurgy*, Almaty: Rauan, 1994, 126 p.

3 Garrels R.I., Christ I.A. *Solutions, minerals, equilibrium*, Moscow: Mir, 1968, 386 p.

4 Matayev M.M., Aldabergenov M.K., Abdraimova M.R., Doszhanova N.A. *Theoretical and Experimental Chemistry*: Materials of IV International scientific-practical conference dedicated to 80th anniversary of prof. M.I.Bakeev, Karaganda, 2010, p. 223–227.

ХИМИЯЛЫҚ ТЕХНОЛОГИЯ ЖӘНЕ МҰНАЙ ХИМИЯСЫ
ХИМИЧЕСКАЯ ТЕХНОЛОГИЯ И НЕФТЕХИМИЯ

УДК 66.097.3

Р.Р.Токпаев, С.А.Абдуллаева, А.А.Атчабарова, А.Т.Кабулов,
К.К.Кишибаев, С.В.Нечипуренко, С.А.Ефремов, М.К.Наурызбаев

*Центр физико-химических методов исследования и анализа
Казахского национального университета им. аль-Фараби, Алматы
(E-mail: rustamtokpaev@mail.ru)*

Углерод-металлические катализаторы для получения целевых продуктов из синтез-газа

В статье получены новые углеродсодержащие носители на основе обогащенных шунгитовых пород и карбонизатов растительного сырья. Исследованы основные физико-химические характеристики носителей, по результатам которых установлено, что лучшими характеристиками обладает носитель на основе карбонизата абрикосовых косточек: удельная поверхность — 480,0 м^2/г, pH водной вытяжки — 9,4, йодное число — 78,6 мг/г, влажность — 1,1 %, зольность — 3,2 %. На основе разработанных носителей методом пропитки с упариванием раствора получены родий-углеродные катализаторы, которые были испытаны в реакциях получения спиртов из синтез-газа. Использование катализаторов позволило получить метанол и этанол с выходом 56,32 и 43,76 %.

Ключевые слова: шунгит, активированный уголь, носитель, катализатор, синтез-газ, этанол, метанол.

Введение

Интенсивное промышленное освоение месторождений, развитие производства, расширение ресурсной базы требуют со стороны государства адекватных мер по защите окружающей природной среды, сохранению биоразнообразия, обеспечению рационального природопользования. Особую опасность для здоровья населения представляют выбросы токсичных веществ в атмосферу [1]. Большинство городов и промышленных центров страдают от загрязнения воздуха выбросами заводов, ТЭЦ, выхлопных газов автомобилей и др. В связи с этим переработка печного газа на сегодняшний день является актуальной проблемой. Основными компонентами, входящими в состав печного газа, являются CO, CO_2, H_2, SO_2 и другие газы, специфичные для каждого индивидуально взятого предприятия, например, для фосфорного производства — это P_2O_5 и PH_3. Для решения данной экологической проблемы используют 2 основных метода:

1. Очистка выбросов с помощью абсорбентов и адсорбентов.
2. Сжигание в «факелах» [2, 3].

Одним из наиболее перспективных и эффективных методов борьбы является комплексный подход: очистка печного газа и получение целевых продуктов из синтез-газа. Это становится возможным благодаря использованию каталитических систем [4], в результате действия которых можно получить из синтез-газа ряд продуктов, имеющих практический интерес: метанол и этанол. Метанол является одним из основных продуктов многотоннажной химии, широко используется для получения формальдегида, сложных эфиров, аминов, растворителей, уксусной кислоты и др. Технический этанол, в свою очередь, применяется при производстве лакокрасочной продукции, моющих средств и добавок к топливу.

В настоящее время наблюдается рост научных исследований в области каталитических методов получения спиртов из синтез-газа. Авторами работы [5] исследован механизм синтеза спиртов из синтез-газа на сульфидах переходных металлов. Сульфиды переходных металлов, модифицированные щелочным металлом, представляют собой перспективные каталитические системы для получения спиртов из CO и H_2. В отличие от широко применяемых в промышленности катализаторов на основе оксида меди, сульфидные катализаторы устойчивы к содержащимся в сырье сернистым соединениям.

В работе [6] представлен способ получения спиртов из углеродсодержащего сырья, в котором углеродсодержащее сырье сначала превращают в синтез-газ, затем — в метанол, который впоследствии превращают в уксусную кислоту, далее подвергают этерификации и гидрированию с получением этанола. Предпочтительный катализатор синтеза метанола представляет собой смесь меди, оксида цинка и промотора, например оксида хрома или оксида алюминия.

В настоящее время одним из активных катализаторов процесса получения этанола из синтез-газа является карбонил родия — $Rh_4(CO)_{12}$. Родиевые катализаторы имеют длительный срок службы (2–3 года), для них разработаны надежные и эффективные методы количественной регенерации родия из потерявших активность каталитических систем. Все это позволяет рассматривать родиевую технологию как перспективное направление развития технического оксосинтеза [7].

Вследствие перспективности родиевой технологии авторами настоящей статьи были получены и исследованы родиевые катализаторы на новых углеродсодержащих носителях на основе продуктов обогащения шунгитовых пород Восточного Казахстана, а также карбонизатов растительного сырья (абрикосовые косточки, скорлупа грецкого ореха).

Шунгитовые породы — невостребованное углерод-минеральное сырье, которое представляет собой отходы других производственных процессов. Шунгитовые породы образуют природные толщи и отвалы после добычи и обогащения полиметаллических руд, ресурсы которых достаточны для использования в промышленных масштабах. Растительное сырье для получения носителей, представленное в виде абрикосовых косточек и скорлупы грецких орехов, появляется в больших количествах при производстве кураги, соков, зерен в Южном Казахстане и в соседних странах Центрально-Азиатского региона.

Цель настоящей работы заключается в получении новых, эффективных углерод-металлических каталитических систем для процессов синтеза спиртов из синтез-газа.

Экспериментальная часть

С целью увеличения содержания углерода в образцах было произведено обогащение шунгитовой руды методом пенной флотации. После флотационного обогащения содержание углерода в образцах увеличилось с 20 % масс. до 45 % масс. Для получения носителей концентрат, обогащенный по углероду, подвергали термической обработке в инертной среде аргона при температуре 800 ºС в течение 1 ч, затем активировали перегретым водяным паром при температуре 850–900 ºС в течение 40 мин, в результате чего происходило увеличение удельной поверхности за счёт выгорания аморфного углерода [8].

Носители на основе растительного сырья были приготовлены аналогично носителям на основе углерод-минерального сырья. Основные стадии: дробление, термическая обработка (карбонизация) в инертной среде аргона при температуре 700 ºС, активация водяным паром при температуре 850–900 ºС. В результате карбонизации растительного сырья происходит выгорание смолистых веществ, гемицеллюлозы и др.

Традиционными методами были определены основные физико-химические характеристики полученных носителей согласно ГОСТ-методикам. Массовая доля воды (влажность) носителей была определена согласно ГОСТу 12597–67 [9], массовая доля золы (зольность) — по ГОСТу 12596–67 [10], pH водной вытяжки — по ГОСТу 4453–74 [11], сорбционная емкость — по йоду по ГОСТу 6217–74 [12].

Удельная поверхность была определена динамическим методом тепловой десорбции с использованием метода Брунауэра-Эммета-Тейлора (БЭТ) на приборе «Сорбтометр» (РФ).

Получение катализаторов методом пропитки. Метод приготовления катализаторов состоял из нескольких стадий: 10 г носителя на основе растительного и минерального сырья подвергали предварительной сушке при температуре 100–150 ºС, готовили раствор хлористого родия с таким расчетом, чтобы после импрегнирования в исходных носителях содержание родия составляло 1,5 % масс. Импрегнирование проводили методом пропитки (порционно) с упариванием раствора, сушку катализаторов проводили в течение 2 ч при комнатной температуре и затем при 200 ºС в сушильном шкафу.

Синтез спиртов из синтез-газа в присутствии катализаторов. Каталитическую реакцию проводили в проточном реакторе: образец катализатора массой 0,5 г помещали в U-образный реактор. Катализатор подвергали предобработке при температуре 400 ºС в течение 4 ч в потоке инертного газа при скорости пропускания v = 50 л/ч. Затем проводили восстановление катализатора в потоке H_2 при температуре 500 ºС в течение 4 ч. После этого температуру реакции снижали до 200 ºС, давление при этом составляло 1,8 атм., затем через катализатор пропускали газовый поток, соотношение $CO{:}H_2 = 1{:}3$. Температура реакции варьировалась в диапазоне 200–350 ºС. На выходе реактора периодически отбирали пробы при T = 200, 250, 300, 350 ºС, которые анализировали с помощью метода газовой хроматографии.

Газохроматографический анализ. Анализируемый образец объемом 0,2 мкл вводили в устройство для ввода проб газового хроматографа с масс-спектрометрическим детектором Agilent 6890N/5973, нагретое до температуры 240 ºС в режиме деления потока 500:1. Хроматографирование проводили с использованием капиллярной колонки DB-WAXetr длиной 60,0 м, внутренним диаметром 0,25 мм и толщиной пленки 0,5 мкм. Газ-носитель (гелий марки «А») подавали в режиме постоянной скорости, составляющей 1,0 мл/мин. Температуру термостата колонки программировали от 40 ºС (выдержка 15 мин) до 240 ºС (выдержка 5 мин) со скоростью нагрева 15 ºС/мин. Полное время хроматографирования составляло 31 минуту. Температуры интерфейса, квадруполя и источника ионов МСД составляли 240, 150 и 230 ºС соответственно. Полученные данные были обработаны на базе программы Enhanced Data Analysis, масс-спектры полученных пиков хроматограмм сравнивали с библиотеками NIST mass spectral library, Wiley mass spectral library.

Результаты и обсуждение

В результате проведенной работы были получены 3 вида углеродсодержащих носителей:

– образец на основе активированного карбонизата шунгита — носитель № 1;

– образец на основе активированного карбонизата скорлупы грецкого ореха — носитель № 2;

– образец на основе активированного карбонизата абрикосовых косточек — носитель № 3.

Физико-химические характеристики полученных носителей представлены в таблице 1.

Таблица 1

Физико-химические характеристики носителей

Характеристика	Носитель		
	№ 1	№ 2	№ 3
Сорбционная активность по йоду, %	24,6	59,5	78,6
pH водной вытяжки	7,5	9,1	9,4
Влажность, %	1,7	1,2	1,1
Зольность, %	53,7	3,8	3,2
Удельная поверхность, м^2/г	153,2	383,0	480,0

Анализ физико-химических характеристик носителей свидетельствует о том, что носители на основе растительного сырья обладают высокой сорбционной активностью по йоду, что способствует лучшей адсорбции активных металлов на поверхности носителя. pH водной вытяжки носителей на растительной основе смещен в щелочную сторону, что свидетельствует о лучшей сорбционной активности носителей в растворах с кислой средой. Влажность и зольность носителей № 2–3 не выходит за пределы 5 % масс. Это характеризует относительно высокую точность и сравнительно небольшую погрешность при взвешивании носителей для анализов. Как известно, влажность в значительной степени зависит от условий хранения и транспортировки. Носитель на основе минерального сырья имеет низкое значение йодного числа, pH водной вытяжки носит слабощелочной характер, влажность — в допустимых пределах. Высокое содержание золы обусловлено природой происхождения шунгитовых пород. Известно, что в состав шунгитовых пород, кроме углерода входят SiO_2, Al_2O_3, Fe_2O_3 и др., которые, в свою очередь, осуществляют вклад в каталитическую активность носителей.

Из представленных данных следует, что носители на основе растительного сырья обладают более развитой поверхностью, чем носитель на основе минерального сырья. Высокие значения удельной поверхности обусловлены наличием у носителей № 2–3 микропор и субмикропор.

На основе полученных носителей методом пропитки с упариванием раствора была получена серия углерод-родиевых катализаторов для синтеза спиртов из синтез-газа. Содержание активного металла во всех катализаторах составило 1,5 % масс., которое подтверждалось с помощью рентгеновского энергодисперсионного анализа. Маркировка катализаторов произведена в соответствии с нумерацией носителей. На рисунке 1 в качестве примера приведена рентгенограмма катализатора № 2.

Элемент	% масс.
C	90,96
O	4,12
Si	0,33
S	0,18
Cl	1,35
K	0,67
Ca	0,87
Rh	1,52

а — таблица элементного состава

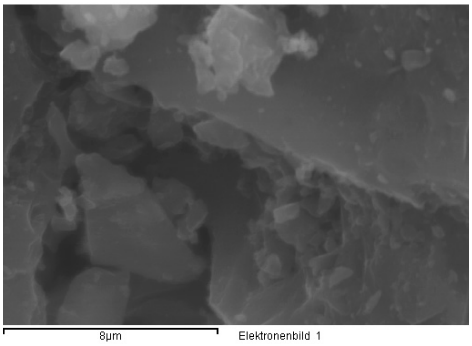

б — микрофотография катализатора, ×2500

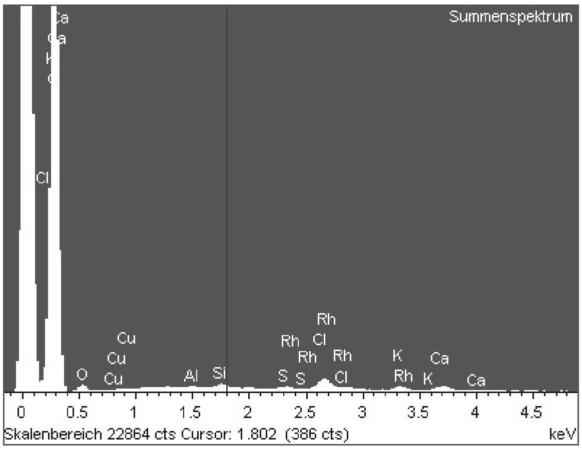

в — рентгенограмма

Рисунок 1. Данные рентгеновского энерго-дисперсионного анализа катализатора № 2

Разработанные катализаторы были испытаны в реакциях получения спиртов из синтез-газа. На рисунках 2, 3 и в таблицах 2, 3 представлены результаты газохроматографического анализа продуктов каталитической реакции при использовании представительных проб катализаторов на основе углерод-минерального и растительного сырья, отобранных при $T = 350$ ºС.

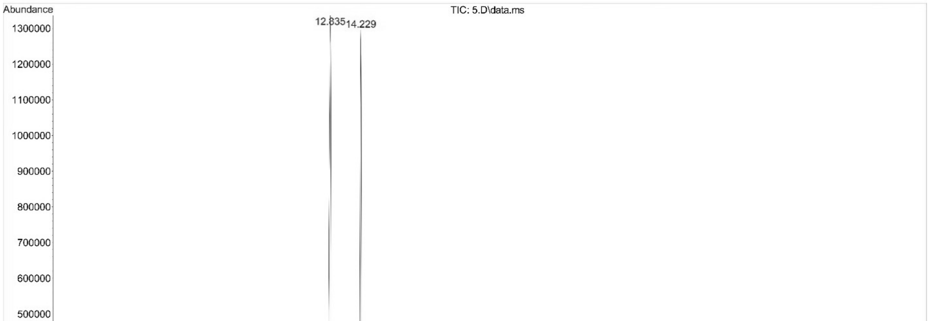

Рисунок 2. Хроматограмма продуктов реакции на катализаторе № 1 ($T = 350$ ºС)

Таблица 2

Продукты каталитической реакции на катализаторе № 1 при *T* = 350 ºC

Соединение	Время удерживания, мин	Площадь пика, у.е.	Выход, %
1-метоксиацетилен	9,201	2557056	1,841
Углекислый газ — CO_2	9,231	866695	0,624
Метанол — CH_3OH	12,835	78241666	56,322
Изопропиловый спирт —$CH_3CH(OH)CH_3$	13,903	2788717	2,007
Этанол — C_2H_5OH	14,229	52414769	37,730
Вода — H_2O	17,621	2050284	1,476

Анализ продуктов реакции при использовании катализатора № 1 (*T* = 350 ºC) свидетельствует об образовании необходимых целевых продуктов: метанола с выходом 56,32 % и этанола с выходом 37,73 %.

Образование метанола протекает по обратимой экзотермической реакции

$$CO + 2H_2 \rightarrow CH_3OH \tag{1}$$

$$-\Delta^0_{298} = 110{,}8 \text{ кДж/моль.}$$

На промышленных установках синтеза метанола чаще всего работают при давлении 20–35 МПа в интервале температур 370–420 ºC. Ввиду высокой экзотермичности реакции и в связи с необходимостью тонкого регулирования температуры, повышение которой отрицательно сказывается как на равновесии, так и на избирательности процесса, в реакционных аппаратах обычно предусмотрен ввод холодного синтез-газа в пространство между полками, на которых размещен катализатор — оксиды меди, с добавками оксидов хрома и цинка. Использование полученных углерод-родиевых катализаторов привело к снижению температуры синтеза: метанол начинает образовываться при *T* = 200 ºC с выходом — 22 % и максимального выхода достигает при *T* = 350 ºC — 56,32 %. Также при синтезе метанола идет образование другого целевого продукта — этанола, по реакции гомологизации метанола

$$CH_3OH + CO + 2H_2 \underset{-H_2O}{\rightarrow} CH_3CH_2OH \tag{2}$$

В качестве побочных превращений при синтезе метанола наблюдается образование углекислого газа, воды, метоксиацетилена и изопропилового спирта, представляющих меньший практический интерес.

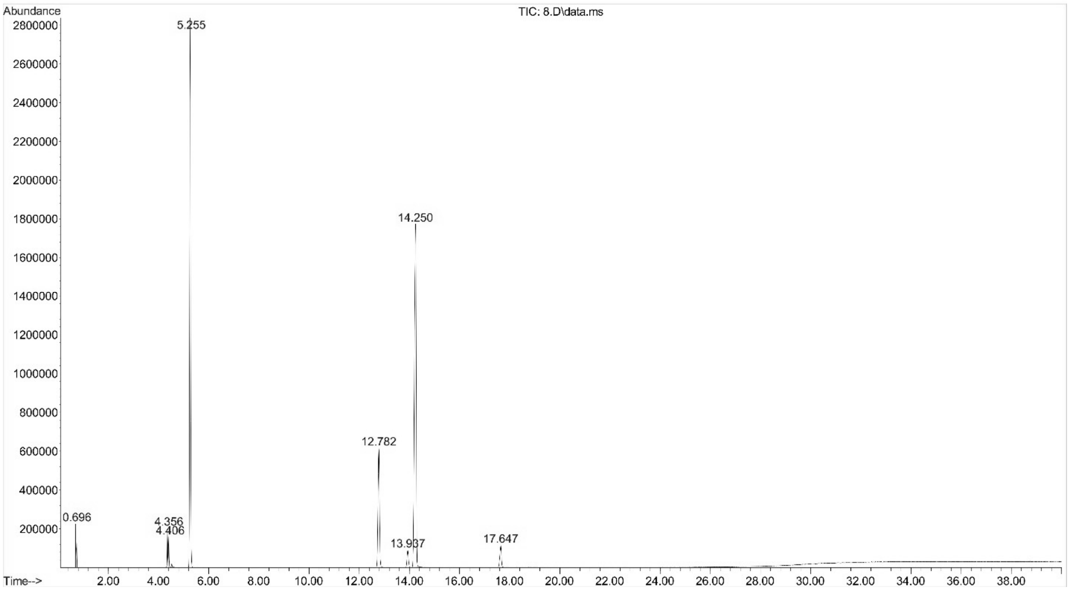

Рисунок 3. Хроматограмма продуктов реакции на катализаторе № 3 (*T* = 350 ºC)

Таблица 3

Продукты каталитической реакции на катализаторе № 3 при T = 350 ºС

Соединения	Время удерживания, мин	Площадь пика, у.е.	Выход, %
Ацетилен — C_2H_2	0,696	3611096	1,753
Изобутан — $(CH_3)_3CH$	4,356	3092628	1,502
Бутан — C_4H_{10}	4,406	2475307	1,202
Этиловый эфир — $C_2H_5OC_2H_5$	5,255	72291418	35,099
Метанол — CH_3OH	12,782	25917472	12,584
Изопропиловый спирт — $CH_3CH(OH)CH_3$	13,937	3538927	1,718
Этанол — C_2H_5OH	14,250	90129996	43,760
Вода — H_2O	17,647	4906746	2,382

Использование катализатора № 3 в каталитической реакции (T = 350 ºС) ведет к образованию основных целевых продуктов: этанола с выходом — 43,76 % и метанола с выходом — 12,58 %. Образование данных продуктов идет по ранее приведённым реакциям (1), (2). В качестве побочных продуктов образуются: вода, ацетилен, изобутан, бутан, этиловый эфир и изопропиловый спирт, некоторые из них также представляют практический интерес.

Для изучения оптимальных параметров получения этанола и метанола из синтез-газа были построены зависимости выхода этанола и метанола от температуры (рис. 4, 5).

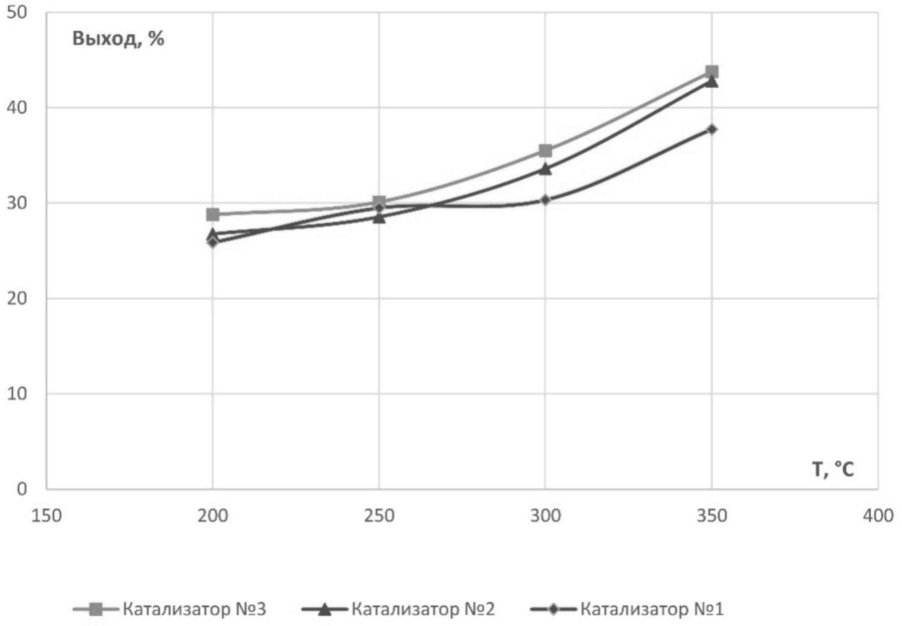

Рисунок 4. Зависимость выхода этанола от температуры

Из данных рисунка 4 можно сделать вывод о том, что с ростом температуры происходит постепенное повышение выхода этанола на катализаторах № 2 и 3 на основе растительного сырья. Катализатор № 1 на основе минерального сырья в интервалах температур 200–300 ºС сохраняет стабильное значение выхода по этанолу, которое незначительно увеличивается при температуре 350 ºС. Возможно, что при температуре выше 350 ºС выход по этанолу увеличится, но при такой температуре происходит возгорание углеродного материала и, как следствие, разрушение углеродсодержащих носителей. Так как катализатор № 3 показал самый высокий выход по этанолу 43,76 %, он может быть рекомендован для процессов получения этанола из синтез-газа при T = 350 ºС.

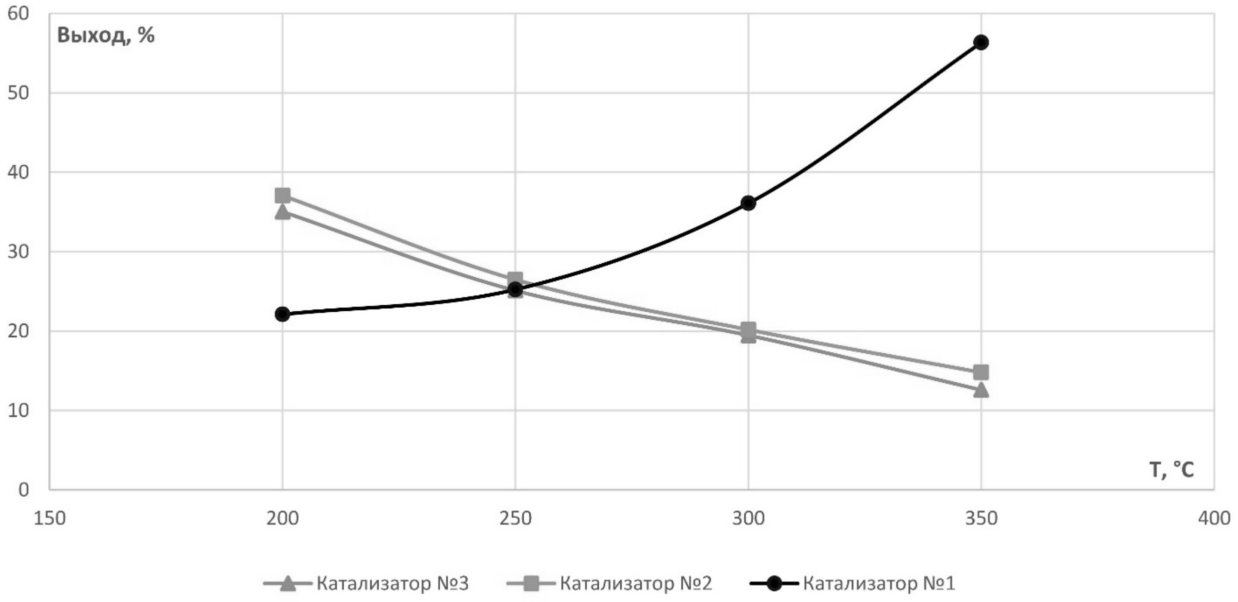

Рисунок 5. Зависимость выхода метанола от температуры

Как показано на рисунке 5 при проведении каталитической реакции в присутствии катализатора на основе углерод-минерального сырья с ростом температуры наблюдается увеличение выхода по метанолу. При использовании катализаторов на основе растительного сырья мы наблюдаем обратный процесс — снижение выхода метанола, что объясняется преимущественным протеканием реакции гомологизации, в которой метанол гомологизирует до этанола. Превалирование данного процесса можно объяснить природой углерод-минерального носителя и наличием других элементов в его составе, помимо углерода. Таким образом, катализатор № 1 проявил высокую каталитическую активность в реакции получения метанола из синтез-газа и может быть рекомендован к дальнейшей промышленной разработке.

Заключение

В ходе выполнения работы были получены и исследованы новые углеродсодержащие носители для углерод-металлических каталитических систем. По результатам анализа физико-химических характеристик установлено, что лучшими характеристиками обладает углеродный носитель на основе карбонизата абрикосовых косточек, удельная поверхность 480,0 м^2/г, pH водной вытяжки 9,4, йодное число 78,6 мг/г, влажность 1,1 %, зольность 3,2 %.

Для получения катализаторов было произведено импрегнирование носителей раствором хлористого родия методом пропитки с упариванием раствора. Содержание родия во всех приготовленных катализаторах составляло 1,5 % масс., которое контролировалось с помощью энергодисперсионного элементного анализа.

Полученные катализаторы были исследованы в реакциях получения целевых продуктов из синтез-газа. Высокую каталитическую активность в реакции получения этанола проявил родий-углеродный катализатор на основе активированного карбонизата абрикосовых косточек. Выход этанола в результате использования данного катализатора составил 43,76 % при T = 350 ºC. При получении метанола высокую каталитическую активность проявил катализатор на основе активированного карбонизата шунгита, выход метанола при этом составил 56,32 %.

Проведенные исследования показывают перспективность использования каталитических систем на основе углеродсодержащих материалов для процессов получения спиртов из синтез-газа.

Список литературы

1 *Варенков А.Н., Костиков В.И.* Химическая экология и инженерная безопасность металлургических производств: Учеб. пособие. — М.: Интернет инжиниринг, 2000. — 382 с.

2 *Криксунов Е.А., Пасечник В.В., Сидорин А.П.* Экология. — М.: Дрофа, 1995. — 240 с.

3 *Чернова Н.М., Былова А.М.* Экология: Учеб. пособие. — М.: Просвещение, 1988. — 272 с.

4 *Мухутдинов Р.Х., Самойлов Н.А.* Теория и практика каталитической очистки отходящих газов. — Уфа: Гилем, 2002. — 252 с.

5 *Дорохов В.С., Елисеев О.Л., Лапидус А.Л., Коган В.М.* Исследование механизма синтеза спиртов из синтез-газа на сульфидах переходных металлов // Сб. тез. докл. VI Молодежной конф. ИОХ РАН, посвящ. 80-летию со дня основания ИОХ РАН. — М.: МАКС Пресс, 2014. — С. 16–17.

6 *Караханов Э.А.* Синтез-газ как альтернатива нефти. — Ч. 2. Метанол и синтезы на его основе // Соросовский образовательный журнал. — 1997. — № 12. — С. 65–69.

7 *Haider M.A., Gogate M.R., Davis R.J.* Fe-promotion of supported Rh catalysts for direct conversion of syngas to ethanol // Journal of Catalysis. — 2009. — Vol. 261, No. 1. — P. 9–16.

8 *Efremov S.A.* Shungite rock processing technology // Russian Journal of Applied Chemistry. — 2010. — Vol. 83, Iss. 1. — P. 23–26.

9 ГОСТ 12597–67. Сорбенты. Метод определения массовой доли воды в активных углях и катализаторах на их основе.

10 ГОСТ 12596–67. Угли активные. Метод определения массовой доли золы.

11 ГОСТ 4453–74. Уголь активный осветляющий древесный порошкообразный. Технические условия. П. 4.7 «Определение pH водной вытяжки».

12 ГОСТ 6217–74. Уголь древесный дробленный. Технические условия. П. 4.4 «Метод определения сорбционной емкости по йоду».

Р.Р.Токпаев, С.А.Абдуллаева, А.А.Атчабарова, А.Т.Кабулов,
К.К.Кишибаев, С.В.Нечипуренко, С.А.Ефремов, М.К.Наурызбаев

Синтез-газдан мақсатты өнімдерді алуға арналған көміртек-металды катализаторлар

Мақалада байытылған шунгит жыныстары және өсімдіктекті карбонизаттар негізінде жаңа көміртек құрамды тасымалдағыштар алынды. Тасымалдығыштардың негізгі физика-химиялық сипаттамалары зерттелді. Нәтижелер бойынша өрік дәнегі карбонизаты негізіндегі тасымалдағыштар жақсы сипаттамаларды көрсетті: меншікті бет ауданы — 480,0 м^2/г, сулы ерітіндісінің pH-ы — 9,4, йод саны — 78,6 мг/г, ылғалдылық — 1,1 %, күлділік — 3,2 %. Ерітінділерді буландыру арқылы сіңіру әдісімен алынған тасымалдағыштар негізінде родий-көміртекті катализаторлар алынды. Олар синтез-газдан спирт алу реакцияларында сынақтан өткізілді. Катализаторларды қолдану шығымдары 56,32 және 43,76 % болатын метанол мен этанол алуға мүмкіндік берді.

R.R.Tokpayev, S.A.Abdullayeva, A.A.Atchabarova, A.T.Kabulov,
K.K.Kishibayev, S.V.Nechipurenko, S.A.Yefremov, M.K.Nauryzbayev

Carbon-metal catalysts for obtaining of desired products from synthesis gas

In this paper, new carbon containing supports based on products of shungite enrichment and carbonizate of raw materials were obtained and studied. The main physico-chemical characteristics of the supports were studied. It was established that the support based on carbonizate of apricot pits has the best characteristics. There are specific surface is 480.0 m^2/g, pH of aqueous extract is 9.4, iodine number is 78.6 mg/g, moisture is 1.1 %, ash content — 3.2 %. Rhodium-carbon catalysts were obtained based on the elaborated supports by method of impregnation with solution evaporation. The studied catalysts were assayed in the obtained catalysts were tested in the obtaining processes of alcohols from synthesis gas. The using of given catalysts have allowed to obtain methanol and ethanol in a yield of 56.32 % and 43.76 %.

References

1 Varenkov A.N., Kostikov V.I. *Chemical ecology and safety engineering of metallurgy industry*: Textbook, Moscow: Internet Engineering, 2000, 382 p.

2 Kriksunov E.A., Pasechnik V.V., Sidorin A.P. *Ecology*, Moscow: Drofa, 1995, 240 p.

3 Chernova N.M., Bylova A.M. *Ecology*: Textbook, Moscow: Prosveshchenie, 1988, 272 p.

4 Mukhutdinov R.Kh., Samoilov N.A. *Theory and practice of the catalytic purification of exhaust gases*, Ufa: Gilem, 2002, 252 p.

5 Dorokhov V.S., Eliseev O.L., Lapidus A.L., Kogan V.M. *Abstracts of the VI Youth Conference IOC RAS, dedicated to the 80th anniversary of the Institute of Organic Chemistry RAS*, Moscow: MAKS Press, 2014, p. 16–17.

6 Karakhanov E.A. *Soros Educational Journal*, 1997, 12, p. 65–69.
7 Haider M.A., Gogate M.R., Davis R.J. *Journal of Catalysis*, 2009, 261(1), p. 9–16.
8 Efremov S.A. *Russian Journal of Applied Chemistry*, 2010, 83, 1, p. 23–26.
9 GOST 12597–67. *Sorbents. Method of water determination in the active carbons and catalysts based on them.*
10 GOST 12596–67. *Active coal. Method of ash content determination.*
11 GOST 4453–74. *Lightening active charcoal powdery coal. Specifications. Section 4.7. pH determination of aqueous extract.*
12 GOST 6217–74. *Crushed charcoal. Specifications. Section 4.4. Method of determination the sorption capacity for iodine.*

УДК 551.311.234.5:631.41

В.А.Бурахта[1], А.В.Сафина[2]

[1]Западно-Казахстанский инновационно-технологический университет, Уральск;
[2]Западно-Казахстанский аграрно-технический университет им. Жангирхана, Уральск
(E-mail: Anastassiya.93@mail.ru)

Изучение физико-химических характеристик глин Западного Казахстана

В статье изучены физико-химические, структурные и сорбционные свойства глин Западного Казахстана. Установлено, что среди исследуемых глин глины Погодаевского месторождения обладают лучшими сорбционными характеристиками. Выявлено, что после обогащения и термической обработки глин их сорбционная способность увеличивается. Полученные результаты позволяют сделать вывод о целесообразности использования данных глин в качестве сорбентов в технологии обезвоживания эмульсий.

Ключевые слова: глинистые породы, физико-химические свойства глин, сорбция, вода, водонефтяные эмульсии.

Введение

В настоящее время исследованию глинистых пород посвящено множество работ, поскольку изучение их физико-химических свойств позволяет не только оценить качество глин, но и рекомендовать их для практического применения в различных отраслях промышленности и народного хозяйства [1].

На сегодняшний день, благодаря особому строению и физико-химическим характеристикам, глины зарекомендовали себя в качестве сорбентов в технологии очистки сточных вод, регенерации отработанных масел, ликвидации разливов нефти, нефтехимии и т.п. [2]. На данный момент в технологии обезвоживания нефти сорбционные свойства глинистых пород недостаточно изучены. В связи с этим изучение физико-химических характеристик глин с перспективой на дальнейшее применение их в качестве сорбентов в технологии обезвоживания нефти является актуальным.

Целью данной работы является определение структурных, физико-химических характеристик глин месторождений Западного Казахстана для выявления их адсорбционных свойств.

Экспериментальная часть

Для изучения адсорбционных свойств исследованы следующие глины: голубые глины Погодаевского месторождения Зеленовского района Западно-Казахстанской области, расположенного в 56 км от г. Уральска недалеко от поселка Погодаево; белые глины месторождения «Союзное» Айтекебийского района Актюбинской области. Для сравнения в качестве стандарта исследована голубая глина марки «Lutumtherapia» (Россия). Структурные и физико-химические характеристики исследуемых глин определяли химическими и физико-химическими методами [3]. Для определения хлорид-ионов использовали метод, основанный на титровании хлорид-ионов в водной вытяжке глинистого сырья нитратом серебра в присутствии хромовокислого калия. Определение железа проводили при помощи атомной абсорбции на атомно-абсорбционном спектрофотометре марки АА-140 в пламени воздух-ацетилен при длине волны 248 нм. Ионы натрия и калия определяли методом пламенной фотометрии на пламенном фотометре марки PFP7 при длине волны 589 нм для натрия и 768 нм для калия. Определение кальция и магния проводили комплексонометрическим методом, основанным на титровании суммы ионов кальция и магния трилоном Б в присутствии индикатора хрома темно-синего и ионов кальция в присутствии индикатора мурексида. С целью определения адсорбционных характеристик глин по отношению к воде их прокаливали в муфельной печи при температурах 200–800 ºC.

Результаты и обсуждения

Для определения адсорбционных свойств исследованы физико-химические характеристики глин Западного Казахстана. Полученные результаты сравнивали с таковыми аптечной глины марки «Lutumtherapia» (Россия). Результаты исследований представлены в таблице 1.

Таблица 1

Физико-химические характеристики глин Западно-Казахстанской области

№	Характеристика глин	Исследуемая глина		
		Погодаевского месторождения	марки «Lutumtherapia»	месторождения «Союзное»
1	Влага, %	0,68	0,41	0,24
2	Показатель адсорбции глин, мг/г	93,75	50,00	30,00
3	Емкость катионного обмена, мг/экв	29,30	15,62	9,30
4	Cl, мг-экв/дм^3	0,45	0,10	0,70
5	Fe_2O_3, масс.%	0,68	0,75	0,24
6	Влагоемкость глин	3,60	1,40	0,30
7	Массовая доля песчанных фракций, %	33,00	0,00	27,00
8	Ca, мг-экв/дм^3	12,30	8,40	4,20
9	Mg, мг-экв/дм^3	13,80	7,50	5,70
10	Сульфат-ионы, мг-экв/дм^3	0,70	0,10	0,90
11	Na_2O, %	1,92	1,03	0,47
12	K_2O, %	0,74	0,55	0,17

Анализ табличных данных показывает, что содержание влаги в глинах колеблется от 0,24 % для глин месторождения «Союзное» до 0,68 % для глин Погодаевского месторождения. Содержание большего количества влаги в голубой глине по сравнению с белой глиной объясняется наличием в первой разбухающих слоев, способных поглощать и удерживать в межслоевом пространстве влагу из окружающей среды [4].

Для оценки сорбционных свойств глинистых пород использовали раствор индикатора метиленового голубого, стандартно применяемого для адсорбционных свойств сорбентов, и по полученным значениям рассчитывали емкость катионного обмена. Согласно полученным данным максимальный показатель адсорбции имеет глина Погодаевского месторождения — 93,75 мг/г, минимальный результат — глина месторождения «Союзное» — 30,00 мг/г. Исходя из полученных данных, рассчитана емкость катионного обмена, максимальное значение которой имеет глина Погодаевского месторождения и составляет 29,30 мг/экв. Сравнение полученных результатов свидетельствует о том, что глина Погодаевского месторождения обладает лучшими адсорбционными характеристиками.

На процесс катионного обмена между адсорбентом и адсорбируемым веществом оказывают отрицательное влияние хлорид-ионы, содержание которых определяли титрованием нитратом серебра. Согласно полученным данным, наибольший показатель содержания хлорид-ионов имеет белая глина — 0,70 мг-экв/дм^3, наименьший соответствует глине Погодаевского месторождения, что свидетельствует о том, что глина Погодаевского месторождения из всех исследуемых глин имеет лучшие способности к ионному обмену.

Для оценки площади удельной поверхности глин, которая коррелирует с их адсорбционной способностью, определяли содержание оксида железа. Согласно полученным результатам исследования глины марки «Lutumtherapia», Погодаевского месторождения и месторождения «Союзное» содержат 0,75, 0,68 и 0,24 % оксида железа соответственно, что говорит о том, что аптечная глина и глина Погодаевского месторождения обладают наибольшей площадью удельной поверхности.

Согласно литературным источникам, ионы кальция, магния, калия и натрия играют ключевую роль в обменном поглотительном комплексе глины [5]. Как показал анализ исходного сырья, глина Погодаевского месторождения содержит наибольшее количество ионов кальция (12,30 мг-экв/дм^3), магния (13,80 мг-экв/дм^3), калия (1,92 %) и натрия (0,74 %) что согласуется с результатами расчета емкости катионного обмена. Это доказывает, что из всех исследуемых образцов глин голубая глина Погодаевского месторождения лучше предрасположена к реакциям ионного обмена.

Для более подробной характеристики глинистых пород нами проведен микроанализ образцов глин съемкой с помощью бинокулярного микроскопа МС-300 (см. рис.).

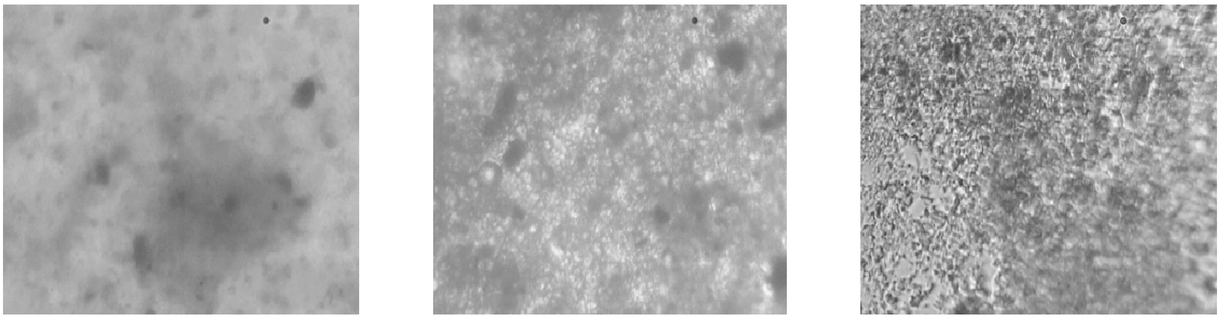

а) аптечная глина, ×100 *б*) погодаевская глина, ×100 *в*) глина месторождения «Союзное», ×100

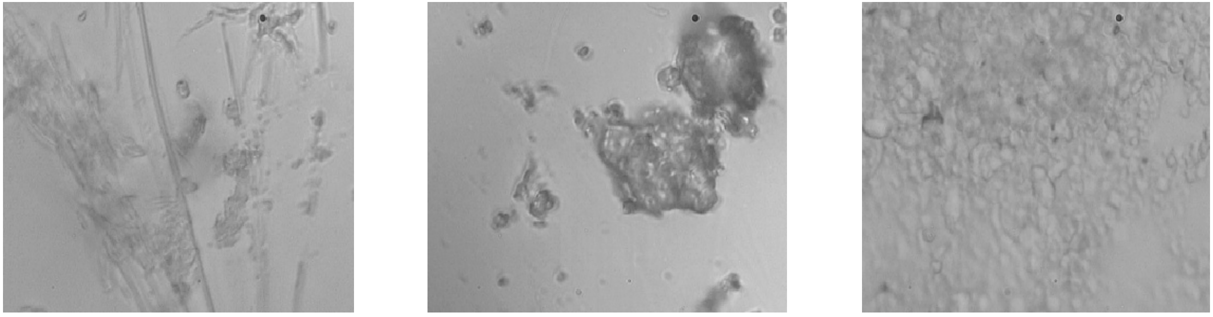

г) аптечная глина, ×1600 *д*) погодаевская глина, ×1600 *е*) глина месторождения «Союзное», ×1600

Рисунок. Микрофотографии глин

Микроструктура аптечной глины (рис. *а*) характеризуется пылевидными частичками, заполняющими пространство между крупными песчаными зернами. Глины месторождения «Погодаево» (рис. *б*) представлены, помимо песчаных и пылевидных зерен, солевыми включениями. Подобную модель описал М.М.Филатов и назвал ее хлопьевидно-ячеистой. Глина месторождения «Союзное» (рис. *в*) представлена отчетливыми песчаными частицами с мелкими соляными включениями. Согласно классификации К.Коллинса и А.Макгауна [6] глинистый минерал (рис. *б*) находится в виде сплошной глинистой матрицы, в которую погружены отдельные песчаные и пылеватные зерна и их скопления, что характерно для сильнонабухающих монтмориллонитовых глин, а минерал (рис. *в*) представлен в виде беспорядочных скоплений, играющих роль связок или мостиков на контактах между пылеватыми и песчаными зернами, что характерно для каолиновых глин.

При увеличении в 1600 раз в глинах Погодаевского месторождения (рис. *д*) видно присутствие первичных глинистых частиц, представленных микрокристаллическими глинистыми минералами, имеющих вид тонких изометричных вытянутых пластин. Помимо этого имеются микрокристаллы аутигенного кальцита, что может свидетельствовать о морском происхождении глинистой породы. При увеличении в 1600 раз в аптечной глине (рис. *г*) наблюдается наличие крупных частиц с четкими контурами, что характеризует преобладание катионов кальция и магния в обменном комплексе. Глина месторождения «Союзное» представлена глинистыми частицами, заполняющими пространство между крупными зернами, образуя мелкоячеистую сетку, что характерно для ячеистой микроструктуры глинистых пород.

Согласно полученным экспериментальным данным можно сделать вывод о том, что наилучшими адсорбционными характеристиками обладают глины месторождения «Погодаево», в связи с этим перспективным является дальнейшее исследование сорбционной способности данных глин в технологии обезвоживания эмульсий.

Для более подробного изучения адсорбционной способности глин месторождения «Погодаево» по отношению к воде нами проведено обогащение глины стандартным методом отмучивания, основанным на отмывке глины от песчаных примесей, с дальнейшим прокаливанием ее при температуре от 200 до 800 ºС. Результаты исследования влагоемкости исследуемых форм глин при нормальных условиях приведены в таблице 2.

Таблица 2

Влагоемкость нативной, обогащенной и термически обработанной глины Погодаевского месторождения

№	Образец глины		Значение влагоемкости, %
1	Нативная		3,6
2	Обогащенная		5,2
3	Термически обработанная при	200 °С	5,6
4	— " —	400 °С	5,7
5	— " —	600 °С	5,9
6	— " —	800 °С	1,9

Как видно из таблицы 2, влагоемкость исследуемой глины после обогащения увеличилась с 3,6 до 5,2 %, т.е. в 1,5 раза, что связано с увеличением концентрации монтмориллонита вследствие удаления пустой породы. После термической обработки происходит увеличение влагоемкости глин, причем максимальное значение влагоемкости соответствует образцу глины, обработанному при 600 °С. Это связано с увеличением порового пространства в структуре минерала монтмориллонита за счет испарения связанной воды и органических примесей. Однако после обработки глин при 800 °С происходит спад значения влагоемкости. Это обусловлено нарушением структуры монтмориллонита и переходом его межпакетного пространства в неподвижное состояние. Таким образом, на основании проведенных исследований можно сделать вывод о том, что максимальной влагоемкостью обладают обогащенные и термически обработанные глины при 600 °С.

Выводы

Таким образом, по результатам исследований структурных, физико-химических и адсорбционных характеристик нами установлено, что наилучшими адсорбционными характеристиками обладают глины месторождения «Погодаево». После процесса обогащения и термической обработки глин, проведенного дополнительно для более точной оценки свойств, определено, что происходит увеличение адсорбционных способностей глин по отношению к воде вследствие удаления пустой породы и увеличения порового пространства. Глины Погодаевского месторождения Западно-Казахстанской области целесообразно рекомендовать в качестве эффективных сорбентов в технологии обезвоживания эмульсий.

Список литературы

1 *Турсынбаева А.* Изучение различных свойств бентонитовых глин для получения строительных материалов // Студенческий научный форум: Материалы V междунар. студ. электрон. науч. конф. — М.: Академия естествознания, 2013. — С. 165–173.

2 *Бурахта В.А., Сафина А.В.* Исследование возможности применения глин в качестве сорбентов в технологии обезвоживания эмульсий // Молодежь и наука в современном мире: Материалы респ. науч.-практ. конф., посвящ. 550-летию Казахского ханства и 70-летию Победы в Великой Отечественной войне. — Уральск: ЗКАТУ, 2015. — С. 172–176.

3 *Нажарова Л.Н., Фомина Р.Е.* Физико-химические свойства силикатного сырья и материалов: Метод. указания к лаб. работам. — Казань: КГТУ, 2008. — 48 с.

4 *Голдовская Л.Ф.* Изотерма сорбции ионов стронция монтмориллонит-гидрослюдистыми глинами // Краткие сообщения. Сорбционные и хроматографические процессы. — 2011. — Т. 11. — С. 165–171.

5 *Дворниченко И.Ф.* Технологические аспекты активации бентонитовых глин // Новое в технологии и технике переработки минерального сырья. — 2013. — № 2. — С. 106–122.

6 *Осипов В.И., Соколов В.Н.* Микроструктура глинистых пород. — М.: Недра, 1989. — С. 31.

В.А.Бурахта, А.В.Сафина

Батыс Қазақстан саз-балшығының физика-химиялық сипаттамаларын зерттеу

Мақалада Батыс Қазақстан облысының сазының физика-химиялық құрылымдық сорбциялық қасиеттері зерттелген. Саз-балшықтардың арасында Погодаев кен орнының саз балшығы ең жақсы сорбциялық сипаттамаларға ие болғандығы анықталды. Саз-балшықты байыту мен термиялық өңдеуден кейін олардың сорбциялық қабілетінің артатыны белгілі болды. Алынған нәтижелер берілген саз-балшықтың эмульсия сусыздандыру технологиясында сорбент ретінде қолдануға мүмкіндік туғызады.

V.A.Burakhta, A.V.Safina

The study of physical and chemical characteristics of clays in Western Kazakhstan

The paper studied the physics-chemical, structural and sorption properties of clays in Western Kazakhstan. It was found that among the studied clay Pogodaev clay deposits have better sorption characteristics. It was revealed that after processing and heat treatment of clays their sorption capacity increases. The results suggest the feasibility of using these clays as sorbents in dewatering technologies emulsions.

References

1 Tursynbayeva A. *Student scientific forum*: Proceedings of the V International Student e-conference, Moscow: Academy of Natural History, 2013, p. 165–173.

2 Burakhta V.A., Safina A.V. *Youth and science in the modern world*: Republican scientific-practical conference, dedicated to the 550th anniversary of the Kazakh Khanate and the 70th anniversary of the Victory in the Great Patriotic War, Uralsk: WKATU, 2015, p. 172–176.

3 Nazharova L.N., Fomina R.E. *Physical-chemical properties of silicate raw materials*: Guidelines for laboratory work, Kazan: KSTU, 2008, 48 p.

4 Goldovskaya L.F. *Brief. Sorption and chromatographic processes*, 2011, 11, p. 165–171.

5 Dvornichenko I.F. *New technology and technology of mineral processing*, 2013, 2, p. 106–122.

6 Osipov V.I., Sokolov V.N. *The microstructure of argillaceous rocks*, Moscow: Nedra, 1989, p. 31.

UDC 662.62.732

K.M.Mamrayeva[1], R.B.Shashchanova[1], M.B.Shashchanova[2]

[1]Ye.A.Buketov Karaganda State University;
[2]Academy «Bolaschak», Karaganda
(E-mail: mamrayeva@mail.ru)

Processing of Shubarkol coal for obtaining chemical products

In the sour coal contain till 35–45 % (on working weight) of gumin of acids, that allows to consider these westers as raw material for reception of chemical substances. As a result of chemical processing sooting coal receive the valuable import-replaced products, which can be used as fertilizer in an agriculture, stabilizers of chisel clay solutions at deep drilling, collectors extending waste water of ions of heavy metals (coop, zinc, lead, mercury).

Key words: coal, gumin of acids, chemical processing of coals, application.

It is well known that the most rational way to increase the economic efficiency of coal mining complex is in the processing of raw coal into the target products at the production site [1].

However, what can be understood by the term «target products»? Coal is so rich with raw materials that the list of products derived from it is around five hundred names. Which of them should be performed? The answer to this question determines all further work on the transition to deep processing of coal at the production site. Let us consider this problem with specific examples.

We will not deal with the problems associated with coking coal of steady sales. The most efficient coal enterprises of Kazakhstan produce mainly coal of D, DG and G grades. These so-called «young» coals are characterized by low calorific value and high demand. However, many of these coals have a low ash content and could be used without enrichment. On the world market, there is only one criterion of value of coal, as well as any fuel — the price of one mega calorie consumer.

The conclusion is, the higher the calorific value of coal becomes, the less the transport component in the price of calories, and, paradoxically, the less the cost of a kilowatt-hour of electricity and Gcal of heat by reducing the cost of internal power station coal is. Thus, the most popular item at the market is a hot commodity high-calorie, low-ash, preferably smokeless, but reactive solid fuel.

In addition, liquid fuels are also of a large and stable demand, as well as the motor ones. Demand for heavy organic liquids such as bitumen and pitch is also being increased. The demand and prices for organic oxygenates, primarily phenol, cresol, xylenols are found to be of high demand and interest.

So, having defined the initial list of products, we shall consider the matter of the technology to be used in developing the products. The main criterion for selecting technologies for processing coal with the desired products produced, is to ensure that their cost will be at least no higher than obtained from alternative raw materials.

The choice must be based on the assessment of current technologies in accordance with the following parameters:

- The presence of the current and forecasted demand on the items produced in Kazakhstan, Russia and abroad;
- The possibility of rapid implementation on an industrial scale;
- Economic efficiency and environmental purity;
- The value of specific capital investment and attractive to potential investors, both in Kazakhstan and abroad.

Nowadays there are more than two dozen coal processing techniques, from simple sorting and enrichment and ending with production of carbon fiber and new forms of carbon. However they have different degrees of readiness for implementation. It would be nice to organize production in Kazakhstan Buckminsterfulleron and sell them out packed in leather briefcases. With the price of crude Buckyball $50 per gram the value of this case study will be a quarter of a million dollars. However, not all even mastered in industry, technologies can be easily implemented in the economic conditions of Kazakhstan.

The attempts to transfer coal into liquid fuel by hydrogenation are of general knowledge. Theoretically, this is a very attractive way, but it is brought to a standstill by some unsolvable technical and economic problems. This is primarily the huge cost of processing in excess of the amount of value added produced. Only the work on the installation of the hydrogenation of coal, together with the processing of heavy oil residues, as part of a petrochemical complex, gives us the hope to reach an acceptable level of profitability. This technology provides a smokeless high-energy solid fuel and liquid low-sulfur fuel. Capital investment unit at $65 per ton processed and refining costs at 6 dollars per ton, provide an opportunity to have a high profitability.

Coal processing technology of soft pyrolysis or, as it is sometimes called in the United States — LPC technology, consists in drying and subsequent heating of coal at 550^0C in an inert atmosphere. The result is a high-energy smokeless char, light fuel oil.

Fuel oil can be divided into gasoline, cresol, diesel fuel and bitumen.

This condition is feasible only in the case of realization of the Russian coal chemists' ideas expressed at the beginning of the century that a mine or its section should be regarded as a component of the so-called energy-technological complex. What does the energy technological complex stand for in contemporary understanding based on modern technologies of coal processing?

It is a complex comprising a number of modular productions that gradually increase added cost to original coal. The first stage of the complex is the introduction of crushing and screening plant that allowing to increase the price of raw coal due to high-quality coal production.

Then, the setting for the briquetting and pelletizing of fine coal is introduced. This allows to avoid coal losses during transportation and to increase the total cost of production. These technologies are widely known and do not require additional comments.

The second step is to build a plant for soft coal pyrolysis of three modules and power plants. This step is also implemented gradually. The introduction of the first module allows to turn high-quality coal into smokeless fuels and light fuel oil, which dramatically increases the efficiency of the entire complex.

Then, the mechanism on distillation to obtain fuel oil diesel cresols and pitch is introduced. Diesel fuel is used in mines and is delivered aside. Cresols are very expensive raw material used for production of plastics and it is highly demanded on the world market. Pitch is used in manufacturing coal briquettes and obtained on the first module of char, it also can also be used in road construction. Smokeless pellets derived from the screenings of char have a price not less than 100–120 dollars per ton. The second module is introduced for processing pellets prepared on its own binder to get a molded coke as a substitute for metallurgical one. The third module is introduced for the processing of pellets from a mixture of semi-coke, limestone and iron ore according to the direct reduction of iron, similar COKEX technology. This technology is becoming more common, forcing the domain industry.

A part of the semi-coke produced at the first module is activated to produce a cheap adsorbent for the purification of water and gases. Such a sorbent, operating on water purification from organic impurities such as phenols, does not require regeneration and can be therefore used at power plants as an additive to the coal, increasing its calorific value. Its expected price comprises $100 per ton.

It is also possible to establish production of the building blocks made of ash and slag, generated during the third module and power station. To solve all these problems the acceleration of the introduction of innovative technologies for processing coal is required. This will improve the economic and environmental conditions in Kazakhstan.

Thus, the energy technological complex consuming non-caking coals of young Kazakhstan, limestone and iron ore, can issue:

- high-quality coal;
- pellets for domestic use;
- molded coke substituting metallurgical coke;
- carbon powder reducing for metallurgy purposes;
- smokeless high-energy solid fuel for power stations
- diesel fuel for motor vehicles; cresols for the chemical industry;
- organic binders (pitch) for road construction;
- electrode and chemical industries;
- cheap absorbents of general use;
- building blocks made of ash and slag materials.

One of the problems associated with the open coal mining is the wastes of coal industry which in most cases do not find practical application. Overburdens containing sooty coal, used to go to spoil and pollute the environment.

Widespread of coal in Kazakhstan, the high value of their organic part necessitate an integrated approach to the use, especially those types of coals, which are not suitable for power generation and coking, and provides a wide range of different products and materials that have no analogues in the processing of other types of natural resources.

Data is necessary for identification existing and working out of new ways of processing of coals for the purpose of reception of gaseous and liquid fuel about laws of decomposition of coal weight in various conditions. Influence of mineral components on thermal destraction coal of the Shubarkolsky deposit is with that end in view studied. Results granulation semicoke structure Shubarkolsky coals are presented in Table.

Table

Results of granulation semicoke structure Shubarkolsky coals

Thermodestruction temperature, ºC	Classes, mm				
	> 40	25–40	13–25	7–13	7
1. The taken class					
50–100 mm	57,1	30,7	9,4	2,8	–
500	48,1	28,1	15,5	4,4	3,3
700	26,1	44,3	18,5	6,8	4,3
900	28,3	29,1	25,0	8,6	9,0
2. The taken class					
6–50 mm	5,2	27,9	40,4	26,5	–
500	–	28,8	36,9	24,6	9,7
700	–	32,4	34,1	25,5	8,0
900	–	20,5	36,9	31,8	10,8

The wastes of previously exposed oxidized coal seams of the Shubarkol deposit itself amount to more than 2 million tons. According to their composition, they can be regarded as a potential raw material.

Among the priorities in the sphere of carbon chemistry one may refer to the research and implementation of industrial technologies and technical solutions of chemical processing of off-balance sheet coal as an organic raw material for the production of humic substances.

It is still an actual and urgent issue for Kazakhstan to establish production of affordable and highly effective sorbents-gatherers and inhibitors of deposits of mineral salts, and corrosion protection of pipelines for the purification of large amounts of waste water. Implementation of the ion exchange purification of waste water from heavy metal ions are constrained by the high cost and scarcity of commercially available cation and anion exchangers.

Humic substances are essential chemical products, widely used as a lignin-alkaline reagent to stabilize the drilling muds, emulsion breakers for the desalting and dehydration of crude oil sorbents for the purification of waste water from heavy metal ions, inhibitors of deposits of mineral salts and pipeline corrosion protection, organic fertilizer for improve soil fertility and productivity of agricultural products [2].

Thus, Kazakhstan has a strong raw material base for the development of high technologies and the creation of the country's chemical industry of chemical processing of the off-balance sheet coal, which has been previously sent to the dumps. The production is important not for the Republic only, it is of great concern abroad too.

The scientific processes of producing organic-mineral fertilizers, lignin-alkaline reagent and corrosion inhibitors are worked out.

The high efficiency of humic fertilizer on different cultures is established in different researches:

– Barayev Institute of Grain Farming (Shortandy village);

– Institute of Soil Science (Almaty city);

– Aral Sea region Research Institute of Agroecology and Agriculture (Kyzyl-Orda city).

The results of the studies show that humic fertilizers increase yield of vegetable crops to 30 % and rice to 22 %. They have not only a fertilizer and soil improving properties, they also have physiological activity.

The results of the research conducted by the Research and Project Institute of Oil and Gas (Aktau city) on the API standard show that the lignin-alkaline reagent quality is not inferior to foreign analogues (SS — 16; carbonox at «BAROID» company), and the cost of CAR is twice or three times cheaper than that of its analogs.

Much of the research is devoted to the practical aspects of chemical processing: development of new technologies of extraction of humic acids in relation to specific coal deposits, their introduction into the production, as well as the search for new fields of application of humic acids and their salts. Fundamental research on the production of inhibitors to protect the pipe from corrosion and coagulant and other modified products from coal are not held. Few studies on modification of humic acids and practical implementation of coal (Kyrgyzstan. Uzbekistan, Russia. Belarus. Estonia and Japan) were held. On a number of coal deposits in the CIS and in Kazakhstan in particular (Maykyuben — West) there are experienced mechanisms of small capacity designed for getting sodium humate.

The data mentioned above show a concern of a number of states of the world community paid to the problems of chemical processing of coal. With state support Kazakhstan for a number of positions could take a leading position in the field of chemical science and technology. The use of off-balance coal for the production of inhibitors of deposits of mineral salts and corrosion protection rude, sorbents for water purification from heavy metals and many other products will solve the problem of import substituted products and environmental problems of the Republic of Kazakhstan. Production of the necessary products from carbon waste is quite competitive with petrochemicals.

Use of an inhibitor (deposition of mineral salts and protecting pipes against corrosion) on the basis of the off-balance coal in the technological cycle of water treatment prevents corrosion of the metal, thereby prolonging the service life of the pipeline. Recycling off-balance coal emitted together with the overburden will reduce pressure on the environment and improve the environment pas open coal mines.

Products of humic acids obtained from the off-balance coal (inhibitors deposits of mineral salts in the water supply piping and pipe protection against corrosion), sorbent for cleaning technical and drinking water from heavy metal ions, a coagulant for drinking water treatment is a new direction in the coal chemistry. They do not have the domestic and foreign analogs.

Humic substances can be used to normalize the situation in non-hazardous areas: Semipalatinsk, Aral and the Aral Sea region (for a set of measures to combat soil erosion, alkalinity, salinity, rich in organic matter, macro- and micronutrients). The use of humic substances improves the physical and chemical properties of soil and binding of heavy metal ions.

One of the major challenges facing the industry of sorbents and adsorbents is to find an alternative source of expanding the range of active carbons with desired and improved performance. Humic products with new properties will be produced from the off-balance coal. Processing and finishing products of the developed technology is waste-free and eco-friendly.

References

1 *Молдыбаев А.Б., Мамраева К.М.* Разработка технологии очистки рудничных и шахтных вод // Респ. конф. молодых ученых: Тез. докл. — Ч. 2. — Алматы: КазНТУ, 2001. — С. 558–578.

2 Патент Казахстана № 2272 / Молдыбаев А.Б. // Промышленная собственность. — 2000. — № 2.

К.М.Мамраева, Р.Б.Шащанова, М.Б.Шащанова

Химиялық өнімдер алу үшін Шұбаркөл көмірін өңдеу процесі

Қазақстандағы көмірлердің химиялық өндірістер аймақтары қарастырылған. Көмірден әр түрлі химиялық заттарды, тынайтқыштарды алу процестері шығымын арттыратындағы дәлелденді. Қазақстанда көмірден шикізатты өңдеудің қазіргі мәселелері, ғылыми ауқымды, экологиялық таза технологияларды қолдана отырып, көмір өндеу өндірістердің даму жолдары зерттелген, сондай-ақ ағынды суларды ауыр металл (мыс, мырыш, қорғасын, сынап) иондарынан тазалау тәсілдері ұсынылған.

К.М.Мамраева, Р.Б.Шащанова, М.Б.Шащанова

Переработка Шубаркольского угля для получения химических продуктов

В окисленных углях содержится до 35–45 % (на рабочем весе) гуминовых кислот, которые позволяют рассматривать эти продукты как сырье для производства химических веществ. В результате химической обработки забалансовых углей получают ценные импортозамещенные продукты, которые используются в качестве удобрения в сельском хозяйстве, в качестве углещелочного реагента для стабилизации буровых растворов, коллекторов, для очистки сточных вод от ионов тяжелых металлов (медь, цинк, свинец, ртуть).

References

1 Moldybaev A.B., Mamraeva K.M. *Republic conf. of young scientists*: Reports, Almaty: KazNTU, 2001, 2, p. 558–578.
2 *The Patent of Kazakhstan № 2272, Moldybaev A.B., The Industrial property*, 2000, 2.

УДК 661.876

Т.Б.Жакибеков, А.Д.Мехтиев, В.В.Югай, О.В.Алдошина

Карагандинский государственный технический университет
(E-mail: barton.kz@mail.ru)

Влияние текстуры хромитовых руд на процессы восстановления

Представлены результаты исследования влияния текстурных особенностей хромитовых руд на процессы углетермического восстановления. Показано, что реакция прямого восстановления оксидов хрома наиболее полно реализуется при непосредственном контакте твердого углерода с хромшпинелидом хромитовых руд. Условие минимальной температуры плавления цементирующей породы хромитовых руд — серпентина является необходимым для оптимизации энергетических затрат при карботермии хромитов. Это условие наиболее полно реализуется при соотношении базовых оксидов SiO_2/Al_2O_3=2,57. Оптимальное соотношение установлено на основе анализа диаграммы состояния конечных шлаков оксидной системы $MgO–SiO_2–Al_2O_3$.

Ключевые слова: хромитовые руды, оксиды хрома, углеротермическое восстановление, хромшпинелид.

Основным технологическим параметром при производстве высокоуглеродистых марок феррохрома является выбор конечного состава шлаков, физико-химические свойства которых (вязкость и электропроводность) определяются свойствами тройной диаграммы оксидной системы $MgO–SiO_2–Al_2O_3$. При этом важное значение имеет подбор состава шлаков в части соотношения MgO/Al_2O_3. Регулирование этого показателя позволяет влиять на качество углеродистого феррохрома по содержанию углерода. Содержание оксида кремния SiO_2 принимается в диапазоне 32–36 %. При соотношении MgO/Al_2O_3=1,7–1,8 и рекомендуемой концентрации SiO_2 достигаются наиболее эффективные технико-экономические показатели процесса, в том числе и минимальный расход электроэнергии. Используемые флюсующие компоненты для формирования рационального состава конечных шлаков содержат оксид кремния SiO_2 и часто, как сопутствующий компонент, оксиды алюминия Al_2O_3. Влияние изменения соотношения SiO_2/Al_2O_3 в составе шлаков производства углеродистых марок феррохрома не исследовалось.

Хромитовые руды южно-кемпирсайского массива имеют различные текстурные особенности [1]. Эти факторы обусловлены природой рудообразующих минералов — хромшпинелидов и формированием сопутствующей породы, представленной в основном серпентином. Особенностью хромитовых руд является четкая, видимая граница раздела рудных минералов, и в зависимости от геометрии границ раздела подразделяют различные типы руд — вкрапленные, полосчатые, нодулярные, сплошные. Вне зависимости от типа текстуры хромитовой руды главной характерной особенностью является чередование минералов — хромшпинелида и серпентина при любом пространственно ориентированном положении. Серпентин — как основная цементирующая связка — обволакивает зерна хромшпинелида, которые имеют обычно размер от 0,5 до 2,5 мм. Текстурные особенности строения хромитовой руды приводят к отсутствию прямого контакта хромшпинелида с восстановителем (кокс, уголь) [2, 3].

Оксид хрома восстанавливается твердым углеродом в результате прямой реакции, возможность газофазного восстановления оксидом углерода в условиях руднотермических электропечей не установлена. Поэтому для развития процессов восстановления, при повышении температуры, необходимо наличие плотного контакта. Однако цементирующая порода (серпентин) препятствует прямому контакту хромшпинелида и кокса. Согласно представленной схеме, поверхность прямого контакта кокса с зернами хромшпинелида, расположенными на гранях куска хромитовой руды, меньше поверхности соприкосновения кокса с серпентином. Рудные зерна шпинели, расположенные в глубине куска хромитовой руды, полностью окружены цементирующей связкой, что препятствует прямому контакту с восстановителем (рис. 1).

Наиболее распространены хромитовые руды средней вкрапленности (рис. 1*б*, *в*). В случае густовкрапленной руды (рис. 1*е*) поверхность контакта хромшпинелида с коксом будет больше. Если руда представлена редковкрапленными разновидностями, точки контакта снижаются. Полосчатые руды (рис. 1*д*) будут приводить к чередованию полного контакта и отсутствия взаимодействия хромшпинелида и кокса. Самый приемлемый вариант полного контакта хромшпинелида с коксом — это наличие руды с массивной текстурой. Однако такая руда содержит более 58 % оксида хрома и практически не используется.

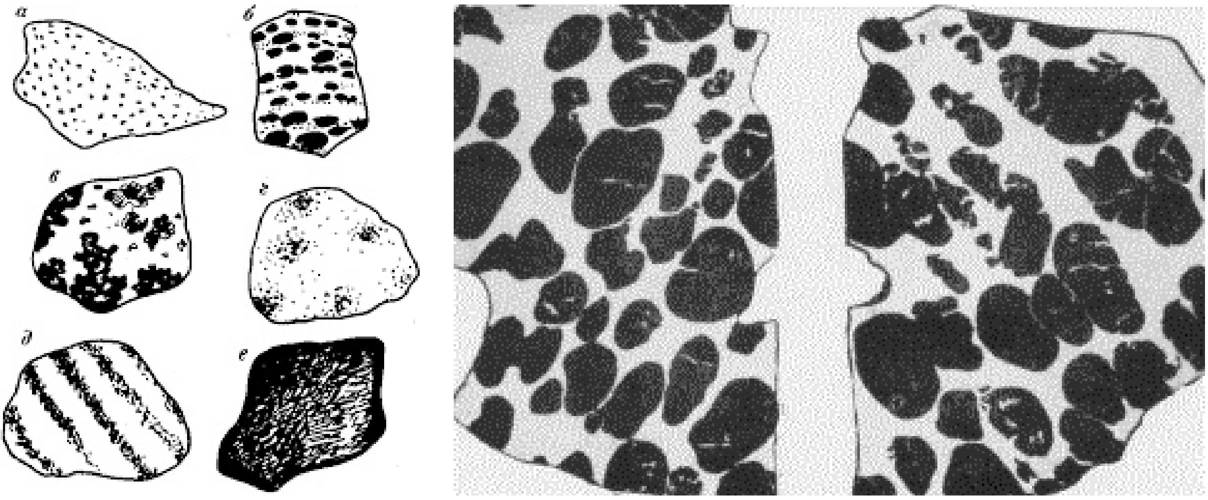

Рисунок 1. Текстура выделений хромшпинелидов

Из анализа текстурных особенностей хромитовых руд и ее взаимодействия с восстановителем следует, что в большинстве случаев отсутствует полное взаимодействие шихтовых материалов.

Кемпирсайские хромитовые руды в своем составе содержат хромшпинелиды, представленные в основном магнохромитом. В тетраэдрических позициях хромшпинелидов располагаются Mg^{2+} и Fe^{2+}, а в октаэдрических позициях — Cr^{3+}, Al^{3+} и Fe^{3+}. Катионный состав хромшпинелидов находится во взаимосвязи с минеральным составом связки.

Согласно [4, 5] хромшпинелиды представлены формулами

$$Mg_{0,62}Fe_{0,05}(Cr_{0,71}Al_{0,015}Fe_{0,14})O_{3,67}$$

$$Mg_{0,54}(Cr_{0,72}Al_{0,4}Fe_{0,14})O_{3,54}$$

Формульный состав хромшпинелидов имеет большое значение для установления химизма и механизма протекания реакции восстановления, образования металлической и оксидных фаз.

Хромшпинелиды не содержат кремния, кальция и других катионов, ионные радиусы которых имеют значения 0,100–0,044 нм.

Согласно экспериментальным и теоретическим исследованиям восстановление оксидов хрома возможно только прямым путем, т.е. при непосредственном взаимодействии хромита с твердым углеродом.

Термохимические константы реакций взаимодействия кислородных соединений хрома с углеродом [6]

$$1/3Cr_2O_3 + 13/9C = 2/9Cr_3C_2 + CO \qquad T_H = 1134\ ^\circ C \qquad (1)$$

$$1/3Cr_2O_3 + 9/7C = 2/21Cr_7C_3 + CO \qquad T_H = 1147\ ^\circ C \qquad (2)$$

$$1/3Cr_2O_3 + 27/23C = 2/69Cr_{23}C_6 + CO \qquad T_H = 1223\ ^\circ C \qquad (3)$$

$$1/3Cr_2O_3 + C = 2/3CrC + CO \qquad T_H = 1260\ ^\circ C \qquad (4)$$

$$Cr_7O_3 + C = 2CrC + CO \qquad T_H = 1207\ ^\circ C \qquad (5)$$

Очевидно, что прямому взаимодействию препятствует серпентин как цементирующая порода, в объеме которого находятся зерна хромшпинелидов. Для высвобождения зерен хромшпинелидов из массы серпентина необходимо постепенное размягчение, оплавление серпентина и ее стекание. При этом более тугоплавкие кристаллы хромшпинелида ($T_{пл}$~2100 °С) имеют возможность полного взаимодействия с коксом под воздействием давления верхних слоев шихтовых материалов. В противном случае восстановительные процессы не будут развиваться. Таким образом, для успешного восстановления хромитовой руды необходимо, чтобы серпентин оплавился и освободил зерна хромита.

Температура плавления серпентина напрямую зависит от его химического состава. Общая формула серпентина — $3MgO{\cdot}2SiO_2{\cdot}2H_2O$. Согласно тройной диаграмме MgO–SiO_2–Al_2O_3 температура плавления серпентина составляет 1700 °С. При наличии флюса (отсевы кварцита ~98 % SiO_2) нижняя температура плавления серпентина составит 1557 °С (эвтектическая точка двойной системы

$MgO–SiO_2$). Эта теоретическая температура плавления серпентина хорошо согласуется с экспериментальными исследованиями [7–9]. Таким образом, реальные температуры восстановления большинства зерен хромшпинелидов составляют более 1557 °С, т.е. после развития процесса плавления серпентина и высвобождения кристаллов шпинели, для их полного контакта с твердым углеродом кокса. Отсюда нетрудно установить, что главным вопросом успешного ведения процесса производства высокоуглеродистого феррохрома является снижение температуры плавления цементирующей связки хромитовой руды. Добиваясь поставленной цели, возможно интенсифицировать восстановительные процессы и снизить энергетические затраты. Вопрос выбора оптимального состава флюсов для снижения температуры плавления серпентина — это важный вопрос технологии при прочих равных условиях.

В литературе неоднократно указывалось на благоприятное влияние — повышение содержания Al_2O_3 в шлаках углеродистого феррохрома. Однако рассматривались в основном конечные составы шлаков и их физико-химические свойства — вязкость и электропроводность.

При более детальном исследовании формирования шлакового расплава очевидно, что в начальном периоде высокотемпературного разложения хромитовой руды, а именно при совместном плавлении серпентина и флюса образуется силикатомагниевый расплав ($T_{пл}$ ~ 1557 °С). Далее после развития восстановления хромитов из зерен хромшпинелида силикатомагниевый расплав взаимодействует с алюмомагнезиальной шпинелью, что приводит к формированию состава конечного шлака.

Процесс начала, развития и завершения шлакообразования при электротермии углеродистого феррохрома протекает в общей тройной системе в области частных подсистем

$$MgO–MgO\cdot Al_2O_3–2MgO\cdot SiO_2 \text{ и } MgO\cdot Al_2O_3–2MgO\cdot SiO_2–2MgO\cdot 2Al_2O_3\cdot 5SiO_2$$

Результирующей для указанных подсистем является квазибинарное сечение

$$2MgO\cdot SiO_2–MgO\cdot Al_2O_3$$

В системе $2MgO\cdot SiO_2–MgO\cdot Al_2O_3–MgO$ образуется тройная эвтектика с температурой плавления 1700 °С.

Реальные температуры плавления шлаков составляют 1550–1650 °С.

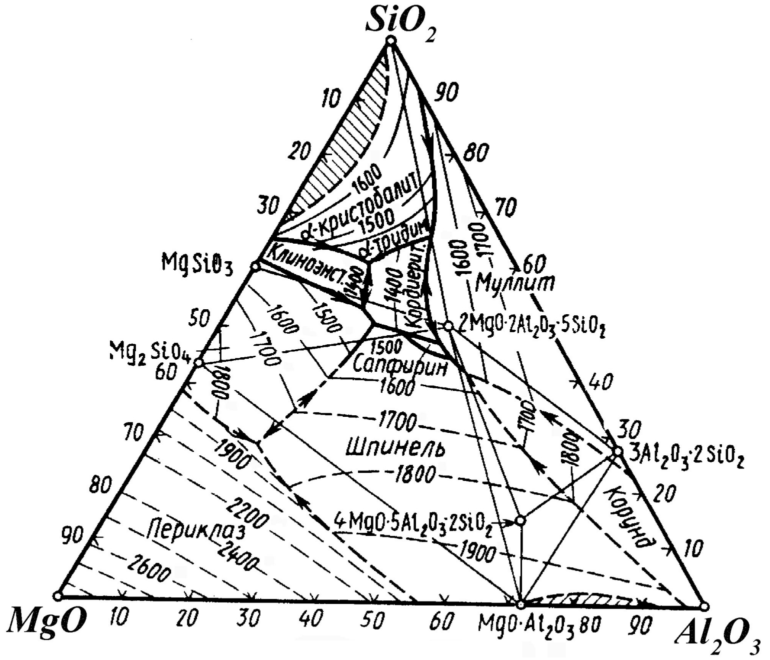

Состав, масс. %

Рисунок 2. Диаграмма состояния системы $MgO–SiO_2–Al_2O_3$

С точки зрения снижения температуры плавления серпентина в рамках реальной тройной системы $MgO–SiO_2–Al_2O_3$, характеризующей формирование оксидов, необходимо найти минимальную точку плавления на этой диаграмме. Самой минимальной точкой является тройная эвтектика с Т = 1355 °С, расположенная в области кристобалита. Если состав серпентина соединить прямой линией с тройной точкой эвтектики и продолжить эту линию до пересечения с системой $SiO_2–Al_2O_3$, то пересечение этих линий укажет на состав флюсов, использование которых позволит снизить температуру плавления серпентина с 1557 ºС до 1355 ºС. Разница составит 202 ºС. Температура 1355 ºС, при которой должно произойти плавление серпентина и высвобождение зерен хромшпинелида для полного прямого контакта с коксом, практически приближается к температурам начала восстановления хромита $Cr_2O_3 \cdot FeO$ и магнезиохромита $MgO \cdot Cr_2O_3$ — 1151 и 1273 ºС соответственно). Из указанных особенностей строения хромитовых руд и реализации восстановительных процессов следует, что в реальных условиях реакция взаимодействия оксидов хрома с углеродом начинается при температурах более 1355 ºС, после высвобождения зерен хромшпинелида из обволакивающей ее цементирующей породы. Восстановление оксидов хрома и железа протекает одновременно. Точка пересечения, указывающая на необходимый состав флюсов, соответствует соотношению $SiO_2/Al_2O_3 = 2,57$. Очевидно, что при таком составе применяемых флюсов минимизируются энергетические расходы, восстановительные процессы протекают при более низких температурах и достигаются оптимальные ТЭП технологии производства углеродистого феррохрома.

Таким образом, на основе анализа текстурных особенностей хромитовой руды и с учетом закономерностей температуры плавления оксидов в тройной системе $MgO–Al_2O_3–SiO_2$ теоретически установлен наиболее оптимальный состав флюсов по концентрации оксидов кремния и алюминия, который должен соответствовать соотношению $SiO_2/Al_2O_3 = 2,57$. Именно данное соотношение приводит к минимальной температуре плавления серпентина, что позволяет интенсифицировать восстановление оксидов хрома и железа и снизить энергетические затраты производства углеродистого феррохрома.

Распределение температурных зон при работе руднотермических электропечей, традиционных для производства ферросплавов, отличается наличием значительного градиента. В зоне работы электрических дуг температура достигает значений от 5000 до 15000 ºС. На поверхности колошника температура составляет 500–600 ºС. Присутствуют все значимые температуры для размягчения, плавления, диссоциации и восстановления шихтовых материалов. Однако поиск и наведение в составе шихты эвтектических точек плавления путем подбора необходимых флюсующих компонентов приводят в конечном результате к снижению энергетических затрат.

При выборе флюсующих компонентов наиболее целесообразно использовать комплексные шихтовые материалы, сочетающие в себе несколько необходимых для технологии свойств. Так, например, если подобрать высокозольные угли с составом зольных компонентов в части соотношения SiO_2/Al_2O_3, равном или близком к требуемому, то это решение снизит технологические затраты. В соответствии с данным подходом была реализована технология производства высокоуглеродистого феррохрома с использованием фракционированных углей месторождения «Борлы» с зольностью 36,8 %, содержащей, %: 58,4 SiO_2; 32,4 Al_2O_3; 0,073 CaO; 1,61 MgO; 1,01 FeO; 0,85 K_2O+Na_2O; 0,35 S; 0,007 P.

Традиционный кокс частично (до 30 %) был заменен на высокозольный уголь, что составило 5,5 % от массы хромитовой руды. Наряду с прямым экономическим эффектом, обусловленным рыночной разницей в цене восстановителей, были достигнуты положительные технологические показатели в обеспечении повышения энергоэффективности — снижение расхода электроэнергии составило 3,13–4,56 % на каждую тонну произведенной продукции.

Таким образом, предложен механизм влияния состава базовых оксидных компонентов SiO_2/Al_2O_3 конечных шлаков производства высокоуглеродистых марок феррохрома на технико-экономические параметры производства и указано его влияние на расход электроэнергии. Установлено, что при соотношении $SiO_2/Al_2O_3 = 2,57$ достигаются оптимальные параметры. Использование высокозольных каменных углей при выплавке высокоуглеродистых марок феррохрома взамен части металлургического кокса не только выгодно с экономических позиций, но и необходимо как полезный компонент шихты, обеспечивающий требуемый состав конечных шлаков.

Список литературы

1 *Павлов Н.В., Кравченко Г.Г., Чупрынина И.И.* Хромиты кемпирсайского плутона. — М.: Наука, 1968. — 178 с.

2 *Гасик М.И., Лякишев Н.П., Емлин Б.И.* Теория и технология производства ферросплавов. — М.: Металлургия, 1988. — 784 с.

3 *Есенжулов А.Б., Островский Я.И., Веселовский И.А. и др.* Производство высокоуглеродистого феррохрома из бедных уральских хромитовых руд // Сталь. — 2007. — № 8. — С. 54.

4 *Кадарметов Х.Н.* Металлургическая характеристика актюбинских хромитовых руд // Научно-технические труды НИИМ. — 1960. — Вып. 2. — С. 65–73.

5 *Жучков В.И., Заякин О.В., Афанасьев В.И.* Перспективные направления переработки отечественных бедных хромитовых руд // Проблемы и перспективы развития металлургии: Тр. науч.-техн. конф. — Екатеринбург: Изд. УрО РАН, 2011. — Т. 1. — С. 193–197.

6 *Топорищев Г.А., Волков В.С., Гетманчук В.И.* О механизме углетермического восстановления окиси хрома // Восстановительные процессы в производстве ферросплавов. — М., 1977. — С. 132–135.

7 *Кадарметов Х.Н.* Механизм восстановления хромшпинелидов Кемпирсайского месторождения твердым углеродом // Изв. вузов. Черная металлургия. — 1986. — № 1. — С. 35–39.

8 *Гриненко В.И., Поляков О.И., Гасик М.И. и др.* Хром Казахстана. — М.: Металлургия, 2001. —С. 177–222.

9 *Жакибеков Т.Б., Гриненко В.И., Такенов Т.Д.* Моделирование фазовых равновесий при карбо- и металлотермии хромитовых руд // Физико-химические и технологические вопросы металлургического производства Казахстана. — Алматы: Искандер, 2002. — С. 106–115.

Т.Б.Жакибеков, А.Д.Мехтиев, В.В.Югай, О.В.Алдошина

Хромдалған руда текстурасының қайта қалпына келтіру үрдісіне әсері

Хромдалған руда текстура ерекшеліктерінің көміртермиялық қайта қалпына келтіру үрдісіне әсерінің зерттеу қорытындылары келтірілген. Хромшпинелидті хромдалған рудасы бар қатты көміртекпен әсерлескен кезде, хром оксидінің тура қалпына келтіру реакциясы толық көлемде іске асатыны көрсетілген. Хромдалған руда цементтік тегінің минималды еру температурасының шарты — серпентиннің, хром карботермиясы кезінде энергиялық шығынды оңтайландыру үшін қажет. Бұл шарт базалық оксидтердің $SiO_2/Al_2O_3 = 2{,}57$ қатынасында толық көлемде жүзеге асады. $MgO–SiO_2–Al_2O_3$ оксидті жүйелерінің шекті қождар диаграммаларын талдау негізінде оңтайлы орнатылған.

T.B.Zhakibekov, A.D.Mekhtiev, V.V.Yugay, O.V.Aldoshina

Influence of chromite's texture ores on restoration processes

Results of research on influence of chromite's texture ores on processes of carbon thermal restoration are presented. It is shown that reaction of direct restoration of chrome's oxides is most fully realized at direct contact of solid carbon with hromshpinelidy chromite ores. The condition of the minimum temperature of melting of the cementing breed of chromite ores — serpentine is necessary for optimization of power expenses at a carbothermy of chromites. This condition is most fully realized at a ratio of basic $SiO_2/Al_2O_3 = 2{,}57$ oxides. The optimum ratio is established on the basis of the chart's analyzes of a condition of oxidic $MgO–SiO_2–Al_2O_3$ system's final slags.

References

1 Pavlov N.V., Kravchenko G.G., Chuprynina I.I. *Chromites of Kempirsaysky Pluton*, Moscow: Nauka, 1968, 178 p.

2 Gasik M.I., Lyakishev N.P., Emlin B.I. *Theory and production technology of ferroalloys*, Moscow: Metallurgiya, 1988, 784 p.

3 Esenzhulov A.B., Ostrovsky Ya.I., Veselovsky I.A. et al. *Steel*, 2007, 8, p. 54.

4 Kadarmetov Kh.N. *Scientific and technical works NIIM*, 1960, 2, p. 65–73.

5 Zhuchkov V.I., Zayakin O.V., Afanasyev V.I. *Problems and Prospects of Development of Metallurgy*: Works of the sci. and techn. conf., Yekaterinburg: Prod. OURO RAHN, 2011, 1, p. 193–197.

6 Toporishchev G.A., Volkov V.S., Getmanchuk V.I. *Recovery processes in production of ferroalloys*, Moscow, 1977, p. 132–135.

7 Kadarmetov Kh.N. *Izvestiya vuzov. Ferrous metallurgy (Steel in Translation)*, 1986, 1, p. 35–39.

8 Grinenko V.I., Polyakov O.I., Gasik M.I. et al. *Chrome of Kazakhstan*, Moscow: Metallurgiya, 2001, p. 177–222.

9 Zhakibekov T.B., Grinenko V.I., Takenov T.D. *Physical and chemical and technological questions of metallurgical production of Kazakhstan*, Almaty: Iskander, 2002, p. 106–115.

UDC 678+67.03

A.V.Omasheva[1], K.A.Sevostyanova[1], M.A.Zavgorodnyaya[2]

[1]*Ye.A.Buketov Karaganda State University;*
[2]*Tomsk State University of Control Systems and Radio Electronics, Russia*
(E-mail: kristina.sevostyanova.93@mail.ru)

Adhesives of cold curing based on chloroprene rubber brand Skaypren G-40T

New formulation of adhesives based on cold curing chloroprene rubber stamp Skaypren G-40T have been developed with a complex of adhesion, strength, performance properties that meet the requirements of modern technology. Mode of preparation of glue was installed for laboratory's glue-stir. These adhesives have been tested for compliance with technical requirements. Formulation of adhesive was based on finding the optimal balance between the physical and mechanical properties, providing the set requirements, the technological properties which satisfy the conditions of the existing production process and economic efficiency. At the same time sought to maximize unification adhesives. For the preparation of adhesives cold rejection was used chloroprene rubber stamp Skaypren G-40T instead of the previously used Nairit chloroprene rubber stamps.

Key words: adhesives, chloroprene rubber, glue, economic efficiency, Skaypren G-40T, physical and mechanical properties, sealing materials, Nairit rubber stamps, cold-curing adhesives.

Currently it is difficult to imagine engineering and instrumentation, furniture and shoe industries, construction, aircraft construction, space and military equipment, shipbuilding without adhesives. This is due to the bonding is one of the most economical and efficient ways of assembling parts. Efficacy of adhesives due to a number of significant advantages adhesive compounds compared to the compounds of other types. The adhesive firmly glues variety of materials, and in some cases gluing is the only possible way of a secure connection. The variety of fields of application and use of adhesives led to the creation of a wide range of products. There are more than 15,000 manufacturers of adhesive materials, which suggests over 250,000 different adhesives and sealing materials [1].

Development of adhesives — one of the most traditional areas of the use of polymers [2]. The statistical analysis shows the demand for adhesives is a major stimulator of growth in the production of polymeric materials. However, the chemical industry develops independently, and the range of adhesives is influences by the existing range of polymer materials.

Adhesive compounds have a number of significant advantages over conventional types of compounds. This is due to the problems of producing polymers with specific adhesion properties with the correct selection of all the ingredients of the adhesive composition, the peculiarities of manufacturing technology and application of adhesives and methods of preparation of substrates. Adhesives with the establishment of complex desired properties is extremely challenging. n the rubber Industry and in the mode of life are widely uses adhesives based on polychloroprene, which are intended for fastening to each other rubbers and to metals. Despite the prevalence of this type of adhesives, they are characterized by relatively low adhesion performance. Development of adhesive compositions based on the novel polymers is not always economically justified and therefore the use of adhesion promoters in the adhesive formulations administered in small amounts and that enhance the performance properties of adhesives are commercially available and use of new grades of polychloroprene rubbers is an important task. The purpose of research — development of new formulations of cold-curing adhesives based on chloroprene rubber stamp Skaypren G-40T with a complex adhesion, strength, performance properties that meet the requirements of modern technology [3]. To achieve the goal the formulation of adhesives have been developed based on cold curing chloroprene rubber stamp Skaypren G-40T. These adhesives have been tested for compliance with technical requirements.

Formulation of adhesive was based on finding the optimal balance between the physical and mechanical properties, providing the set requirements, the technological properties which satisfy the conditions of the existing production process and economic efficiency [4].

Rubber stamps Skaypren G-40T is characterized by a higher viscosity, and for the preparation of cold-cure adhesive was used chloroprene rubber stamp Skaypren G-40T replace previously used in the majority of Nairit chloroprene rubber stamps. Chloroprene rubber characterized by the ability to crystallize in comparison with rubber stamps Nair said that the benefits of using Skaypren G-40T in cold-curing adhesive compositions.

Comparative characteristics of rubbers uses in the adhesive compositions shown in Table 1.

Table 1

Comparative characteristics of rubber stamps Skaypren G-40T and Nairit uses in adhesive compositions

Index	Skaypren G-40T	Nairit DV-80	Nairit DV-100
Mooney viscosity, 100 ºC	96–113	71–89	90–110
Crystallizability	High	High	High

The study was developed 6 recipes adhesives based on chloroprene rubber stamp Skaypren G-40T, and according to these recipes in the laboratory were prepared prototypes cold curing adhesives. The developed formulation contain in their composition different vulcanizing agents, resin 2 values, solvents and solvent mixtures, as well as builders, the data shown in Table 2.

Table 2

Comparative characteristics of composition and properties of prototypes adhesives № 1,2 and 3 cold cure

№ of Sample	Composition	Weight the proportion of dry substances	Bond Strength Peel c/o 24 hours
1	Skaypren G-40T; Curatives; resin brand Ribetak 7522E; organic solvent (ethyl-acetate:nefras:toluene 2:2:1)	29,2	2,50
2	Skaypren G-40T; Curatives; resin brand Ribetak 7522E; organic solvent (ethyl-acetate:nefras:toluene 1:1:1)	24,2	2,33
3	Skaypren G-40T; Curatives; resin brand Ribetak 7522E; organic solvent (ethyl-acetate:nefras:toluene 1:1,5:2,5)	31,3	3,0

Note. In the manufacture of a composition № 2 first prepared rubber composition consisting of chloroprene rubber stamps Skaypren G-40T, magnesium oxide, zinc oxide, altaks, thiuram D on rollers on the set mode.

These data shows that the greatest strength has adhesive composition that was used in the manufacture of pre-cooked chelate resins Ribetac 7522E. So it was decided to replace the resin in the resin Ribetac 7522E 101K. Resin 101 K was used previously in many adhesive compositions, as it has good adhesive characteristics.

On the basis of the following recipes were offered cold curing adhesives based on chloroprene rubber Skaypren G-40T, the data obtained are given in Table 3.

Table 3

Comparative characteristics of composition and properties of prototypes adhesives № 4,5 and 6 cold cure

№ of Sample	Composition	Weight the proportion of dry substances	Bond Strength Peel c/o 24 hours
4	Skaypren G-40T; Curatives; resin brand 101 K; organic solvent (ethyl-acetate:nefras:toluene 2:2:1)	32,4	2,62
5	Skaypren G-40T; Curatives; resin brand 101 K; organic solvent (ethyl-acetate:nefras:toluene 2:2:1)	31	3,2
6	Skaypren G-40T; Curatives; resin brand 101 K; organic solvent (ethyl-acetate:nefras:toluene 1:1.2:1.6)	31,3	3,24

Note. In the preparation of the adhesive composition № 5 Mixture: resin, burnt magnesia, an organic solvent and a small amount of water, the reaction proceeds for 6 hours at 30 °C. Then, the resulting solution is added to the rubber composition containing the remaining components.

After analyzing the data, it can be concluded: the best strength properties has adhesive which prepared two-step process (Table 4).

Table 4

Comparative characteristics of cold-curing adhesives based on chloroprene rubber stamp Skaypren G-40T

Name of glue		Bond Strength Peel c/o 24 hours	
		Norm standard 50307471-08-2008	Results
1	88-НД-GR № 1	2,31	2,33
2	88-НД-GR № 1		2,62
3	88-НД-GRнB		2,50
4	88-НДСк-40GT № 1		3,00
5	88-НДСк-40GT № 2		3,20
6	88-НД-GR № 3		3,30

Thus we can conclude that the formation of a durable adhesive bond is significantly affected by the preliminary formation of chelate resins with magnesium oxide, applied mark resins (since the resin provides adhesion strength of the adhesive composition), the use of crosslinkers and accelerators of vulcanization.

However, the use of hardeners in adhesive formulations significantly reduces their viability, as well as an inconvenience in use, as it requires pre-mixing before gluing.

Increasing the technological properties of adhesives with promoting additives that can be incorporated directly in the manufacture of adhesives and of high environmental performance, it is an urgent problem that requires further study.

References

1 *Петрова А.П.* Клеящие материалы: Справочник / Под ред. чл.-кор. РАН, д-ра техн. наук С.В.Резниченко. — М.: Редакция журнала «Каучук и резина», 2002. — 196 с.

2 Большой справочник резинщика. Ч. 1. Каучуки и ингредиенты / Под ред. С.В.Резниченко, Ю.Л.Морозова. — М.: Изд. центр «Техноформ» МАИ, 2012. — 648 с.

3 Справочник по клеям / Сост. Л.Х.Айрапетян, В.Д.Заика, Л.А.Яншина. — Л.: Химия, 1980. — 304 с.

4 Клеи, адгезия, технология склеивания / Пер. с англ. под ред. Г.В.Комарова. — СПб.: Профессия, 2007. — 376 с.

А.В.Омашева, К.А.Севостьянова, М.А.Завгородняя

Скайпрен G-40T маркалы хлоропренді каучукке негізделген суық қатайту желімдер

Заманауи техникалық талаптарын қанағаттандыратын адгезиялық, төзімді, пайдаланушылық қасиеттеріне ие комплексімен Скайпрен G-40T маркалы хлоропренді каучукке негізделген суық қатайту желімдерінің жаңа рецептуралары өңделген. Зертханалық желім бұлғауышқа желімдерді дайындау тәртібі анықталған. Алынған желімдердің техникалық талаптарға сәйкестігі зерттелген. Желімді дайындау рецептурасы қойылған талаптарды қамтитын физика-механикалық қасиеттері арасындағы, істегі өндірістік үрдістің және экономикалық тиімділіктін жағдайларын қанағаттандыратын технологиялық қасиеттері арасындағы оңтайлы балансты табу негізінде жүргізілген. Бұл жағдайда желімдерді максималды унификациялауға тырыстық. Суық катайту желімдерін дайындау үшін бұрын қолданылып жүрген Наирит маркалы хлоропренді каучуктің орнына Скайпрен G-40T маркалы хлорпренді каучук қолданылды.

А.В.Омашева, К.А.Севостьянова, М.А.Завгородняя

Клеи холодного отверждения, основанные на хлоропреновом каучуке марки Скайпрен G-40T

Разработаны новые рецептуры клеев холодного отверждения на основе хлоропренового каучука марки Скайпрен G-40T с комплексом адгезионных, прочностных, эксплуатационных свойств, удовлетворяющих требованиям современной техники. Установлены режимы приготовления клеев к лабораторной клеемешалке. Полученные клеи были исследованы на соответствие техническим требованиям.

Разработка рецептуры клея проводилась на основе отыскания оптимального баланса между физико-механическими свойствами, обеспечивающими поставленные требования, технологическими свойствами, удовлетворяющими условиям действующего производственного процесса, и экономической эффективностью. При этом стремились к максимальной унификации клеев. Для приготовления клеев холодного отверждения был использован хлоропреновый каучук марки Скайпрен G-40T взамен используемого ранее хлоропренового каучука марки Наирит.

References

1 Petrova A.P. *Adhesives*: Handbook, Ed. by S.V.Reznichenko, Moscow: Redakciya Zhurnala «Kauchuk i Rezina», 2002, 196 p.

2 *Large handbook of rubbermaker. Part 1. Rubbers and ingredients*, Ed. by S.V.Reznichenko, Yu.L.Morozov, Moscow: Izdatelskij centr «Texnoform» MAI, 2012, 648 p.

3 Airapetyan L.Kh., Zaika V.D., Yanshina L.A. *Handbook of adhesives*, Leningrad: Khimiya, 1980, 304 p.

4 *Adhesives, adhesion, gluing technology*, Transl. from Eng. and ed. by G.V.Komarov, Saint Petersburg: Professiya, 2007, 376 p.

ӘОЖ 561.66.023

Ж.К.Каирбеков[1], Ж.К.Мылтықбаева[2], Ж.Т.Ешова[2], Т.М.Әндіжанова[2]

[1]*Жаңа химиялық технологиялар мен материалдар ғылыми-зерттеу институты, Алматы;*
[2]*Әл-Фараби атындағы Қазақ ұлттық университеті, Алматы*
(E-mail: damasma.tolganay@gmail.com)

Ультрадыбыспен өңделген Ni қаңқалы катализаторында мұнай өнімдерін гидротазалау

Гидротазалау үдерісінде тура айдалған бензин фракциясының құрамындағы күкірт мөлшерін азайтуға Ni қаңқалы катализаторын ультрадыбыспен өңдеу әсері зерттелді. Ультрадыбыс әдісімен гидротазалау үдерісінің катализаторын белсендіру әдісі ұсынылды. Қаңқалы катализаторды ультрадыбысты белсендіру гидротазалау өнімдерінің сапасына әсер еткендігі көрсетілді. Ультрадыбыспен өңделген катализаторды қолданғаннан кейін, бензин фракциясындағы күкірт мөлшері 48 %-ға азайды. Бензин фракциясының эксплуатациялық қасиеттері жақсарғаны байқалды.

Кілт сөздер: бензин, ультрадыбыс, гидротазалау, катализатор, күкіртсіздендіру, құйма, гидрлеу, диспергирлеу.

Кіріспе

Қазіргі таңда мұнай өңдеу саласындағы негізгі міндеттердің бірі оны тереңдетіп өңдеу негізінде пайдалану тиімділігін арттыруға бағытталған жаңа, экологиялық жетілдірілген, энергияны үнемдейтін технологияларды жасау болып табылады. Осындай өзекті мәселелердің бірі — сапасы жоғары, бәсекеге қабілетті мұнай өнімдерін шығару. Себебі алдыңғы қатарлы дамыған мемлекеттерде бензин сапасына қойылатын талаптар күшейтілген нормалар енгізілген. Бұл нормаларға сәйкес бензин құрамындағы күкірт мөлшері 0,001 масс. %-дан аспауы қажет [1–3]. Мұндай заманауи экологиялық талаптарды қанағаттандыратын бензин фракциясын алу технологиясы сапасы төмен мұнай фракцияларын гидротазалауға арналған катализаторларды өндіруді қажет етеді.

Сондықтан дәстүрлі емес әдістерді қолданып, гидротазалауға арналған катализаторларды дайындау технологиясын жасаудың маңызы зор. Мұнай фракцияларын дәстүрлі емес әдістерді қолданып өңдеуге физикалық, атап айтқанда, ультрадыбыспен, лазермен, электрондар шоғырымен әсер ету үдерістері жатады.

Бұл мақалада Павлодар мұнай өңдеу зауытының тура айдалған бензин фракциясын гидротазалауға арналған катализаторды ультрадыбыспен өңдеп, белсенділігін арттыру жолдары зерттелген.

Зерттеу әдістері

Бензин фракциясының көмірсутекті құрамын, физика-химиялық сипаттамаларын талдау аккредитацияланған, аттестаттаудан өткізілген (аттестат № KZ.И.02.1572). Жаңа химиялық технологиялар мен ҒЗИ-ның жаңғыш кендер мен оларды өңдеуден алынған өнімдерді кешенді талдау мен зерттеуге арналған сынақ зертханасында жүргізілді.

Тура айдалған бензиннің фракциялық құрамы 2177–99 МемСТ бойынша мұнай фракцияларының құрамын айқындауға арналған АРН-ЛАБ-11 аппаратында анықталды.

Бензин фракциясы құрамындағы күкірт мөлшерін анықтау Спектроскан S аппаратында 51947–2002 МемСТ немесе 4294–98 ASTMD сәйкес жүргізілді.

Мұнай өнімдерінің көмірсутектік топтық құрамын анықтау газды хроматография әдісімен «Хроматэк-Кристалл 5000» аппаратында жасалынды.

Ni қаңқалы катализаторды ультрадыбыспен өңдеу УЗВ-3/100-ТНМ-44 ультрадыбысты ваннада 60–150 Гц жиілікте, 25–65 °С температуралар аралығында 30 мин жүргізілді.

Тура айдалған бензин фракциясын гидрлеу үдерісі газометрлік бюреткамен жалғанған, потенциометрлік қондырғымен жабдықталған, қарқынды араластырғышы бар, градиентсіз термостатталған «катализдік үйрек» түріндегі шыны реакторда жүргізілді. Диффузиялық тежелулердің әсерін болдырмау үшін реакторды минутына 300–400 рет қарқынды тербелту жасалынды. Реакция жылдамдығы реактормен жалғанған термостатталған газометрлік бюреткадағы сутек көлемінің өзгеруі бойынша есептелінді.

Зерттеу нәтижелері мен оларды талдау

Зерттеу нысаны ретінде Павлодар мұнай өңдеу зауытының ЛК6У ЭЛОУ АТ қондырғысынан тура айдалып алынған бензин фракциясы қолданылды. Павлодар мұнай өңдеу зауытының тура айдалған бензин фракциясының негізгі физика-химиялық көрсеткіштері анықталды. Зерттеуге алынған бастапқы бензин фракциясының құрамына жүргізілген талдау нәтижелері 1-кестеде келтірілген.

1-кесте

Павлодар мұнай өңдеу зауытының тура айдалған бензин фракциясының физика-химиялық көрсеткіштері

Көрсеткіштері	Бастапқы тура айдалған фракция	Нормативтер
20 °C температурадағы тығыздығы, кг/м^3	831,6	МемСТ 3900–85
20 °C температурадағы кинематикалық тұтқырлығы, м^2/с	414,5	МемСТ 31391
Жабық тигельдегі тұтану температурасы, °C	81	МемСТ 6356
Күкірт мөлшері, масс. %	0,031	ASTMD 4294–98
Фракциялық құрамы		
Қайнау температурасының басталуы, °C	36	МемСТ 2177–99, ASTM D 86
5 %	75	
10 %	103	
Қайнау температурасының соңы, °C	148,6	

Кестеде көрсетілгендей, рентгенфлюоресцентті әдіспен анықталған күкірт мөлшері бастапқы бензин фракциясында 0,031 масс. % құрайды. Бензин фракциясының қайнау температурасының басталуы — 36 °C, ал соңғы қайнау температурасы 148,6 °C тең.

Қазіргі уақытта дәстүрлі емес әдістерді қолданып, мұнай өңдеуге арналған катализаторды дайындау технологиясын жасау жұмыстарына басты назар аударылған. Мұндай дәстүрлі емес әдістерге физикалық: ультрадыбыспен, лазермен, электрондар шоғырымен әсер ету үдерістері жатады. Бұл әдістерді өңдейтін шикізатқа немесе катализаторға, не болмаса олардың екеуіне қолданып жүргізуге болады.

Катализ саласындағы зерттеулерде ультрадыбыспен әсер ету әр түрлі кезеңдерде қолданылады: катализаторды алу үдерісінде, дайын болған катализаторды өңдеу, құрамында катализатор бар реакциялық қоспаны өңдеу және үдерсіке қолданылып болған катализаторды қайта қалпына келтіру үдерісінде қолдану [4].

Бұл жұмыста белсенділігін арттыру мақсатында дайын катализаторға ультрадыбыспен әсер ету жүргізілді. Гидротазалау катализаторы ретінде Ni–Al–Fe–Cr–Ti (51,1 %; 46,9; 0,075; 0,8593; 0,914 %) құймасынан алынған Ni қаңқалы катализатор алынған. Гетерогенді катализде, мысалы, гидрлеуде, гидрогенолизде никелді катализаторлардың маңызы ерекше. Бұл жұмысқа дейін Ni қаңқалы катализаторлар мұнайдан, көмірден алынған мотор отындарының сапасын жақсарту үшін қолданылған [5].

Бензин фракциясының сапасына ультрадыбыспен өңделген Ni қаңқалы катализатордың әсері гидротазалау үдерісінде зерттелді. Ультрадыбыспен өңделген катализатор қатысында тура айдалған бензин фракциясын гидротазалау бойынша зерттеу нәтижелері 2-кестеде берілген.

2-кесте

Бастапқы фракция мен гидрогенизаттың физика-химиялық көрсеткіштері

Көрсеткіштері	Бастапқы бензин	Өңделмеген Ni қаңқалы катализатор қатысында	Ультрадыбыспен өңделген Ni қаңқалы катализатор қатысында		
			60 Гц	90 Гц	150 Гц
1	2	3	4	5	6
25 °C температурада					
ρ, кг/м^3	831,6	641,7	680,2	749,2	779,9
η, м^2/с	414,5	435,2	431,7	397,2	397,2
S, масс. %	0,031	0,028	0,042	0,039	0,035
Қ.б., °C	32,8	42,7	42,2	40,2	39,1
Қ.с., °C	148,6	152,4	152,0	150,6	146,8

1	2	3	4	5	6
40 ºС температурада					
ρ, кг/м^3	831,6	641,7	635,9	720,6	636,3
η, м^2/с	414,5	435,2	432,1	773,6	442,1
S, масс. %	0,031	0,028	0,024	0,015	0,029
Қ.б., ºС	32,8	42,7	42,1	42,1	33,5
Қ.с., ºС	148,6	152,4	154,3	154,3	155,9
65 ºС температурада					
ρ, кг/м^3	831,6	641,7	718,6	618,3	635,9
η, м^2/с	414,5	435,2	438,6	445,5	417,9
S, масс. %	0,031	0,028	0,038	0,031	0,040
Қ.б., ºС	32,8	42,7	35,7	38,3	38,1
Қ.с., ºС	148,6	152,4	157,1	156,1	154,1

Гидротазалау бойынша жүргізілген зерттеу нәтижелеріне талдау жүргізетін болсақ, тура айдалған бензин фракциясының физика-химиялық көрсеткіштерінің өзгергенін аңғаруға болады. 40 ºС температура мен 60 Гц жиілікте өңделген Ni қаңқалы катализатор қатысында гидротазалау жүргізілген бензин фракциясының құрамында күкірт мөлшері бастапқы 0,031 %-дан 0,024 %-ға дейін төмендеген. Бензин фракциясының бастапқы қайнау нүктесі — 42,1 ºС, ал соңғы қайнау нүктесінің 154,3 ººС температураға дейін жоғарлағанын көруге болады. Ультрадыбыспен өңдеу жиілігін 90 Гц арттырғанда гидрогенизат құрамындағы күкірт мөлшері 0,015 %-ға дейін азайған. Бұл жағдайда да бензин фракциясының бастапқы қайнау нүктесі — 42,1 ºС, ал соңғы қайнау нүктесі 154,3 ºС температураға дейін көтерілген.

Катализаторды ультрадыбыспен алдын ала өңдеу температурасын — 65 ºС, ал жиілікті 150 Гц көтергенде гидрогенизат құрамындағы күкірт мөлшерінің төмендеуіне айтарлықтар әсер етпейтіні байқалды. Күкірт мөлшерін төмендету мақсатында гидротазалау үдерісіне белсенділігін арттыру мақсатында катализаторды алдын ала өңдеудің оңтайлы жағдайлары 40 ºС температура мен 60 Гц жиілік болатынын жүргізілген зерттеу нәтижелері айқындады.

Гидротазалау үдерісінде жүретін бензин фракциясы құрамындағы өзгерістерді айқындау мақсатында бастапқы бензин фракциясы мен гидротазалаудан кейін алынған гидрогенизат құрамдары ИҚ-спектроскопия әдісімен зерттелді (1-сур.).

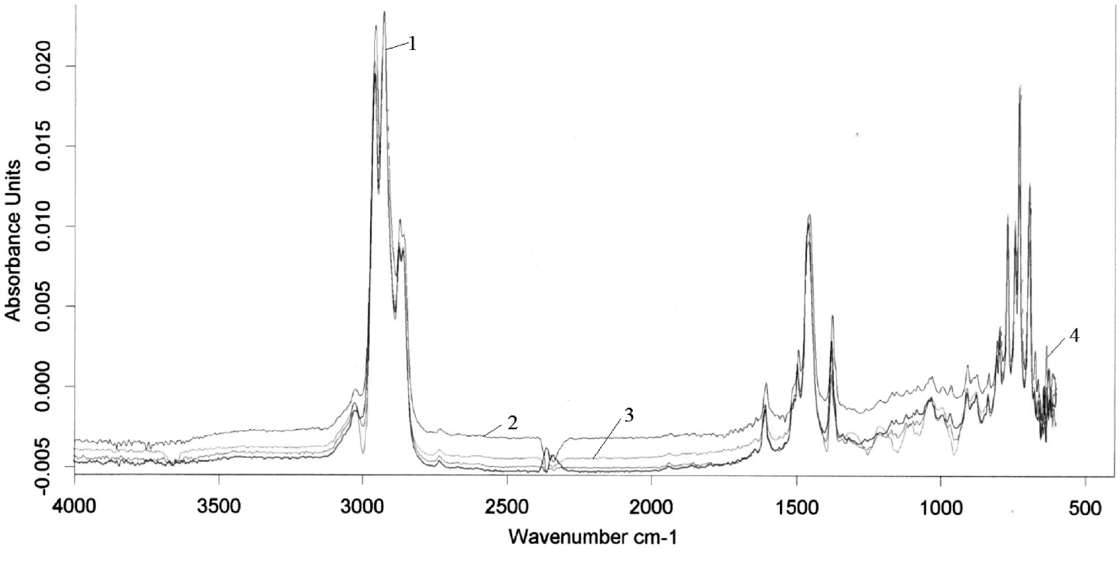

1 — 60 Гц; *2* — бастапқы бензин; *3* — 150 Гц; *4* — 90 Гц

1-сурет. 40 ºС температура мен 60, 90, 150 Гц жиіліктерде ультрадыбыспен өңделген катализатор қатысында жүргізілген гидротазалау өнімдерінің ИҚ-спектрлері

Тура айдалған бензин фракциясы спектріндегі жұтылу сызықтарында келесідей топтар: ароматты қосылыстардағы С–Н байланысына тән валенттік тербелістер 3025,71 см$^{-1}$, алкандар құрамындағы CH_3 топтарына тән жұтылу жолақтары 2957,9 см$^{-1}$, метиленді топтарға тән 2925,45 см$^{-1}$, метилді топтардағы С–Н байланысына тән деформацияланған тербелістер 2872,53 см$^{-1}$, диендер 1606,55 см$^{-1}$, CH_3 топтарына тән антисимметриялық тербелістер 1495,58 және 1458,66 см$^{-1}$, диметилді топтар 1378,13 см$^{-1}$, кеталдер мен ацеталдер 1169,89 см$^{-1}$, транс-алкендер 965,46 см$^{-1}$, цис-диендердегі (=СН) байланыстарына тән жолақтар 750–650 см$^{-1}$ аймағында анықталған (1-сур.).

Гидротазалаудан кейін бензин фракциясы құрамы айтарлықтай өзгереді. Мысалы, 965,46 см$^{-1}$ аймағындағы транс-алкендерге тән жұтылу жолақтары; үшіншілік спирттердегі, кеталдердегі С–О валенттік тербелістеріне тән 1169,89 см$^{-1}$, 1155,82 см$^{-1}$, 1120 см$^{-1}$ аймақтарындағы жұтылу сызықтары 60 Гц жиілікте ультрадыбыспен өнделген катализатор қатысында гидротазалаудан кейін алынған өнімде байқалмайды.

Ультрадыбыспен өңдеуге дейінгі және өңдеуден кейінгі катализатор үлгілері электронды микроскопиялық әдіспен зерттелді (2-сур.).

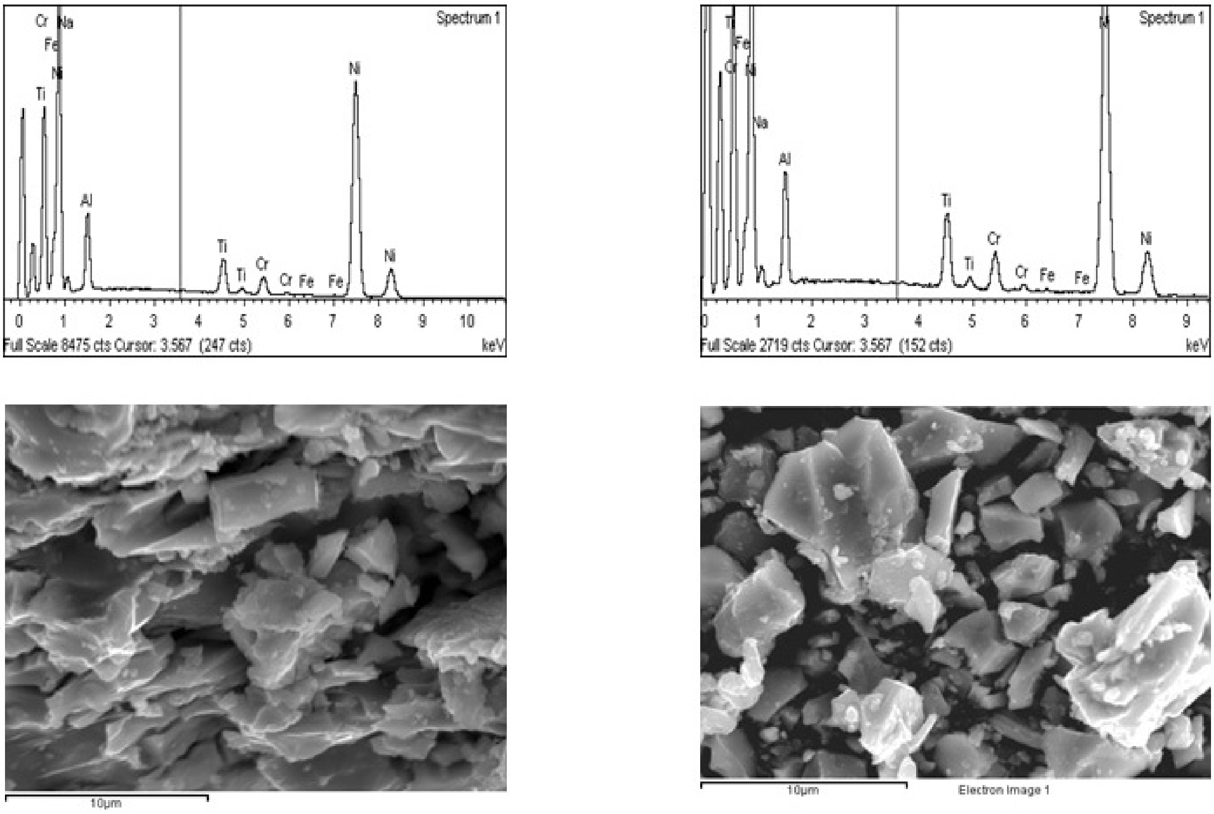

а) ультрадыбыссыз

ә) ультрадыбыспен өңделген

2-сурет. Ni қаңқалы катализаторды электронды микроскопиялық зерттеу нәтижелері

Зерттеу нәтижелері ультрадыбыстық өңдеу катализатор құрамында майда бөлшектердің көптігін және біркелкі таралатынын көрсетеді (2-сур.). Ультрадыбыстық өңдеу нәтижесінде катализатор бөлшектері диспергирленіп, гиротазалау үдерісінде фазааралық бет ауданын артып, әсерлесу бетінде химиялық реакциялар қарқынды жүреді. Ал бұл жағдай өз кезегінде бензин фракциясының күкіртсізденуіне ықпал етеді. Ультрадыбыспен өңделген каталдизатордың сызықтық спектрінде Ni мен Ti үшін рентгендік сәулеленудің қарқындылығы өңделмеген катализаторға қарағанда біршама артатыны байқалады.

Сонымен, тура айдалған бензин фракциясын гидротазалау үдерісінде ультрадыбыспен өңделген Ni қаңқалы катализаторын қолдану күкірт мөлшерін төмендетуге айтарлықтай ықпал ететіні айқындалды.

Гидротазалау үдерісінде катализаторды ультрадыбыспен өңдеудің оңтайлы жағдайлары анықталды. Зерттеу нәтижелері 40 ºС температура мен 90 Гц жиілікте катализаторды ультрадыбыспен өңдеу бензин фракциясы құрамнынан күкірт мөлшерін 48 %-ға дейін төмендететінін көрсетті.

Әдебиеттер тізімі

1 *Анисимов А.В., Тараканов А.В.* Окислительное обессеривание углеводородного сырья // Российский химический журн. — 2008. — Т. LII, № 4. — С. 30.

2 Технический регламент Таможенного союза (ТР ТС) 013/2011 о требованиях к автомобильному и авиационному бензину, дизельному и судовому топливу, топливу для реактивных двигателей и мазуту (в ред. решений Совета Евразийской экономической комиссии от 23.06.2014 № 4, от 28.04.2015 № 36).

3 *Томина Н.Н., Пимерзин А., Моисеев К.* Сульфидные катализаторы гидроочистки нефтяных фракций // Российский химический журн. — 2008. — Том LII, № 4. — С. 41.

4 *Новицкий Б.Г.* Применение акустических колебаний в химико-технологических процессах. — М.: Химия, 1983. — 185 с.

5 *Айты Қ., Суймбаева С.М., Каирбеков Ж.К., Мылтықбаева Ж.К.* Модифицирленген никель қаңқалы катализаторында бензин фракциясын гидротазалау // Мир науки. — Алматы, 2010. — С. 107.

Ж.К.Каирбеков, Ж.К.Мылтыкбаева, Ж.Т.Ешова, Т.М.Андижанова

Гидроочистка нефтепродуктов на Ni скелетном катализаторе, обработанном ультразвуком

Изучено воздействие ультразвуковой обработки Ni скелетного катализатора на снижение содержания серы в прямогонной бензиновой фракции в процессе гидрогенизации. Предложен способ активации катализатора ультразвуком для гидрогенизационного процесса. Было показано, что ультразвуковая активация скелетного катализатора положительно влияет на качество продуктов гидроочистки. После применения катализатора, обработанного ультразвуком, содержание серы в бензиновой фракции снизилось на 48 %. Установлено улучшение эксплуатационных свойств бензиновой фракции.

Zh.K.Kairbekov, Zh.K.Myltykbaeva, Zh.T.Eshova, T.M.Andizhanova

Hydrotreating process of petroleum products on sonicated skeletal Ni catalyst

An effect of ultrasonic treatment of skeletal Ni catalyst to reduce the sulfur content of straight-run gasoline fraction in the hydrogenation process is studied. It is suggested a method for activation of hydro treating catalyst on the basis of ultrasound. It has been shown that son chemical activation of the skeletal catalyst affects the quality of products hydro treating. After applying ultrasonically treated catalysts, the sulfur content of the gasoline fraction has decreased by 48 %. The improvement of the operating properties of the gasoline fraction is established.

References

1 Anisimov A.V., Tarakanov A.V. *Russian Chemical Journal*, 2008, 52, 4, p. 30.

2 *Technical regulations Customs union (TR CU) 013/2011 about the requirements to automobile and aviation gasoline, diesel and marine fuel, jet fuel and heating oil* (in the red. Decisions of the Board of the Eurasian Economic Commission of 23.06.2014 № 4 from 28.04.2015 № 36).

3 Tomina N.N., Pimerzin A., Moiseev K. *Russian Chemical Journal*, 2008, 52, 4, p. 41.

4 Novitskiy B.G. *The use of acoustic vibrations in chemical-technological processes*, Moscow: Khimiya, 1983, 185 p.

5 Aity K., Suimbaeva S.M., Kairbekov Zh.K., Myltykbaeva Zh.K. *Mir nauki*, Almaty, 2010, p. 107.

АВТОРЛАР ТУРАЛЫ МӘЛІМЕТТЕР
СВЕДЕНИЯ ОБ АВТОРАХ

Abdullayeva, S.A. — Senior Laboratory assistant, Center of physico-chemical methods of research and analysis (CPCMRA), al-Farabi Kazakh National University, Almaty.

Absat, Z.B. — Associate professor, Candidate of chemical sciences, Lecturer of the Department of chemical technology and environment, Ye.A.Buketov Karaganda State University.

Aldabergenova, S.K. — Associate professor, Candidate of chemical sciences, Lecturer of the Department of inorganic and technical chemistry, Ye.A.Buketov Karaganda State University.

Aldoshina, O.V. — Senior lecturer, Technology and communication systems chair, Karaganda State Technical University.

Amerkhanova, Sh.K. — Professor of physical and analytical chemistry Department, Doctor of chemical sciences, Ye.A.Buketov Karaganda State University.

Andizhanova, T.M. — Master on the speciality «Petrochemistry», Faculty of Chemistry and chemical technology, al-Farabi Kazakh National University, Almaty.

Atchabarova, A.A. — Junior Research Fellow, Center of physico-chemical methods of research and analysis (CPCMRA), al-Farabi Kazakh National University, Almaty.

Azwan Mat Lazim — PhD, Doctor, Faculty of science and technology, University Malaysia Kebangsaan, Kuala Lumpur, Malaysia.

Bohari M. Yamin — Doctor, Professor, Faculty of science and technology, University Malaysia Kebangsaan, Kuala Lumpur, Malaysia.

Burakhta, V.A. — Vice-rector for SW, Doctor of chemical sciences, Professor, West-Kazakhstan Engineering and Technological University, Uralsk.

Fomin, V.N. — Associate professor of inorganic and technical chemistry Department, Candidate of chemical sciences, Ye.A.Buketov Karaganda State University.

Gogol, D.B. — Leading Scientist, Candidate of chemical sciences, Institute of problems of complex development of mineral resources, Karaganda.

Golovanova, O.A. — Professor of Department of inorganic chemistry, Doctor of chemical sciences, F.M.Dostoevsky Omsk State University, Russia.

Kabulov, A.T. — Junior research fellow, Center of physico-chemical methods of research and analysis (CPCMRA), al-Farabi Kazakh National University, Almaty.

Kairbekov, Zh.K. — Doctor of chemical sciences, Professor, Faculty of chemistry and chemical technology, al-Farabi Kazakh National University, Almaty.

Khassenova, G.T. — PhD Doctorate, Charles University, Prague, Czech Republic.

Kishibayev, K.K. — Junior research fellow, Center of physico-chemical methods of research and analysis (CPCMRA), al-Farabi Kazakh National University, Almaty.

Klivenko, A.N. — The third year PhD student, al-Farabi Kazakh National University, Almaty.

Kudaibergenov, S.E. — Doctor of chemical sciences, Professor, Head of laboratory of engineering profile, K.I.Satpayev Kazakh National Research Technical University; Director of Institute of Polymer Materials and Technology, Almaty.

Kuimova, M.V. — Head of Department Tomsk Polytechnic University, Tomsk Polytechnic University Department of Foreign Languages Institute nondestructive testing, Russia.

Mamrayeva, K.M. — Associate professor, Department of inorganic and technical chemistry, Ye.A.Buketov Karaganda State University.

Mekhtiev, A.D. — Ph.D.Associate professor, Head of the Department of Technology and Communication, Karaganda State Technical University.

Minayeva, Ye.V. — Lecturer of Chair of organic chemistry and polymers, Candidate of Chemical Sciences, Ye.A.Buketov Karaganda State University.

Myltykbaeva, Zh.K. — Candidate of chemical sciences, Docent, Faculty of Chemistry and chemical technology, al-Farabi Kazakh National University, Almaty.

Nauryzbayev, M.K. — Doctor of technical science, Professor, Director, Center of physico-chemical methods of research and analysis (CPCMRA), al-Farabi Kazakh National University, Almaty.

Nechipurenko, S.V. — Candidate of technical sciences, Head of Laboratory, Senior research fellow, Center of physico-chemical methods of research and analysis (CPCMRA), al-Farabi Kazakh National University, Almaty.

Nurgalieva, M. — Student, Ye.A.Buketov Karaganda State University.

Nurxat Nuraje — Head of Laboratory, PhD, Professor, Department of chemical engineering, Texas Tech University, Lubbok, USA.

Omarov, Kh.B. — Doctor of technical sciences, Professor, Vice-Rector, Ye.A.Buketov Karaganda State University.

Omasheva, A.V. — Candidate of chemical sciences, Docent of Department of organic chemistry and polymers, Ye.A.Buketov Karaganda State University.

Ponomarev, D.L. — Leading scientist, Public association «Grazhdane Kazakhstana», Karaganda.

Rakhimzhanova, N.J. — Candidate of chemical sciences, Docent, Docent of Laboratory, Ye.A.Buketov Karaganda State University.

Rozhkovoy, I.E. — Master student, Ye.A.Buketov Karaganda State University.

Safina, A.V. — Master student, Zhangir Khan West-Kazakhstan Agrarian-Technical University, Uralsk.

Salkeyeva, A.K. — Lecturer of physics chair, Candidate of physical-mathematical sciences, Karaganda State Technical University.

Salkeyeva, L.K. — Head of Chair of organic chemistry and polymers, Professor, Doctor of chemical sciences, Ye.A.Buketov Karaganda State University.

Sevostyanova, K.A. — Master's second year «Petrochemistry», Ye.A.Buketov Karaganda State University.

Shashchanova, M.B. — Managing chair IS, Academy «Bolashak», Karaganda.

Shashchanova, R.B. — Lecturer of Chair of inorganic and technical chemistry, Ye.A.Buketov Karaganda State University.

Shlyapov, R.M. — Associate professor of chemical engineering and petroleum chemistry, Candidate of chemical sciences, Ye.A.Buketov Karaganda State University.

Siyazova, A.B. — Master of engineering sciences, Specialist of Center of technology commercialization, Ye.A.Buketov Karaganda State University.

Sugralina, L.M. — Professor of Chair of organic chemistry and polymers, Associated professor, Candidate of chemical sciences, Ye.A.Buketov Karaganda State University.

Taishibekova, Ye.K. — Teacher of Chair of organic chemistry and polymers, Ye.A.Buketov Karaganda State University.

Tatykhanova, G.S. — Vice-head of laboratory of engineering profile, Candidate of chemical sciences, K.I.Satpayev Kazakh National Research Technical University, Almaty.

Tokpayev, R.R. — Junior research fellow, Center of physico-chemical methods of research and analysis (CPCMRA), al-Farabi Kazakh National University, Almaty.

Uali, A.S. — Associate professor of chemical engineering and petroleum chemistry Department, Candidate of chemical sciences, Ye.A.Buketov Karaganda State University.

Yefremov, S.A. — Doctor of chemical sciences, Full professor, Deputy director for Innovation and Technological Activities, Center of physico-chemical methods of research and analysis (CPCMRA), al-Farabi Kazakh National University, Almaty.

Yeshova, Zh.T. — Candidate of chemical sciences, Docent, Faculty of chemistry and chemical technology, al-Farabi Kazakh National University, Almaty.

Yugay, V.V. — Doctoral candidate of PhD, «Technologies and Communication Systems» chair, Karaganda State Technical University.

Zavgorodnyaya, M.A. — Master-engineer direction «Innovation Management», Tomsk State University of Control Systems and Radio Electronics, Russia.

Zhakibekov, T.B. — Candidate of technical sciences, Senior lecturer, «Technologies and Communication Systems» chair, Karaganda State Technical University.

Zhakupov, R.M. — Master student, Ye.A.Buketov Karaganda State University.

Zhortarova, A.A. — PhD Doctorate, Charles University, Prague, Czech Republic.

2015 жылғы «Қарағанды университетінің хабаршысында» жарияланған мақалалардың көрсеткіші. «Химия» сериясы

БЕЙОРГАНИКАЛЫҚ ХИМИЯ

	№	*б.*
Дүйсекеева А.Т., Бектұрғанова А.Ж., Рүстембеков К.Т., Қасенов Б.Қ., Махатова Н.А., Стоев М. Магний қос теллуритінің термохимиясы	2	23
Жылысбаева Г.Н., Нұрділлаева Р.Н., Баешов А.Б., Жылысбаева А.Н. Өндірістік айнымалы токпен поляризациялау арқылы қорғасынның бейорганикалық қосылыстарын синтездеу	2	27
Матаев М.М., Әбдірайымова М.Р., Тұрсынова Ж.И., Батырбекова Ж.Д. Иондаған сәулелерден қорғануға арналған жаңа материалдар	2	31
Мұстафин Е.С., Омаров Х.Б., Хавличек Д., Қасенов Р.З., Қайкенов Д.А., Мұратбекова А.А., Тулетаев Д.К., Канчер И.А. $Yb_2M^I_3Fe_5O_{12}$ (M^I — Li, Na, K) қосылыстарының синтезі, рентгенографиялық және термодинамикалық зерттеуі	2	35

ОРГАНИКАЛЫҚ ХИМИЯ

	№	*б.*
Баринов Д.В., Қалықова Ә.С., Сақыпова З.Б. ФС-1 субстанциясын спектралды әдіспен идентификациялау	1	26
Бүркеев М.Ж., Тажбаев Е.М., Жақыпбекова Э.Ж., Ковалева А.К., Көпбосынова А.А. Полипропиленгликольмалеинатфталат пен акрил қышқылы негізіндегі сополимерлердің қасиеттерін синтездеу және зерттеу	1	31
Жалмаханбетова Р.И. Сесквитерпенді лактондардың галоциклопропанды туындыларының құрылымы және биологиялық белсенділігі	1	12
Жалмаханбетова Р.И., Жұмағалиева Ж.Ж. Циклопропан сақинасы бар табиғи қосылыстар: синтездеу әдістері және биологиялық белсенділігі	1	18
Кенжетаева С.О., Сәрсембаева А.Ш., Файзуллина І.К. Фосфонсірке қышқылы жаңғыштықты бәсеңдетуші құрал ретінде	2	4
Кливенко А.Н., Татыханова Г.С., Нұршат Нұраджи, Құдайбергенов С.Е. Алтынның нанобөлшектері иммобилденген N,N-диметиламиноэтилметакрилат және метакрил қышқылы негізіндегі макроторлы амфотерлі криогель көлемінде *п*-нитрофенолды гидрлеу	4	10
Мерхатұлы Н., Әбеуова С.Б., Омарова А.Т., Тоқтарова Л.Н., Сулейменова Ж.Е. Эстафиатин және оның туындыларының синтезі мен өсуді реттегіш белсенділігі	1	8
Мерхатұлы Н., Щепеткин И.А., Әбеуова С.Б., Омарова А.Т., Искандеров А.Н., Тоқтарова Л.Н. Эстафиатиннің гетероатомқұрамды туындыларының синтезі және қабынуға қарсы, цитотоксикалық белсенділігі	1	4
Мұсабаева Б.Х., Оразжанова Л.К., Құдайбергенов С.Е., Жиенбекова А.Е. Табиғи минералдар және полиакриламид негізінде композициялық гидрогельді материалдардың қасиеттерін зерттеу	3	4
Нұркенов О.А., Сейілханов Т.М., Фазылов С.Д., Исаева А.Ж., Қабиева С.К., Тақыбаева А.Т., Татеева А.Б., Арынова А.Е. ЯМР спектроскопия әдісі арқылы лупининнің β-циклодекстринге енгізілген супрамолекулярлық кешенін алу және зерттеу	3	14
Сәлкеева Л.Қ., Каколина Г.М., Тайшибекова Е.К., Сұғралина Л.М., Хасенова Г.Т., Паншина С.Ю., Горбач Д.Ю., Мұратбекова А.А., Сәлкеева А.Қ. Этиленпропиленді каучуктердің пероксидті вулканизаттарының қасиеттеріне термиялық ескірудің әсері	2	8
Сәлкеева Л.Қ., Минаева Е.В., Тайшибекова Е.К., Жортарова А.А., Хасенова Г.Т., Жакупов Р.М., Сугралина Л.М., Сәлкеева А.К. Минералды қышқылдармен протондау арқылы 2-амино-4-фенилтиазолдың және 2-амино-4-оксотиазолдың негізділік деңгейін зерттеу	4	4
Фазылов С.Д., Нұркенов О.А., Кулаков И.В., Арынова А.Е., Сатпаева Ж.Б., Закарин С.З., Исаева А.Ж., Кәріпова Г.Ж., Исабекова Д.С. Конвекционды жылыту мен микротолқынды активация шарттарында *d*-трео-2-метиламино-1-фенил-1-пропанолының 4-морфолилбензальдегидімен өзара әсерлесуі	3	10

ФИЗИКАЛЫҚ ХИМИЯ

ХИМИЯЛЫҚ ТЕХНОЛОГИЯ ЖӘНЕ МҰНАЙ ХИМИЯСЫ

ХИМИЯНЫҢ ӘДІСТЕМЕСІ

Указатель статей, опубликованных в «Вестнике Карагандинского университета» в 2015 году. Серия «Химия»

№ с.

НЕОРГАНИЧЕСКАЯ ХИМИЯ

ОРГАНИЧЕСКАЯ ХИМИЯ

ФИЗИЧЕСКАЯ ХИМИЯ

Amerkhanova Sh.K., Bohari M. Yamin, Azwan Mat Lazim, Uali A.S., Nurgalieva M. Complexing ability of 2,8,14,20-tetrabenzol-sulfo-calix[4]resorcenarene in relation to Cs$^+$, Pd^{2+}, Ce^{3+}, Eu^{3+} ions in aqueous solution	4	16
Amerkhanova Sh.K., Golovanova O.A., Belgibaeva D.S., Uali A.S., Abdiken F.S. Study of complex formation of Cs$^+$, ZrO^{2+}, Sm^{3+}, Eu^{3+} ions with histidine in aqueous solutions	3	28
Amerkhanova Sh.K., Shlyapov R.M., Uali A.S. Evaluation of interrelation of electrochemical properties and thermal storage capacity of the melt of crystal hydrates of inorganic substances on the basis of $Na_2S_2O_3 \cdot 5H_2O$	4	27
Fomin V.N., Dik A.V. Using one-way analysis of variance in the stochastic determinated design of experiment	2	13
Fomin V.N., Rozhkovoy I.E., Gogol D.B., Ponomarev D.L. Thermodynamic parameters of reactions of basic copper carbonates formation with participation of organic complexing agents	4	22
Golovanova O.A., Kuimova M.V. Study of the influence of inorganic and organic additives on the possibility and regularity of the precipitation process of brushite from aqueous solutions	4	34
Khalitova A.I., Kushekova N.D., Kurmanova A.F. Research of complexation of quercetin with tin (II) in water-ethanol medium	3	24
Masalimov A.S., Tur A.A., Tuktybayeva A.E., Nikolskiy S.N. Quantum-chemical investigations of the dual protolytic activity of several semiquinone radicals	1	51
Nikolskiy S.N., Tur A.A., Yelchibekova A.A., Kutzhanova K.Zh., Masalimov A.S. Investigation of intermolecular proton exchange 3,6-di-tert-butyl-2-hydroxyphenoxyl with phenol by ESR spectroscopy method	1	47
Omarov Kh.B., Absat Z.B., Aldabergenova S.K., Rakhimzhanova N.J., Siyazova A.B. Comparative analysis of arsenates, antimonates and calcium bismuthates based on *E*–pH diagrams	4	47
Голованова О.А., Шляпов Р.М., Амерханова Ш.К., Уали А.С., Зырянова И.М. Особенности образования минеральной фазы в системе $Ca(NO_3)_2$–$Mg(NO_3)_2$–Na_2HPO_4–H_2O в присутствии катионов магния	1	37
Парамонов Ф.П., Масакбаева С.Р., Ковтарева С.Ю. Расчет средних длин волн участка тормозного спектра, способного возбудить Kα_1-линию элемента (Zn, Ge, Se)	1	57
Шамбилова Г.К., Мангыстауова Р.Т., Насиров Р. Анион-радикал бензола и теоретическое обоснование его ЭПР-спектра	2	19

ХИМИЧЕСКАЯ ТЕХНОЛОГИЯ И НЕФТЕХИМИЯ

Fengyun Ma, Baikenov M.I., Baikenova G.G., Tateeva A.B., Muratbekova A.A., Makanova N.E. The calculation of the thermodynamic functions of the hydrocarbon composition of the light fraction of primary coal tar with the boiling point 175 ºC	3	47
Kenzhetayeva S.O., Abdygalimova S.Sh. Investigation of influence of colloids formation process on parameters of rare metals extraction	3	63
Mamrayeva K.M., Shashchanova R.B., Shashchanova M.B. Processing of Shubarkol coal for obtaining chemical products	4	66
Mussabayeva B.Kh., Iminova D.E., Orazzhanova L.O., Sabitova A.N. Structure of catalysts with gold nanoparticles	3	53
Mussabayeva B.Kh., Orazzhanova L.K., Kudaibergenov S.E., Kassymbayeva D.S. Selection of depressor additives for transportation of high-viscositive Kazakhstan oils	2	59
Omasheva A.V., Sevostyanova K.A., Zavgorodnyaya M.A. Adhesives of cold curing based on chloroprene rubber brand Skaypren G-40T	4	76
Pudov A.M., Mustafin E.S., Omarov Kh.B., Kasenov R.Z., Pudov I.M., Havlichek D., Sevostyanova K.A. Automatic industrial water treatment plant for the production of steam for boiler room JSC «Road construction materials», Karaganda	3	42
Zhou Qixiong, Niu Ben, Li Zhijuan, Ma Fengyun, Absat Z.B., Kochegina E.V., Karimova A.B., Rakhimzhanova N.Zh., Mukusheva G.K., Bulax J. Effect of iron-based catalysts on hydropyrolysis behavior of coal	2	42
Амерханова Ш.К., Шляпов Р.М., Курбаналиев Н.М. Разработка режима флотационного обогащения медно-свинцовой руды месторождения «Аяк-Коджан» с использованием смеси флотореагентов	1	62

МЕТОДИКА ПРЕПОДАВАНИЯ ХИМИИ